

LIGNIN DERIVATIVES AS BIOAROMATIC MONOMERS: SYNTHESIS,  
CHARACTERIZATION, AND PROPERTIES OF LIGNOPOLYESTERS

by

DEMICHAEL DWAYNE WINFIELD

(Under the Direction of Jason Locklin)

ABSTRACT

Lignin is a promising bio-based feedstock for aromatic platform chemicals. Of particular interest to polymer chemist are the various hydroxycinnamic acid derivatives that can be obtained from lignin depolymerization. The valorization of these derivatives and their subsequent polymerizations are well described in the literature, but robust mechanical and degradation properties of these materials is lacking. The systematic study of the thermal, mechanical, and degradation properties of both novel and previously reported lignopolyesters is described. The properties of polyesters functionalized with alkyl linkers at the phenolic moiety were investigated by conventional techniques. These polymers exhibited excellent thermal stability, allowing for extrusion and injection molding. These semi-aromatic polymers show a wide array of mechanical properties, including a highly ductile thermoplastic, a strong and rigid thermoplastic, and an elastomer. Composting biodegradation tests showed both degradable and nondegradable polymers can be achieved in this class. Of the polymers synthesized, one exhibited shape memory characteristic of thermoplastic polyester elastomers (TPEEs). TPEEs are

unique in that they behave like elastomers but lack any crosslinking. To improve its mechanical properties, reactive extrusion with epoxide chain extenders was used to induce branching. The degree of branching can be controlled by epoxide loading, allowing for tuning of the elastic modulus and ductility. Elastic modulus was increased by up to 3 orders of magnitude and shape memory was retained. The rheological properties of the branched TPEE were also significantly enhanced. These materials were blended with commercial biopolymers to further probe their applications. Formulations with PBS and PHA were melt compounded with and without compatibilizers. Generally, all blends showed increased toughness. PHA's elongation at break of 18% was dramatically increased, with its ultimate elongation with and without compatibilizers increasing to 136% and 247% respectively. Further applications and melt rheology of the blends is described. Optimization of high melting polymers derived from lignin is also described. The conventional synthesis was substantially improved in terms of molecular weight and sustainability. The scalability and extensive characterization of lignopolyesters demonstrates their potential to replace petrol polymers. Further investigation into the structure-property relationships of these structures could aid in developing new generations of lignopolyesters.

INDEX WORDS: Biobased polymers, bioaromatic polymers, polymer chemistry, green chemistry, polyesters, extrusion, polymer synthesis, polymer characterization

LIGNIN DERIVATIVES AS BIOAROMATIC MONOMERS: SYNTHESIS,  
CHARACTERIZATION, AND PROPERTIES OF LIGNOPOLYESTERS

by

DEMICHAEL DWAYNE WINFIELD

B.S., Georgia College and State University, 2016

A Dissertation Submitted to the Graduate Faculty of The University of Georgia in  
Partial Fulfillment of the Requirements for the Degree

DOCTOR OF PHILOSOPHY

ATHENS, GEORGIA

2021

© 2021

DeMichael Dwayne Winfield

All Rights Reserved

LIGNIN DERIVATIVES AS BIOAROMATIC MONOMERS: SYNTHESIS,  
CHARACTERIZATION, AND PROPERTIES OF LIGNOPOLYESTERS

by

DEMICHAEL DWAYNE WINFIELD

Major Professor: Jason Locklin  
Committee: Steven Wheeler  
Suraj Sharma

Electronic Version Approved:

Ron Walcott  
Vice Provost for Graduate Education and Dean of the Graduate School  
The University of Georgia  
December 2021

## DEDICATION

This dissertation is dedicated to my sister and best friend, Anastasia, for her unconditional love and support throughout my life. Thank you for always believing in me, even when I didn't believe in myself.

## ACKNOWLEDGEMENTS

I would like to thank my family and friends for their support throughout this journey. To my parents, thank you for instilling the value of education in me at a young age. Thank you for the immense sacrifices you made so that I could have opportunities that you never had. You always pushed me to do my best, and never settled for good enough. I wouldn't have made it this far without your love and support. To Emily, thanks for your support and encouragement. You helped me get through the difficult parts of this process and always know how to cheer me up. I would like to thank the rest of my family for their words of encouragement, as well as my friends who have cheered me on throughout this journey.

I would also like to thank my advisor Jason Locklin, for his support and guidance throughout this journey. Thank you for allowing me the freedom to shape my project, hearing out my crazy ideas, and reeling me back in when I go too far off the rails. I appreciate you giving me a chance and building me up during my first few years. To my committee members, Steven Wheeler and Suraj Sharma, thank you for your useful feedback and insight during my graduate career.

To the labmates I've worked with alongside over the past 5 years, Evan, Karson, Li, Qiahong, Yutian, Grant, Jessica, Jess, Scott, Apisata, Tim, Cato, Maddi, Josh, Ryan, Ethan, and Virginia, thank you for your friendship and for making this experience more enjoyable.



## TABLE OF CONTENTS

ACKNOWLEDGEMENTS.....	v
LIST OF TABLES .....	ix
LIST OF FIGURES .....	xi
CHAPTER 1: INTRODUCTION .....	1
Sustainable Feedstocks .....	1
Bio PET .....	2
Lignin Biomass.....	4
Lignopolyesters.....	5
Sustainability of Lignopolymers.....	6
Objectives .....	8
CHAPTER 2: SEMI-AROMATIC BIOBASED POLYESTERS DERIVED FROM LIGNIN AND CYCLIC CARBONATES .....	18
Abstract.....	19
Introduction .....	20
Experimental .....	23
Results and Discussion.....	31
Conclusion .....	46
References.....	48

CHAPTER 3: PROPERTIES OF BRANCHED THERMOPLASTIC POLYESTER ELASTOMER POLY(ISOPROPYL PHLORETATE) BY EPOXY CHAIN EXTENDER.....	58
Abstract.....	59
Introduction .....	60
Experimental .....	63
Results and Discussion.....	66
Conclusion .....	76
References.....	77
CHAPTER 4: ENHANCEMENT OF POLY(BUTYLENE SUCCINATE'S) CRYSTALLINITY, STIFFNESS, AND TOUGHNESS BY BLENDING WITH SEMI-AROMATIC LIGNOPOLYESTERS.....	81
Abstract.....	82
Introduction .....	83
Experimental .....	85
Results and Discussion.....	87
Conclusion .....	91
References.....	92
CHAPTER 5: POLYESTERS AS DUAL TOUGHENING AGENTS AND PROCESSING AIDS IN POLY(HYDROXYL ALKANOATE) BLENDS .....	96
Abstract.....	97

Introduction .....	98
Experimental .....	101
Results and Discussion.....	104
Conclusion .....	110
References.....	111
CHAPTER 6: SCREENING AND OPTIMIZATION OF BASE CATALYST FOR THE SYNTHESIS OF HIGH TM BIOBASED POLYESTERS FROM HYDROXYCINNAMIC ACIDS .....	115
Abstract.....	116
Introduction .....	117
Experimental .....	120
Results and Discussion.....	122
Conclusion .....	130
References.....	132
CHAPTER 7: Outlook .....	136
Conclusion .....	136
Future Work .....	136
Final Remarks.....	137
Appendix .....	138

## LIST OF TABLES

Table 2.1 Summary of polymerization results.....	34
Table 2.2 Summary of tensile properties .....	39
Table 2.3 Results from cyclic tensile testing of PiPP. Final strain is the strain at which stress is zero. Shape recovery ratio ( $R_r$ ) is the percentage of strain that was recovered in each cycle .....	43
Table 3.1 Results of REX. Molecular weights of epoxy modified PiPP determined by GPC. Degrees of branching (DB) determined by equation 1. $T_g$ was determined by DSC. ....	66
Table 3.2 Tensile test with cyclic loading rate $20\% \text{ min}^{-1}$ of to 150% strain for 10 cycles .....	72
Table 3.3 Shear Modulus of polymers based on shear rate sweeps .....	75
Table 4.1 Thermal properties from second cycle of DSC. X is the fraction of crystallinity, calculated by eq. 4.1. PBSe refers to neat PBS that has been hot melt extruded.....	88
Table 4.2 Tensile data of PBS and blends .....	90
Table 5.1 Thermal properties from second cycle of DSC. X is the fraction of crystallinity, calculated by eq. 5.1 .....	104
Table 5.2 Tensile properties of PHA and PHA blends .....	106
Table 5.3 Tensile properties of all blends evaluated in this study.....	108

Table 6.1 Preliminary acid catalyst screening for PPA synthesis. AcPA was melted under N <sub>2</sub> at 180°C, then ramped to the final temperature, followed by 4 hours of vacuum.....	119
Table 6.2 Results of optimization of PPA synthesis with hydroxide based catalyst. All polymerizations were conducted under N <sub>2</sub> at 140°C for 4 hours, 160°C for 1 hour, 200°C for 1 hour, then 2 hours at the final temperature under vacuum for 2 hours. ....	128
Table A.1 E-Factor evaluation of alkylation via cyclic carbonate over two steps. Sulfuric acid assumed to be negligible .....	164
Table A.2 E-Factor evaluation of alkylation via halo alcohol.....	164
Table A.3 EcoScale Rubric.....	165
Table A.4 EcoScale evaluation of alkylation with ethylene carbonate .....	166
Table A.5 EcoScale Evaluation of alkylation with 2-chloroethanol.....	167
Table A.6 Tensile properties of PiPP tested at different rates .....	170

## LIST OF FIGURES

Figure 1.1 Structure of terephthalic acid and its common polyesters .....	3
Figure 1.2 Structure of FDCA and PEF .....	4
Figure 1.3 Representative structure of lignin .....	4
Figure 1.4 Select structures of lignin-derived small molecules .....	5
Figure 2.1 Structures of hydroxycinnamic acids that can be obtained from lignin depolymerization and a common route to hydroxycinnamic acid-based polymers .....	22
Figure 2.2 (a) Structures of the monomers synthesized in this study (b) Synthesis, E-Factor, and EcoScale of conventional haloalcohol alkylation (left) and cyclic carbonate alkylation (right). E-Factors shown assume solvent is recovered (c) Polymerization conditions .....	32
Figure 2.3 (a) Second heating cycle from DSC after cold quenching (b) TGA curves under N <sub>2</sub> atmosphere .....	36
Figure 2.4 DMA temperature sweeps of the synthesized polyesters (a) Loss modulus (b) Storage modulus (c) tan delta.....	37
Figure 2.5 Representative stress/strain curves from tensile testing (a) Ductile polymers (b) Brittle polymers .....	40
Figure 2.6 Elastomeric properties of PiPP. (a) Stress relaxation at 5% instantaneous strain. (b) Creep cycles at a constant stress of 0.200 MPa for 10 minutes followed by a 20-minute relaxation period. Strain recovery is presented as	

percentage above each relaxation cycle. (c) Cyclic tensile test with a cyclic loading of 20 mm min <sup>-1</sup> for 10 cycles. (d) 10 cycles with a cyclic loading of 5 mm min <sup>-1</sup> .	42
Figure 2.7 Normalized biodegradation of PEP, PiPP, and PEHF relative to cellulose. Error bars represent one standard deviation from the mean based on triplicates .....	44
Figure 3.1 Summary of PiPP properties .....	61
Figure 3.2 Branched PiPP structures obtained by REX using Joncryl 4368. Joncryl 4368 is a multifunctional chain extender that has a linear backbone with epoxide side chains.....	62
Figure 3.3 Synthesis of PiPP by polycondensation .....	63
Figure 3.4 GPC traces of PiPP and epoxy modified polymers .....	68
Figure 3.5 Tensile properties of polymers in this study (a) Stress/Strain curves (b) Ultimate tensile strength (c) Elastic modulus (d) Elongation at break.....	70
Figure 3.6 Linear regressions and adjusted R <sup>2</sup> values for tensile properties.....	71
Figure 3.7 Rheological data of polymers from oscillatory experiments. All experiments were conducted at 1% strain at 120°C. Data is plotted as a function of angular frequency.....	73
Figure 3.8 Rheological data of polymers from shear sweep experiments. Shear rate was ramped in a logarithmic fashion. (a) Viscosity of polymers over different shear rates. (b) Shear Stress/Strain curve .....	74
Figure 3.8 Rheological data of polymers from shear sweep experiments. Shear rate was ramped in a logarithmic fashion. (a) Viscosity of polymers over different shear rates. (b) Shear Stress/Strain curve .....	74

Figure 4.1 Properties of PBS FZ91 used in this study .....	84
Figure 4.2 Structure of lignopolyesters used in this work .....	85
Figure 4.3 DSC overlays of PBS and blends. Second cycle of cooling scan (top) and heating scan (bottom) is shown .....	87
Figure 4.4 Stress/Strain curves of polymer blends at 20 mm min <sup>-1</sup> .....	89
Figure 5.1 Properties of the PHA used in this study .....	100
Figure 5.2 Properties of lignopolyesters used in this study .....	101
Figure 5.3 Second scans from DSC of polymer blends. (a) second heating cycle (b) second cooling cycle .....	104
Figure 5.4 Stress/Strain curves of PHA, PBG, and lignopolyester blends .....	105
Figure 5.5 Generalized scheme for the synthesis of aliphatic polyesters and their structures. PBSA 5 refers to PBA copolymer content of 5%.....	107
Figure 5.6 Stress/Strain curves of PHA and all blends evaluated in this study.	109
Figure 6.1 General synthetic scheme for acidolysis polymerization of PPA .....	117
Figure 6.2 Generalized mechanism for the polymerization of AcPA to PPA by metal-based Lewis acid catalyst .....	118
Figure 6.3 Generalized scheme for the synthesis of PPA from AcPA with carboxylate end groups .....	120
Figure 6.4 <sup>1</sup> H NMR of AcPA. The integrations of the protons at 2.96 and 2.68 ppm are compared to the integration of methyl end group at 2.29 to calculate D <sub>p</sub> ...	122
Figure 6.5 Thermal analysis of AcPA for polymerization optimization. (a) Heating scan by high pressure DSC (b) Zoom in of heating scan in a showing the slight	



exotherm resulting from homopolymerization of AcPA (c) TGA of AcPA at 10°C min <sup>-1</sup> under N <sub>2</sub> atmosphere .....	123
Figure 6.6 <sup>1</sup> H NMR of AcPA polymerization after 3 hours at 140°C .....	124
Figure 6.7 High pressure DSC runs of AcPA with 10% of selected catalyst. Traces shown are the change in heat flow from AcPA run with no catalyst. (a) Carboxyl catalyst (b) Hydroxide based catalyst (c) Organobase catalyst (d) Traditionally used zinc catalyst for reference .....	125
Figure 6.8 Second heating cooling scan of PPA synthesized from optimized conditions. ....	129
Figure A.1 <sup>1</sup> H NMR spectrum of methyl 3-(4-hydroxyphenyl)propanoate .....	139
Figure A.2 <sup>1</sup> H NMR spectrum of 3-(4-(2-hydroxyethoxy)-3-methoxyphenyl)propanoic acid .....	140
Figure A.3 <sup>13</sup> C NMR spectrum of 4-(2-hydroxyethoxy)phenylpropanoic acid ...	141
Figure A.4 <sup>1</sup> H NMR spectrum of 3-(4-(2-hydroxypropoxy)phenyl)propanoic acid .....	142
Figure A.5 <sup>13</sup> C NMR spectrum of 3-(4-(2-hydroxypropoxy)phenyl)propanoic acid .....	143
Figure A.6 <sup>1</sup> H NMR spectrum of 4-(3-hydroxypropoxy)phenylpropanoic acid...	144
Figure A.7 <sup>13</sup> C NMR spectrum of 4-(3-hydroxypropoxy)phenylpropanoic acid .	145
Figure A.8 <sup>1</sup> H NMR spectrum of 3-(4-hydroxy-3-methoxyphenyl)propionic Acid .....	146

Figure A.9	$^1\text{H}$ NMR spectrum of methyl 3-(4-hydroxy-3-methoxyphenyl)propanoate .....	147
Figure A.10	$^1\text{H}$ NMR spectrum of 3-(4-(2-hydroxyethoxy)-3-methoxyphenyl)propanoic acid .....	148
Figure A.11	$^{13}\text{C}$ NMR spectrum of 3-(4-(2-hydroxyethoxy)-3-methoxyphenyl)propanoic acid .....	149
Figure A.12	$^1\text{H}$ NMR spectrum of 3-(4-hydroxy-3,5-dimethoxyphenyl)propanoic acid .....	150
Figure A.13	$^1\text{H}$ NMR spectrum of methyl 3-(4-hydroxy-3,5-dimethoxyphenyl)propanoate .....	151
Figure A.14	$^1\text{H}$ NMR spectrum of 3-(4-(2-hydroxyethoxy)-3,5-dimethoxyphenyl)propanoic acid .....	152
Figure A.15	$^{13}\text{C}$ NMR spectrum of 3-(4-(2-hydroxyethoxy)-3,5-dimethoxyphenyl)propanoic acid .....	153
Figure A.16	$^1\text{H}$ NMR spectrum of polyethylene phloretate .....	154
Figure A.17	$^{13}\text{C}$ NMR spectrum of polyethylene phloretate .....	155
Figure A.18	$^1\text{H}$ NMR spectrum of polyisopropyl phloretate (PiPP) .....	156
Figure A.19	$^{13}\text{C}$ NMR spectrum of polyisopropyl phloretate (PiPP) .....	157
Figure A.20	$^1\text{H}$ NMR spectrum of polypropylene phloretate (PPP) .....	158
Figure A.21	$^{13}\text{C}$ NMR spectrum of polypropylene phloretate (PPP) .....	159
Figure A.22	$^1\text{H}$ NMR spectrum of polyethylene dihydroferulate .....	160
Figure A.23	$^{13}\text{C}$ NMR spectrum of polyethylene dihydroferulate .....	161
Figure A.24	$^1\text{H}$ NMR spectrum for polyethylene dihydrosinapate .....	162

Figure A.25 $^{13}\text{C}$ NMR spectrum of polyethylene dihydrosinapate.....	163
Figure A.26 Second heating and cooling cycle of PEP.....	168
Figure A.27 Second heating and cooling cycle of PPP.....	169
Figure A.28 Stress strain curve of PiPP tested at different rates.....	170
Figure A.29 Cumulative $\text{CO}_2$ production of compost without sample (blank), cellulose positive control, and tested samples.....	172
Figure A.30 Absolute biodegradation of cellulose triplicates .....	173
Figure A.31 Absolute biodegradation of PEP triplicates .....	174
Figure A.32 Absolute biodegradation of PEHF .....	175
Figure A.33 Absolute biodegradation of PiPP.....	176

## CHAPTER 1: INTRODUCTION

### **Sustainable Feedstocks**

Petroleum feedstocks are crucial for the production of industrially relevant plastics, pharmaceuticals, construction materials, agricultural materials, and consumer goods.<sup>1</sup> However, current estimates predict that the economic viability of harvesting petroleum sources will plummet in 50 years.<sup>2</sup> While this estimate is controversial, almost all experts agree that petroleum sources will be depleted by the end of the century at the latest.<sup>2</sup> Additionally, drilling of petrol sources is known to cause substantial ecological degradation and negative effects on the health of the world's inhabitants.<sup>3,4</sup> In fact, petroleum feedstocks are tied to virtually every environmental problem being faced today. Utilization of petrol feedstocks causes a substantial degree of pollution and is a major contributor to global warming.<sup>1,3,5–</sup>

7

Due to growing environmental concerns, utilization of sustainable and/or biological based feedstocks for sourcing of platform chemicals has been of growing significance in the literature. In terms of polymeric materials, lignocellulosic biomass has been widely utilized for biobased polymers.<sup>1,8–10</sup> Lignocellulose consists of cellulose, hemicellulose, and lignin connected by triglyceride linkers.<sup>1,9</sup> From this biomass, a number of biopolymers have been developed. However,

many of these polymer materials have been aliphatic. Aromatic and semi-aromatic polyesters are valuable commodity plastics. Accounting for roughly 10% of the global plastic economy, they boast easy processability and robust thermal and mechanical properties.<sup>11,12</sup> Despite the rapid advancement in biopolymers, aromatic monomers used for the synthesis of these polyesters are derived almost exclusively from petroleum feedstocks.<sup>13,14</sup> While many aliphatic polyesters derived from biosources have seen commercial success in recent years, examples of biobased aromatic monomers are less common.<sup>15,16</sup>

## **Bio PET**

Most commercial aromatic polyesters utilize terephthalic acid (TA) as an aromatic diacid (**Figure 1.1**).<sup>10,17</sup> Of significant commercial relevance is poly(ethylene terephthalate) (PET), accounting for 7.7% of the global plastics economy.<sup>18</sup> PET is used in a wide array of applications ranging from packaging, films, and fibers.<sup>18</sup> There have been many efforts to make biobased terephthalic acids, but it is exorbitantly expensive compared to petrol based TA.<sup>17</sup> In fact, 'biobased' PET and PBAT are partially biobased. The diols used are biobased, while TA is not.<sup>13</sup> In fact, roughly 0.2% of bio PET produced in 2017 contained biobased TA.<sup>17</sup> Additionally, PET does not degrade in the natural environment, producing persistent microplastics.<sup>14,19</sup> However, random copolymers with aliphatic diacids can degrade so long as the TA makes up roughly half or less of the diacid monomers.<sup>20</sup> Poly(butylene adipate co terephthalate) (PBAT) is a

commercially available biodegradable polymer with TA.<sup>20–22</sup> PBAT is a highly flexible and ductile polyester with a lower  $T_m$ .<sup>23</sup>

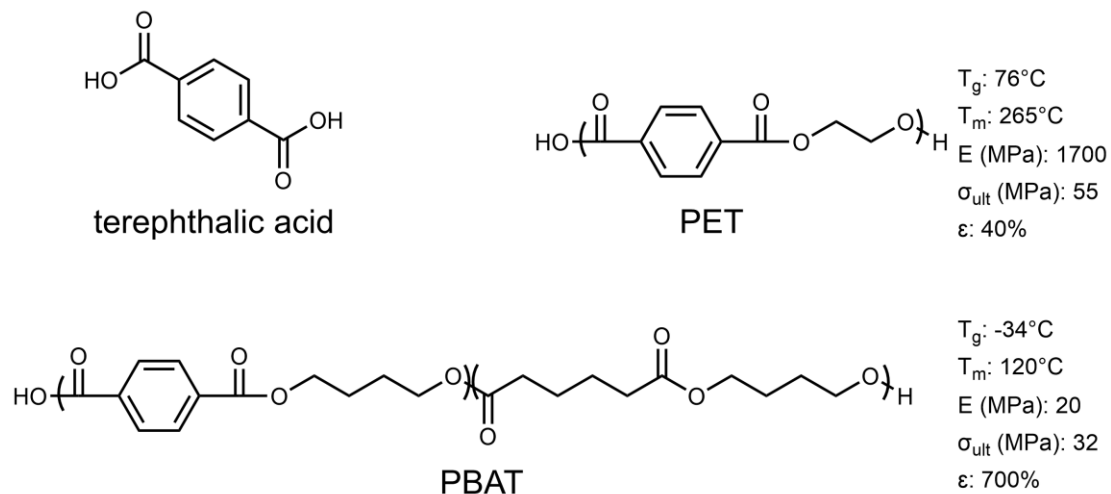


**Figure 1.1** Structure of terephthalic acid and its common polyesters

Poly(ethylene 2,5-furandicarboxylate) (PEF) has been proposed as a biobased alternative to PET (**Figure 1.2**).<sup>18,24</sup> PEF boasts several advantages, namely its superior barrier properties, higher modulus, and biodegradability.<sup>18</sup> It is worth noting however, that PEF is the slowest reported degrader by industrial composting taking up to 385 days to fully degrade.<sup>25</sup> Still, this is an advantage as PET is nondegradable. Application of PEF has been limited, as the production of 2,5-furandicarboxylic acid (FDCA) is expensive and lengthy due to the complexity of purification.<sup>19,24</sup> The synthesis of PEF is also quite challenging due to the poor solubility of FDCA in the melt, making high molecular weight difficult to achieve.<sup>26,27</sup> Due to the aforementioned reasons, there is need for more research of bioaromatic monomers.

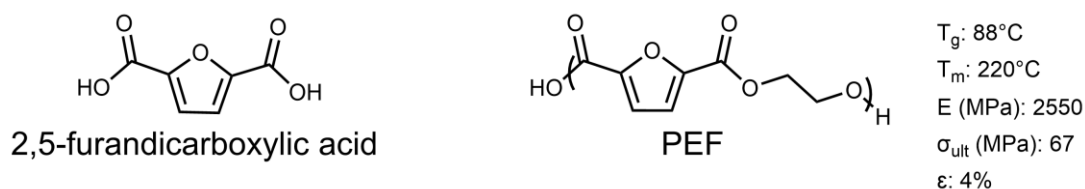


**Figure 1.2** Structure of FDCA and PEF

## Lignin Biomass

Considering the structure of lignocellulosic biomass, lignin is the obvious choice for bioaromatic monomers. Lignin is the second most abundant biopolymer on earth second to cellulose.<sup>28</sup> It is a polyphenolic polymer found in the cell walls of most vascular plants.<sup>28</sup> While the growing and cultivating of lignin can be done in a sustainable fashion, lignin is also produced as a byproduct of agro-industrial industries. The paper milling process produces lignin inadvertently as cellulose is isolated to make paper products.<sup>28–30</sup> Most lignin produced from these industries is burned for energy recovery. Due to its natural abundance, there have been many efforts to utilize lignin as a feedstock for materials.<sup>31–35</sup>

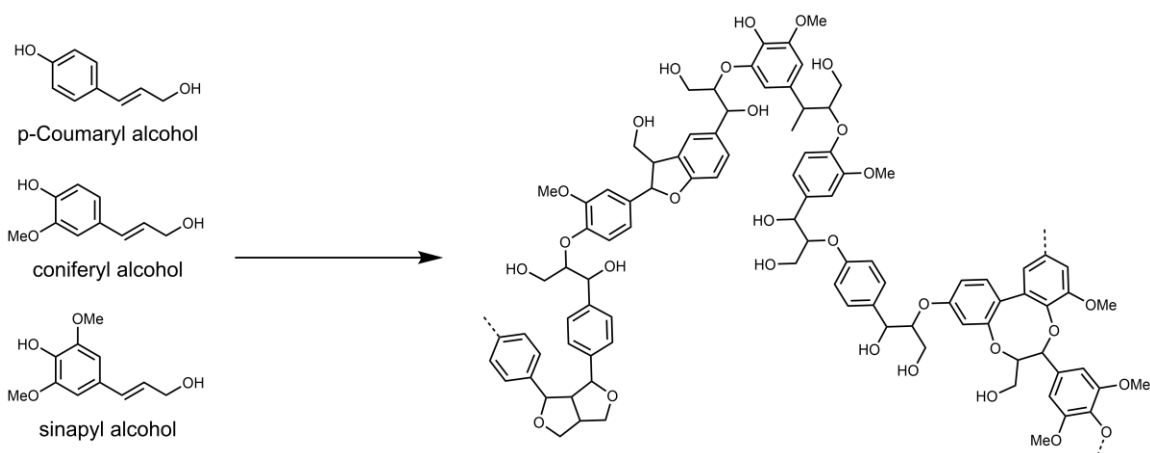


**Figure 1.3** Representative structure of lignin

In nature, lignin is synthesized by radical polymerization of the monolignols (**Figure 1.3**).<sup>36</sup> Due to the highly reactive and oxidative nature of this polymerization, lignin is a highly variable heterogeneous material.<sup>36</sup> Thus, using lignin directly in materials is difficult.<sup>37,38</sup> Instead, several groups have sought to utilize lignin depolymerization and functionalization strategies to produce platform and value-added chemicals.<sup>28</sup> A variety of useful starting materials have been isolated from lignin, including hydroxycinnamic acids, hydroxybenzoic acids, benzaldehydes, and styrenics (**Figure 1.4**).<sup>34,39–43</sup>

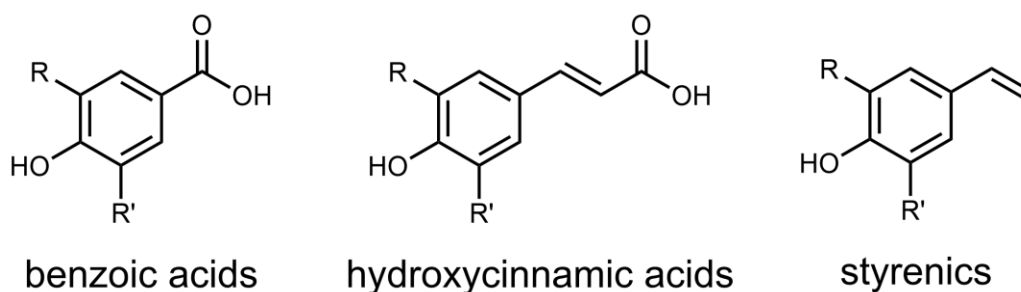


**Figure 1.4** Select structures of lignin-derived small molecules

### Lignopolyesters

Several classes of polymers have been synthesized from lignin biomass. As the focus of this dissertation is on lignin derived polyesters, this topic will be the focus of this section. The Miller group has made many contributions to the synthesis of lignopolyesters. In 2010, the group published a report on utilizing reduced hydroxycinnamic acid derivatives to produce high melting polyesters.<sup>30</sup> These materials rival PET in thermal properties. Sequentially, many polyesters made from lignin derived hydroxybenzoic acids have been reported. Miller et al. reported the



synthesis and thermal properties of benzoic, vanillic, and syringic acid homopolymers functionalized with short chain aliphatic linkers.<sup>44</sup> Notably, many of these materials appear to have robust thermal properties, but obtaining the polymers in reasonable yield without decomposition is challenging. Recently, much interest has been placed on vanillic acid homopolymers from this class. Poly(propylene vanillate) (PPV) specifically is considered a sustainable engineering plastic due to its high melting transitions and mechanical properties.<sup>29</sup>

Beyond this, there is some particularly appealing work that has been done with lignin derived hydroxy cinnamic acid derivatives. After functionalization with haloalcohols, Miller et al. reported the homopolymerization of these materials.<sup>45</sup> The thermal properties of these polyesters are highly varied. Both semicrystalline and wholly amorphous materials were achieved. These materials were also copolymerized with poly(lactic acid) and poly(caprolactone) to yield a series of copolymers.<sup>46</sup> While these works are interesting from a synthetic perspective, the application of these materials has been poorly explored. The mechanical properties of these lignopolyesters cannot be found in the literature, and the molecular weight of the reported polymers is quite low.<sup>45,46</sup> This significantly limits the potential of these polyesters to make significant impact as biobased materials.

### **Sustainability of Lignopolymers**

While utilization of bio feedstocks has obvious advantages, further consideration of the sustainability of biobased polymers is necessary. In a critical review, the sustainability of over a 100 lignin-based polymers was assessed by Fadallah et

al.<sup>47</sup> In general, many methods used to build up monomer precursors for lignin-derived polymers are less than ideal from a sustainability perspective. Several quantifiable metrics can be employed to evaluate sustainability. The simplest include metrics such as E-factor and atom economy. E-factor is simply a ratio of waste to product produced.<sup>48</sup> Ideally, an E-factor of zero should be targeted, as this would mean that all inputs were incorporated into the product. Atom economy is a very similar metric. It is based on the idea that in an ideal scenario, the atoms present in the reagents should be incorporated into the product or recovered by other means.

Outside of simple green metrics, there are more complex and specific criteria that can be employed for evaluating different processes. In particular interest to synthesis is EcoScale. EcoScale takes into account several factors, including yield, energy input, toxicity, environmental harm of the reagents, waste, and complexity of performing the process.<sup>49</sup> EcoScale is a more robust metric for evaluating the 'greenness' of different chemical processes due to its thoroughness. Phosgene for example is highly 'sustainable' by a number of green metrics.<sup>50,51</sup> This is due to the fact that phosgene's exceptional reactivity and atom economy yields high numbers in many green metrics. However, use of phosgene is obviously less than ideal due to its danger and the stoichiometric halogenated waste it produces. Thus, simple green metrics are useful for quick assessments, but many factors need to be considered to make a reasonable claim on the 'greenness' of a process.

## **Objectives**

Elucidation of the application of lignopolyesters through thorough thermomechanical characterization is the primary concern of this dissertation. Chapter 2 describes the synthesis, characterization, and composting of a selection of lignopolyesters. Of the materials studied, a variety of properties are achieved. These range from ductile thermoplastic, highly rigid and strong materials, as well as a shape memory elastomer. Chapter 3 deals with the chemical modification of our lignopolyester based elastomer through reactive extrusion with multifunctional epoxides. Elastic modulus can be readily tuned allowing for the targeting of soft and hard rubbers. Chapter 4 and 5 discuss blending of our lignopolyesters with other biobased polyesters. Poly(butylene succinate) (PBS) blends were made by melt mixing with and without epoxy compatibilizer. Significant improvement to the tensile properties and crystallinity were achieved. Blends with poly(hydroxy alkanates) (PHA) were also investigated. The tensile properties of PHA were substantially improved, with increases in both toughness and strength achieved at once. A library of aliphatic polyesters was also synthesized and blended with PHA to assess the effectiveness of our lignopolyesters in the broader context of polyesters. Finally, Chapter 6 shifts gears to discuss the optimization of poly(phloretic acid) (PPA) synthesis, a high melting polymer that historically has been difficult to synthesize. Our optimized conditions are not only greener than the conventionally used methods, but also yielded higher molecular weight. Thermal properties, further optimization, and remaining challenges are discussed.

## References

- (1) Steinbüchel, A. *Biopolymers*; Wiley-VCH, 2001.
- (2) Subbotina, E.; Rukkijakan, T.; Marquez-Medina, M. D.; Yu, X.; Johnsson, M.; Samec, J. S. M. Oxidative Cleavage of C-C Bonds in Lignin. *Nat. Chem.* **2021**. <https://doi.org/10.1038/s41557-021-00783-2>.
- (3) Tamis, J. E.; Jongbloed, R. H.; Karman, C. C.; Koops, W.; Murk, A. J. Rational Application of Chemicals in Response to Oil Spills May Reduce Environmental Damage. *Integr. Environ. Assess. Manag.* **2012**, 8 (2), 231–241.
- (4) Piorkowska, E. Overview of Biobased Polymers. In *Thermal Properties of Biobased Polymers*; Di Lorenzo, M. L., Androsch, R., Eds.; Springer International Publishing: Cham, 2019; pp 1–35.
- (5) Chiroma, H.; Abdul-kareem, S.; Khan, A.; Nawi, N. M.; Gital, A. Y.; Shuib, L.; Abubakar, A. I.; Rahman, M. Z.; Herawan, T. Global Warming: Predicting OPEC Carbon Dioxide Emissions from Petroleum Consumption Using Neural Network and Hybrid Cuckoo Search Algorithm. *PLoS One* **2015**, 10 (8), e0136140.
- (6) Franta, B. Early Oil Industry Knowledge of CO<sub>2</sub> and Global Warming. *Nat. Clim. Chang.* **2018**, 8 (12), 1024–1025.
- (7) Kessel, D. G. Global Warming — Facts, Assessment, Countermeasures. *J. Pet. Sci. Eng.* **2000**, 26 (1), 157–168.

- (8) Dai, Z.; Guo, F.; Zhang, S.; Zhang, W.; Yang, Q.; Dong, W.; Jiang, M.; Ma, J.; Xin, F. Bio-based Succinic Acid: An Overview of Strain Development, Substrate Utilization, and Downstream Purification. *Biofuels Bioprod. Biorefin.* **2020**, *14* (5), 965–985.
- (9) Isikgor, F. H.; Remzi Becer, C. Lignocellulosic Biomass: A Sustainable Platform for the Production of Bio-Based Chemicals and Polymers. *Polym. Chem.* **2015**, *6* (25), 4497–4559.
- (10) Nguyen, H. T. H.; Suda, E. R.; Bradic, E. M.; Hvozdoch, J. A.; Miller, S. A. Polyesters from Bio-Aromatics. In *Green Polymer Chemistry: Biobased Materials and Biocatalysis*; ACS Symposium Series; American Chemical Society, 2015; Vol. 1192, pp 401–409.
- (11) Miller, S. A. Sustainable Polymers: Opportunities for the Next Decade. *ACS Macro Lett.* **2013**, *2* (6), 550–554.
- (12) Sinha, V.; Patel, M. R.; Patel, J. V. Pet Waste Management by Chemical Recycling: A Review. *J. Polym. Environ.* **2010**, *18* (1), 8–25.
- (13) European Bioplastics. *Bioplastics Market Data 2020*; Nova-Institute, 2020.
- (14) Wang, G.-X.; Huang, D.; Ji, J.-H.; Völker, C.; Wurm, F. R. Seawater-Degradable Polymers-Fighting the Marine Plastic Pollution. *Adv. Sci.* **2020**, *8* (1), 2001121.
- (15) Borrelle, S. B.; Ringma, J.; Law, K. L.; Monnahan, C. C.; Lebreton, L.; McGivern, A.; Murphy, E.; Jambeck, J.; Leonard, G. H.; Hilleary, M. A.; Eriksen, M.; Possingham, H. P.; De Frond, H.; Gerber, L. R.; Polidoro, B.;

- Tahir, A.; Bernard, M.; Mallos, N.; Barnes, M.; Rochman, C. M. Predicted Growth in Plastic Waste Exceeds Efforts to Mitigate Plastic Pollution. *Science* **2020**, 369 (6510), 1515–1518.
- (16) Tokiwa, Y.; Calabia, B. P.; Ugwu, C. U.; Aiba, S. Biodegradability of Plastics. *Int. J. Mol. Sci.* **2009**, 10 (9), 3722–3742.
- (17) Benavides, P. T.; Dunn, J. B.; Han, J.; Biddy, M.; Markham, J. Exploring Comparative Energy and Environmental Benefits of Virgin, Recycled, and Bio-Derived PET Bottles. *ACS Sustainable Chem. Eng.* **2018**, 6 (8), 9725–9733.
- (18) Sousa, A. F.; Patrício, R.; Terzopoulou, Z.; Bikiaris, D. N.; Stern, T.; Wenger, J.; Loos, K.; Lotti, N.; Siracusa, V.; Szymczyk, A.; Paszkiewicz, S.; Triantafyllidis, K. S.; Zamboulis, A.; Nikolic, M. S.; Spasojevic, P.; Thiagarajan, S.; van Es, D. S.; Guigo, N. Recommendations for Replacing PET on Packaging, Fiber, and Film Materials with Biobased Counterparts. *Green Chem.* **2021**. <https://doi.org/10.1039/D1GC02082J>.
- (19) Sang, T.; Wallis, C. J.; Hill, G.; Britovsek, G. J. P. Polyethylene Terephthalate Degradation under Natural and Accelerated Weathering Conditions. *Eur. Polym. J.* **2020**, 136, 109873.
- (20) Herrera, R.; Franco, L.; Rodríguez-Galán, A.; Puiggali, J. Characterization and Degradation Behavior of Poly(Butylene Adipate- Co -Terephthalate)S : Poly(Butylene Adipate- Co -Terephthalate)s. *J. Polym. Sci. A Polym. Chem.* **2002**, 40 (23), 4141–4157.

- (21) Ferreira, F. V.; Cividanes, L. S.; Gouveia, R. F.; Lona, L. M. F. An Overview on Properties and Applications of Poly(Butylene Adipate- Co -Terephthalate)-PBAT Based Composites. *Polym. Eng. Sci.* **2019**, 59 (s2), E7–E15.
- (22) Schneider, J.; Manjure, S.; Narayan, R. Reactive Modification and Compatibilization of Poly(Lactide) and Poly(Butylene Adipate-Co-Terephthalate) Blends with Epoxy Functionalized-Poly(Lactide) for Blown Film Applications. *Journal of Applied Polymer Science* **2016**, 133 (16). <https://doi.org/10.1002/app.43310>.
- (23) Jian, J.; Xiangbin, Z.; Xianbo, H. An Overview on Synthesis, Properties and Applications of Poly(Butylene-Adipate-Co-Terephthalate)–PBAT. *Advanced Industrial and Engineering Polymer Research* **2020**, 3 (1), 19–26.
- (24) Papageorgiou, G. Z.; Papageorgiou, D. G.; Terzopoulou, Z.; Bikiaris, D. N. Production of Bio-Based 2,5-Furan Dicarboxylate Polyesters: Recent Progress and Critical Aspects in Their Synthesis and Thermal Properties. *Eur. Polym. J.* **2016**, 83, 202–229.
- (25) Lead products - Avantium <https://www.avantium.com/lead-products/#pef&fdca/> (accessed Jul 7, 2021).
- (26) Rosenboom, J.-G.; Hohl, D. K.; Fleckenstein, P.; Storti, G.; Morbidelli, M. Bottle-Grade Polyethylene Furanoate from Ring-Opening Polymerisation of Cyclic Oligomers. *Nat. Commun.* **2018**, 9 (1), 2701.
- (27) Papadopoulos, L.; Zamboulis, A.; Kasmi, N.; Wahbi, M.; Nannou, C.; Lambropoulou, D. A.; Kostoglou, M.; Papageorgiou, G. Z.; Bikiaris, D. N.

- Investigation of the Catalytic Activity and Reaction Kinetic Modeling of Two Antimony Catalysts in the Synthesis of Poly(Ethylene Furanoate). *Green Chem.* **2021**, 23 (6), 2507–2524.
- (28) Sun, Z.; Fridrich, B.; de Santi, A.; Elangovan, S.; Barta, K. Bright Side of Lignin Depolymerization: Toward New Platform Chemicals. *Chem. Rev.* **2018**, 118 (2), 614–678.
- (29) Xanthopoulou, E.; Terzopoulou, Z.; Zamboulis, A.; Papadopoulos, L.; Tsongas, K.; Tzetzis, D.; Papageorgiou, G. Z.; Bikiaris, D. N. Poly(Propylene Vanillate): A Sustainable Lignin-Based Semicrystalline Engineering Polyester. *ACS Sustainable Chem. Eng.* **2021**, 9 (3), 1383–1397.
- (30) Mialon, L.; Pemba, A. G.; Miller, S. A. Biorenewable Polyethylene Terephthalate Mimics Derived from Lignin and Acetic Acid. *Green Chem.* **2010**, 12 (10), 1704–1706.
- (31) Jia, Z.; Wang, J.; Sun, L.; Zhu, J.; Liu, X. Fully Bio-Based Polyesters Derived from 2,5-Furandicarboxylic Acid (2,5-FDCA) and Dodecanedioic Acid (DDCA): From Semicrystalline Thermoplastic to Amorphous Elastomer. *J. Appl. Polym. Sci.* **2018**, 135 (14), 46076.
- (32) Upton, B. M.; Kasko, A. M. Biomass-Derived Poly(Ether-Amide)s Incorporating Hydroxycinnamates. *Biomacromolecules* **2019**, 20 (2), 758–766.



- (33) Kaneko, T.; Thi, T. H.; Shi, D. J.; Akashi, M. Environmentally Degradable, High-Performance Thermoplastics from Phenolic Phytomonomers. *Nat. Mater.* **2006**, 5 (12), 966–970.
- (34) Fonseca, A. C.; Lima, M. S.; Sousa, A. F.; Silvestre, A. J.; Coelho, J. F. J.; Serra, A. C. Cinnamic Acid Derivatives as Promising Building Blocks for Advanced Polymers: Synthesis, Properties and Applications. *Polym. Chem.* **2019**, 10 (14), 1696–1723.
- (35) Llevot, A.; Grau, E.; Carlotti, S.; Grelier, S.; Cramail, H. From Lignin-Derived Aromatic Compounds to Novel Biobased Polymers. *Macromol. Rapid Commun.* **2016**, 37 (1), 9–28.
- (36) Boerjan, W.; Ralph, J.; Baucher, M. Lignin Biosynthesis. *Annu. Rev. Plant Biol.* **2003**, 54, 519–546.
- (37) Formela, K.; Zedler, Ł.; Hejna, A.; Tercjak, A. Reactive Extrusion of Bio-Based Polymer Blends and Composites – Current Trends and Future Developments. *eXPRESS Polymer Letters* **2018**, 12 (1), 24–57.
- (38) Wang, X.-W.; Wang, G.-X.; Huang, D.; Lu, B.; Zhen, Z.-C.; Ding, Y.; Ren, Z.-L.; Wang, P.-L.; Zhang, W.; Ji, J.-H. Degradability Comparison of Poly(Butylene Adipate Terephthalate) and Its Composites Filled with Starch and Calcium Carbonate in Different Aquatic Environments: Degradability Comparison of Poly(Butylene Adipate Terephthalate) and Its Composites Filled with Starch and Calcium Carbonate in Different Aquatic Envi. *J. Appl. Polym. Sci.* **2019**, 136 (2), 46916.

- (39) Schijndel, J.; Molendijk, D.; Beurden, K.; Vermeulen, R.; Noël, T.; Meuldijk, J. Repeatable Molecularly Recyclable Semi-aromatic Polyesters Derived from Lignin. *J. Polym. Sci. A* **2020**, *58* (12), 1655–1663.
- (40) Tana, T.; Zhang, Z.; Beltramini, J.; Zhu, H.; Ostrikov, K. (ken); Bartley, J.; Doherty, W. Valorization of Native Sugarcane Bagasse Lignin to Bio-Aromatic Esters/Monomers via a One Pot Oxidation–Hydrogenation Process. *Green Chem.* **2019**, *21* (4), 861–873.
- (41) Mehta, M. J.; Kulshrestha, A.; Sharma, S.; Kumar, A. Room Temperature Depolymerization of Lignin Using a Protic and Metal Based Ionic Liquid System: An Efficient Method of Catalytic Conversion and Value Addition. *Green Chem.* **2021**, *23* (3), 1240–1247.
- (42) Trejo-Machin, A.; Verge, P.; Puchot, L.; Quintana, R. Phloretic Acid as an Alternative to the Phenolation of Aliphatic Hydroxyls for the Elaboration of Polybenzoxazine. *Green Chem.* **2017**, *19* (21), 5065–5073.
- (43) Takeshima, H.; Satoh, K.; Kamigaito, M. Bio-Based Functional Styrene Monomers Derived from Naturally Occurring Ferulic Acid for Poly(Vinylcatechol) and Poly(Vinylguaiacol) via Controlled Radical Polymerization. *Macromolecules* **2017**, *50* (11), 4206–4216.
- (44) Mialon, L.; Vanderhenst, R.; Pemba, A. G.; Miller, S. A. Polyalkylenehydroxybenzoates (PAHBs): Biorenewable Aromatic/Aliphatic Polyesters from Lignin. *Macromol. Rapid Commun.* **2011**, *32* (17), 1386–1392.

- (45) Nguyen, H. T. H.; Reis, M. H.; Qi, P.; Miller, S. A. Polyethylene Ferulate (PEF) and Congeners: Polystyrene Mimics Derived from Biorenewable Aromatics. *Green Chem.* **2015**, 17 (9), 4512–4517.
- (46) Nguyen, H. T. H.; Short, G. N.; Qi, P.; Miller, S. A. Copolymerization of Lactones and Bioaromatics via Concurrent Ring-Opening Polymerization/Polycondensation. *Green Chem.* **2017**, 19 (8), 1877–1888.
- (47) Fadlallah, S.; Roy, P. S.; Garnier, G.; Saito, K.; Allais, F. Are Lignin-Derived Monomers and Polymers Truly Sustainable? An in-Depth Green Metrics Calculations Approach. *Green Chem.* **2021**, 23 (4), 1495–1535.
- (48) Charpe, V. P.; Ragupathi, A.; Sagadevan, A.; Hwang, K. C. Photoredox Synthesis of Functionalized Quinazolines via Copper-Catalyzed Aerobic Oxidative Csp<sup>2</sup>–H Annulation of Amidines with Terminal Alkynes. *Green Chem.* **2021**, 23 (14), 5024–5030.
- (49) Van Aken, K.; Streckowski, L.; Patiny, L. EcoScale, a Semi-Quantitative Tool to Select an Organic Preparation Based on Economical and Ecological Parameters. *Beilstein J. Org. Chem.* **2006**, 2 (1), 3.
- (50) Kricheldorf, H. R.; Böhme, S.; Schwarz, G. Polycondensations of Bisphenol-A with Diphosgene or Triphosgene in Water-Free Organic Solvents. *Macromol. Chem. Phys.* **2005**, 206 (4), 432–438.
- (51) OSAMU HABA, ISAO ITAKURA, MITSURU UEDA, SHIGEKI KUZE. Synthesis of Polycarbonate from Dimethyl Carbonate and Bisphenol-A

Through a Non-Phosgene Process. *Journal of Polymer Science A: Polymer Chemistry* **1999**, 37, 2087–2093.

CHAPTER 2:  
SEMI-AROMATIC BIOBASED POLYESTERS DERIVED FROM LIGNIN AND  
CYCLIC CARBONATES<sup>1</sup>

---

<sup>1</sup>DeMichael Winfield, John Ring, Jessica Horn, Evan M. White, Jason Locklin. *RSC Green Chemistry*, **2021**, Advance Article, DOI: 10.1039/D1GC03135J

## **Abstract**

The synthesis of biobased aromatic polyesters from lignin-derived monomers has become well described in the literature, but robust mechanical and degradation studies of these materials is lacking. In this work, we have systematically investigated the mechanical and biodegradation properties of semi-aromatic polyesters that can potentially be derived from lignin. AB monomers were synthesized from reduced analogues of coumaric, ferulic, and sinapic acids along with cyclic carbonates. Polymerization yielded both semi-crystalline and amorphous polyesters with mechanical properties varying over three orders of magnitude. Detailed characterization revealed a wide array of properties including a highly ductile thermoplastic, a strong and rigid thermoplastic, and an elastomer. Composting biodegradation tests showed both degradable and nondegradable polymers can be achieved in this class. This work demonstrates the versatility of this class of polymers and illustrates their potential to replace non-sustainably derived plastics.

## Introduction

Aromatic polyesters are valuable commodity plastics due to their easy processability and robust thermal and mechanical properties.<sup>1,2</sup> Aromatic and semi-aromatic polyesters account for roughly 10% of the world's plastic economy.<sup>1</sup> However, growing environmental concerns and dwindling fossil fuel resources have led to the exploration of biobased polymers. Many biobased aliphatic polyesters such as polylactic acid (PLA), polybutylene succinate (PBS), and polyhydroxyl alkanoates (PHAs) have seen commercial success in recent years, but the demand for more mechanically robust polymers still remains.<sup>3,4</sup> Despite this, examples of biobased aromatic monomers are not as common as aliphatics. Biobased terephthalic acid can be derived from cellulosic biomass, allowing for the production of biobased polyethylene terephthalate (PET) and polybutylene adipate-co-terephthalate (PBAT), the latter of which is hydrolytically degradable and industrially compostable.<sup>5–7</sup> Polyesters based on biobased 2,5-furandicarboxylic acid with similar properties to PET have been reported, as well.<sup>8</sup> However, production of these monomers from biosources is currently expensive due to the challenging purification process.<sup>9</sup>

There are many examples of biobased monomers that have been sourced from fermentation processes, terpenes, vegetable oils, and lignocellulose.<sup>10–13</sup> In terms of bioaromatic monomers, lignin is a promising feedstock.<sup>12,14,15</sup> Lignin is a complex polyphenolic polymer that is found in most vascular plants.<sup>12,14</sup> It is the second most abundant polymer in nature and a waste product in many industries

that is burned for energy recovery.<sup>12,16</sup> In plants lignin is made from hydroxycinnamyl alcohol monomers with varying methoxy substitution, referred to as monolignols.<sup>12</sup> These monomers are polymerized by an enzymatically catalyzed radical process.<sup>12,17</sup> While there is a significant degree of variation among different varieties of lignin, it generally has high thermal stability and mechanical strength.<sup>17,18</sup>

Lignin can be incorporated into polymers by methods such as blending or chemical modification, but these strategies have significant limitations. Direct incorporation of crude lignin into composites by blending is challenging. The monolignols themselves are well defined, but the oxidative nature of the lignin biosynthesis causes it to be highly variable and heterogeneous.<sup>17,19,20</sup> This poorly defined structure along with the immiscibility of lignin with other polymers has limited its application in composites.<sup>17</sup> Chemical modification of lignin also has its challenges. The most common approach is to utilize the phenolic groups as a reactive handle.<sup>17</sup> However, the concentration of reactive phenols in lignin is quite low, as many of the phenols present undergo etherification during lignin synthesis.

Recently, several lignin depolymerization strategies seeking to take advantage of its high abundance and low cost have been reported.<sup>12</sup> Various processes can be applied to generate hydroxycinnamic acids, hydroxybenzoic acids, benzaldehydes, styrenics, and other useful platform chemicals from lignin biomass.<sup>14,15,21–24</sup> As lignin depolymerization continues to become more economically viable, understanding the properties of polymers containing these



precursors is necessary. In turn, identifying useful polymers that utilize these structures could add to the growing interest in lignin depolymerization.

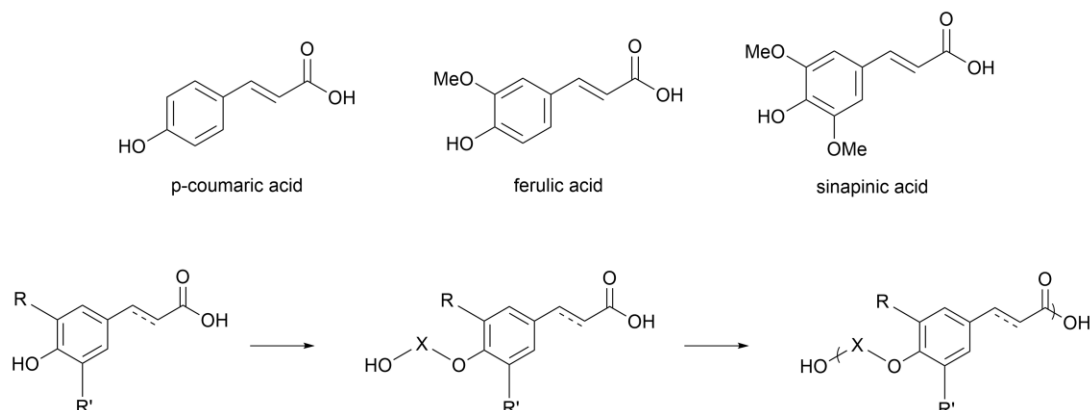


**Figure 2.1** Structures of hydroxycinnamic acids that can be obtained from lignin depolymerization and a common route to hydroxycinnamic acid-based polymers

Hydroxycinnamic acids derived from lignin have been of particular interest for synthesizing biobased polyesters containing aromatic monomers. The structures of hydroxycinnamic acids that are derived from monolignols are shown in **Figure 2.1**. Since the phenolic group is not nucleophilic enough to readily undergo polycondensation, functionalization of the phenol is required.<sup>16</sup> Mialon *et al.* reported the acidolysis of acetylated dihydroferulic acid to the corresponding phenyl ester homopolymer, which has similar properties to PET.<sup>25</sup> Sequentially, numerous examples involving alkylation of the phenoxy group of similar derivatives to generate monomers for polycondensation have been reported. Notably, installation of an alkyl hydroxyl group is an effective strategy to access AB monomers (**Figure 2.1**).<sup>26,27</sup> Various co- and homopolyesters synthesized from these monomers have been reported. These thermoplastic polyesters have a wide

array of thermal properties, and many have been shown to be hydrolytically degradable.<sup>28–30</sup> However, reporting on the mechanical properties of these thermoplastic polymers is lacking, as most mechanical data can only be found for lignin-derived thermosets.<sup>31–33</sup> There is also little in the way of conventional processing methods such as extrusion and injection molding, and degradation data on the reported polymers is largely based on hydrolysis in aqueous media.

Understanding these properties is crucial for defining the applications of biobased polymers, which motivated us to investigate them. In this work, we synthesized five semi-aromatic polyesters based on hydroxycinnamic acid derivatives using the previously mentioned AB strategy. Cyclic carbonates were selected as the alkylating agent since they can be sourced from CO<sub>2</sub> and biobased diols.<sup>34</sup> This route allows for all carbon in the polyester backbone to potentially come from biobased sources. Herein, we report the scalable batch reactor synthesis, processing by extrusion and injection molding, along with the systematic analysis of the thermal, mechanical, and composting properties of this class of polyesters.

## **Experimental**

### *Materials*

Phloretic Acid (98%), Ferulic Acid (98%), Sinapic Acid 97%, 10% Pd/C (wet), 3-chloro-1-propanol (98%) and D-Limonene (97%) were purchased from Oakwood Chemical. 4-methoxyphenol (97%), ethylene carbonate (99%), and propylene carbonate (98%) were purchased from TCI Chemical. Sodium hydroxide (97%)

was purchased from Fisher Scientific. Antimony oxide (99%) and potassium carbonate (99%) were purchased from Sigma Aldrich. All solvents were purchased from Sigma Aldrich in high purity. D-Limonene was purified by distillation. All other reagents were used as received.

*Synthesis of 3-(4-hydroxyphenyl)propanoic acid*

100 g (601 mmol) of phloretic acid were dissolved into 150 mL of methanol. A catalytic amount of sulfuric acid was added, and the reaction was heated to reflux for 6 hours. Upon cooling, the reaction was concentrated and taken up in ethyl acetate and washed with saturated sodium bicarbonate followed by brine. The organic layer was dried over magnesium sulfate and filtered. Removal of solvent yielded 108.44 g of product as a white solid in quantitative yield. <sup>1</sup>H NMR (300 MHz, cdcl<sub>3</sub>) δ 7.07 (d 2H), 6.76 (d 2H), 4.99 (s -OH) 3.67 (s 3H), 2.91 (t, 2H) 2.63 (t, 2H)

*Synthesis of 3-(4-(2-hydroxyethoxy)phenyl)propanoic acid*

60.0 g (333 mmol) of methyl 3-(4-hydroxyphenyl)propanoate, 2.30 g (16.65 mmol) of sodium bicarbonate, and 29.33 g (366 mmol) of ethylene carbonate were added into a 3-neck round bottom flask equipped with a N<sub>2</sub> inlet and gas relief valve. The flask was backfilled with N<sub>2</sub> three times and then heated to 160°C and stirred for 1 hour. The mixture was then allowed to cool below 100°C. 270 mL of 2M NaOH were added, and a reflux condenser was equipped to the round bottom flask. The heterogeneous mixture was allowed to reflux overnight. Once the mixture became homogenous, it was then cooled in an ice bath and acidified. The

resultant solid was collected by vacuum filtration and washed with excess water. 67.2 g of white solid were obtained in a 96% yield and used without further purification.  $^1\text{H}$  NMR (300 MHz, dmsO)  $\delta$  7.13 (d 2H), 6.84 (d 2H), 4.86 (t -OH), 3.95, 3.93 (t 2H), 3.71 (t 2H) 3.66, 2.77 (t 2H), 2.45 (m 2H).  $^{13}\text{C}$  NMR (75 MHz, dmsO)  $\delta$  173.79, 156.99, 132.70, 129.17, 114.28, 69.41, 59.58, 35.61, 29.51.

*Synthesis of 3-(4-(2-hydroxypropoxy)phenyl)propanoic acid*

3-(4-(2-hydroxypropoxy)phenyl)propanoic acid was synthesized in the same manner with propylene carbonate in 83% yield.  $^1\text{H}$  NMR (300 MHz,  $\text{cdCl}_3$ )  $\delta$  7.11 (d 2H), 6.86 (d 2H), 4.20 (m 1H), 3.93 (m 1H), 3.77 (m 1H), 2.91 (t 2H), 2.65 (t 2H), 1.29 (d 3H).  $^{13}\text{C}$  NMR (75 MHz,  $\text{cdCl}_3$ )  $\delta$  178.82, 157.31, 133.01, 129.51, 114.87, 73.50, 66.55, 36.03, 29.96, 18.89.

*Synthesis of 3-(4-(3-hydroxypropoxy)phenyl)propanoic acid*

83 g (500 mmol) of phloretic acid, 50 g (1.25 mol) of NaOH, and 22.5 g (150 mmol) of NaI were dissolved in 500 mL of water. After all solids were dissolved, 63 mL (750 mmol) of 3-Chloro-1-propanol were added slowly by addition funnel to avoid exotherming. After addition the solution was allowed to reflux for 12 hours. After reflux, the solution was distilled to approximately half volume, then cooled in an ice bath. The solution was acidified, and the resultant solids were collected by vacuum filtration. After washing with cold ethanol and water, 48.23 g of crude product containing monomer and dimers were obtained in 50% yield. The product was used without purification.  $^1\text{H}$  NMR (300 MHz,  $\text{cdCl}_3$ )  $\delta$  7.11 (m 2H), 6.83 (m 2H), 4.24 (t 1H), 4.11 (t 1H), 3.87 (t 1H), 2.91 (m 2H), 2.65 (m 2H), 2.04 (m 2H).

$^{13}\text{C}$  NMR (75 MHz,  $\text{cdCl}_3$ )  $\delta$  178.28, 173.20, 157.48, 132.77, 129.46, 114.76, 65.98, 64.46, 61.53, 60.73, 36.31, 35.99, 32.11, 30.29, 29.99, 28.84.

*Synthesis of 3-(4-hydroxy-3-methoxyphenyl)propanoic acid*

In a 3-neck round bottom flask, 72.3 g (372 mmol) of ferulic acid and 7.92 g (74.47 mmol) of 10% Pd/C were added. The round bottom was equipped with a  $\text{N}_2$  inlet, reflux condenser, and addition funnel, then backfilled with  $\text{N}_2$  three times. 370 mL of acetic acid was added under positive  $\text{N}_2$  pressure, and the solution was heated until ferulic acid dissolved. 90.5 mL of limonene was then added dropwise by addition funnel, followed by reflux until the reaction was complete by TLC. The mixture was cooled to room temperature and filtered through a celite. After removal of solvent, the crude solid was taken up in methyl ethyl ketone and extracted with 1 M NaOH. The aqueous layer was cooled in an ice bath and acidified. The resultant white precipitate was collected by vacuum filtration and washed with water. 59.22 g, 95% yield.  $^1\text{H}$  NMR (300 MHz,  $\text{cdCl}_3$ )  $\delta$  6.83 (d 1H), 6.72 (s 1H), 6.69 (s 1H), 3.87 (s 3H), 2.90 (t 3H), 2.65 (t 3H).

*Synthesis of 3-(4-hydroxy-3,5-dimethoxyphenyl)propanoic acid*

3-(4-hydroxy-3,5-dimethoxyphenyl)propanoic acid was synthesized in the same manner in 83% yield.  $^1\text{H}$  NMR (300 MHz,  $\text{dmso}$ )  $\delta$  8.05 (s 2H), 3.72 (s 6H), 2.72 (t 2H), 2.47 (m 2H).

*Synthesis of Methyl 3-(4-hydroxy-3-methoxyphenyl)propanoate*

Methyl 3-(4-hydroxy-3-methoxyphenyl)propanoate was synthesized by the esterification described above in quantitative yield.  $^1\text{H}$  NMR (300 MHz,  $\text{cdCl}_3$ )  $\delta$

6.82 (d 1H), 6.70 (s 1H), 6.68 (s 1H), 3.87 (s 3H), 3.67 (s 3H), 2.88 (t 2H), 2.61 (t 2H).

#### *Synthesis of Methyl 3-(4-hydroxy-3,5-dimethoxyphenyl)propanoate*

Methyl 3-(4-hydroxy-3,5-dimethoxyphenyl)propanoate was synthesized by the esterification described above in quantitative yield. <sup>1</sup>H NMR (300 MHz, cdcl<sub>3</sub>) δ 6.42 (s 2H), 3.87 (s 6H), 3.68 (s 3H), 2.91 (t 2H), 2.61 (t 2H).

#### *Synthesis of 3-(4-(2-hydroxyethoxy)-3-methoxyphenyl)propanoic acid*

3-(4-(2-hydroxyethoxy)-3-methoxyphenyl)propanoic acid was synthesized by the alkylation described above in 92% yield. <sup>1</sup>H NMR (500 MHz, cdcl<sub>3</sub>) δ 6.86 (d 2H), 6.75 (s 1H), 6.73 (s 1H), 4.11 (t 2H), 3.91 (t 2H), 3.83 (s 3H), 2.91 (t 2H), 2.67 (t 2H). <sup>13</sup>C NMR (75 MHz, cdcl<sub>3</sub>) δ 178.50, 149.98, 146.69, 134.42, 120.63, 115.42, 112.35, 71.77, 61.42, 55.98, 35.96, 30.50.

#### *Synthesis of 3-(4-(2-hydroxyethoxy)-3,5-dimethoxyphenyl)propanoic acid*

3-(4-(2-hydroxyethoxy)-3,5-dimethoxyphenyl)propanoic acid was synthesized by the alkylation described above in 94% yield. <sup>1</sup>H NMR (500 MHz, cdcl<sub>3</sub>) δ 6.44 (s 2H), 4.12 (t 2H), 3.85 (s 6H), 3.70 (t 2H), 2.93 (t 2H), 2.70 (t 2H). <sup>13</sup>C NMR (75 MHz, cdcl<sub>3</sub>) δ 178.17, 153.38, 136.67, 134.82, 105.39, 75.37, 61.53, 56.27, 35.83, 31.26.

#### *Synthesis of Polymers*

The polymerizations outlined in Scheme 2 were conducted in a 3-neck round bottom flask equipped with an overhead stirrer, short path distillation apparatus, and heating mantle with temperature probe. Typically, monomer (300

mmol),  $\text{Sb}_2\text{O}_3$  (3 mmol), and 1000 ppm of 4-methoxyphenol were added to the flask, which was then backfilled with  $\text{N}_2$  3 times. The internal temperature was raised to  $140^\circ\text{C}$  and stirred at 150 rpm. Once the monomer melted, the temperature was ramped to  $200^\circ\text{C}$  over 6 hours. Vacuum was then gradually applied over 30 minutes ( $<1$  torr), and the melt was stirred under vacuum for an additional hour at  $200^\circ\text{C}$ . The reaction was then allowed to cool to room temperature, and resultant polymer was melted from the flask and used without further purification. For polyisopropyl phloretate (PiPP), a temperature ramp of  $160$ - $220^\circ\text{C}$  was used instead.

### *Characterization*

All NMR spectra were collected on a Varian Mercury 300 MHz or 500 MHz spectrometer in appropriate deuterated solvent. Spectra are reported in the Appendix. Molecular weight was determined by gel permeation chromatography (GPC), equipped with two pumps (Shimadzu, LC-20AD) and a column oven (Shimadzu, CTO-20A) set to  $40^\circ\text{C}$ . Samples were analyzed at a concentration of  $1\text{ mg mL}^{-1}$  in  $\text{CHCl}_3$  and a flow rate of  $1\text{ mL min}^{-1}$ . Molecular weight is reported according to polystyrene standards.

Thermal properties were measured by differential scanning calorimetry (DSC) on a DSC 250 (TA Instruments). Approximately 5-10 mg of sample was heated at a rate of  $10^\circ\text{C min}^{-1}$  from  $0^\circ\text{C}$  to  $200^\circ\text{C}$ , then cold quenched to  $0^\circ\text{C}$  at a rate of  $100^\circ\text{C min}^{-1}$ , followed by an additional heating and cooling scan at  $10^\circ\text{C min}^{-1}$ . All data reported was taken from the second scans. Degradation

temperature was measured using thermogravimetric analysis (TGA) on a Discovery TGA (TA Instruments). Approximately 10-15 mg of sample was heated from ambient temperature to 700°C at 10°C min<sup>-1</sup> under N<sub>2</sub> atmosphere.

#### *Extrusion and Injection Molding*

Samples were extruded using a HAAKE Minilab 2 twin screw extruder and injection molded using a HAAKE Minijet Pro Piston Injection Molding System. Semi-crystalline polymers were extruded at the endset + 5°C of their melting temperature based on DSC. Amorphous samples were extruded at T<sub>g</sub> + 100°C based on DSC. A screw speed of 100 RPM was used for all samples. The injection molding cylinder was set to the extrusion temperature + 5°C. Samples were injected into either an ASTM Type 5 Tensile bar mold, or a DMA bar mold (60mm x 10mm x 1mm). A pressure of 480 bar with a 5 second hold was used for ASTM Type 5 Tensile bars, and 320 bar with a 5 second hold for DMA bars. For both geometries, the mold temperature for semi-crystalline samples was set to T<sub>c</sub> - 20°C based on DSC cold quench. For amorphous samples, the mold temperature was set to T<sub>g</sub> + 15°C.

In a typical procedure, approximately 3 to 3.5 g of material was fed into the extruder manually and flushed directly into a heated injection molding cylinder without any cycling time. The extrudate was then immediately injected into the mold via ram injection molding system. After the 5 second hold, the mold was immediately opened, and the specimen was removed. For amorphous samples, a



liberal amount of magnesium stearate powder was applied to the mold as a mold release agent. Semi-crystalline samples were aged for 1 week before testing.

### *Mechanical Testing*

Dynamic Mechanical Analysis (DMA) was performed on a DMA Q800 (TA Instruments). Temperature sweep experiments were performed on DMA bars using a dual cantilever clamp. Samples were subjected to 0.1% strain at a frequency of 1 Hz. The temperature was ramped at a rate of  $4^{\circ}\text{C min}^{-1}$  from -80 to  $100^{\circ}\text{C}$ . Stress relaxation experiments were done on DMA bars with tension clamps at both room temperature and  $30^{\circ}\text{C}$ . An instantaneous strain of 5% was applied and held constant while stress was monitored. Creep cycle experiments were done on DMA bars with tension clamps at room temperature. A stress of 0.200 MPa was applied for 10 minutes, followed by a relaxation period of 20 minutes. This was repeated 5 additional times to the same sample.

Tensile properties were measured using a Shimadzu AGS-X series tensile tester. Tensile properties are reported as the average from triplicate testing at room temperature at a rate of  $20\text{ mm min}^{-1}$ . For PiPP, additional rates of 50 and  $80\text{ mm min}^{-1}$  were used. Cyclic tensile testing was performed on PiPP to a set strain of 100% for 10 cycles, at a rate of either 5 or  $20\text{ mm min}^{-1}$ .

### *Industrial Composting Analysis*

Composting biodegradation test were conducted in reactors connected to a 12-channel respirometer (ECHO instruments) under aerobic conditions for 92 days. Compost inoculum was collected from the industrial composting facility at

the University of Georgia from 2 to 4 month aged compost. Each reactor was filled with approximately 300 g of compost with 50% moisture content, along with 6 grams of sample in powder form. Each sample was tested in triplicate. Other reactors containing either no sample (blank), cellulose (positive control), or polypropylene (negative control) were also monitored. The compost was maintained at 58°C and air was pumped into each channel at a flow rate of 180 ml min<sup>-1</sup>. Reactors were stirred weekly, and water was added as necessary to maintain a constant level of moisture throughout the experiment. CO<sub>2</sub> emission was measured every 2 hours by the respirometer's gas sensor. Biodegradation data was reported relative to cellulose mineralization (**Figure A29**). Further details about the calculations and the compost used can be found in the appendix.

## **Results and Discussion**

### *Monomer Synthesis*

The structures of all monomers used in this study are shown in **Figure 2.2a**. These hydroxycinnamic acid derivatives can be obtained directly from lignin depolymerization, or by Knoevenagel condensation of benzaldehydes obtained from lignin.<sup>12,14,16,21</sup> For convenience, we purchased these starting materials from commercial sources. Phloretic acid was converted to the methyl ester and alkylated with either ethylene or propylene carbonate. To install the linear propyl group for **M3**, 3-chloropropanol was used instead of trimethylene carbonate, which is synthetically more challenging and expensive. Synthesis of this carbonate is an ongoing topic of research and may become more economically feasible in the

future.<sup>36</sup> After transfer hydrogenation with limonene, ferulic and sinapic acid derived monomers were prepared in the same fashion. Polymerization and thermal properties of **M1** and **M4** have been previously reported, but the mechanical and degradation properties have not.<sup>28</sup> To the best of our knowledge the remaining three have not been previously reported.

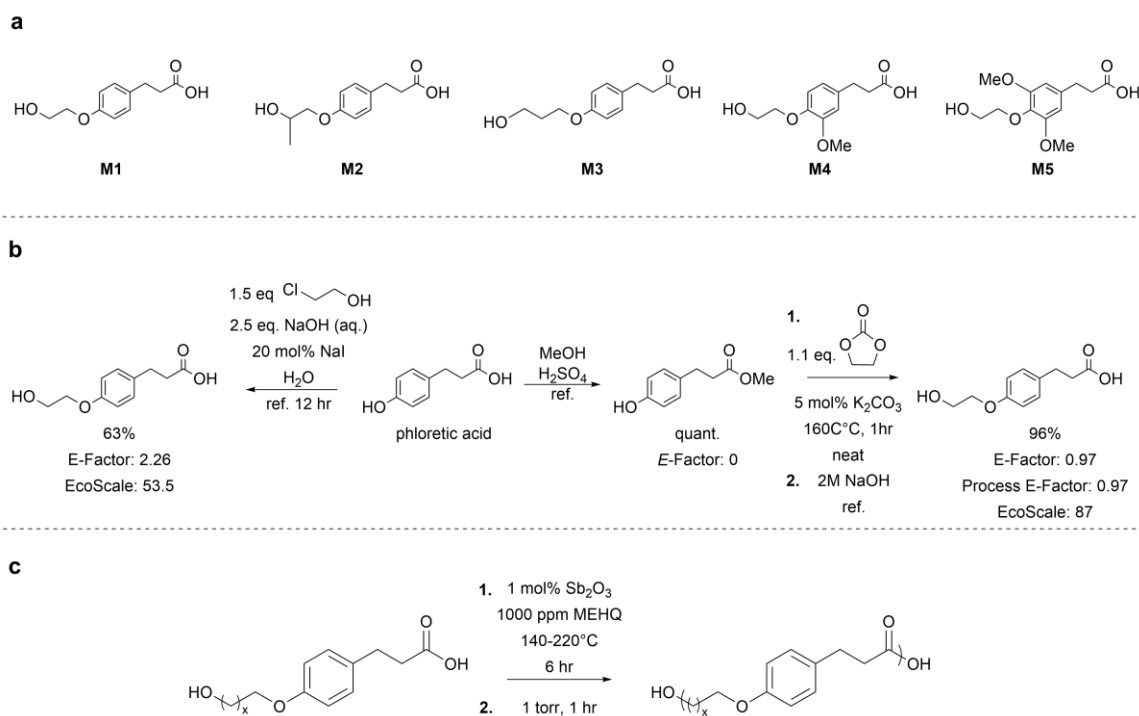


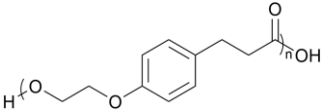
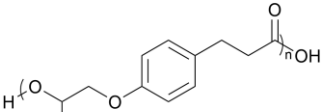
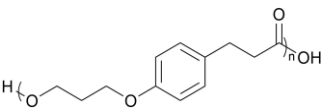
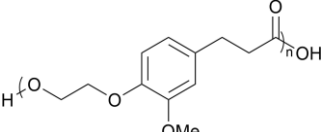
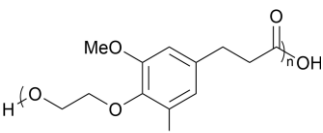
**Figure 2.2** (a) Structures of the monomers synthesized in this study (b) Synthesis, E-Factor, and EcoScale of conventional haloalcohol alkylation (left) and cyclic carbonate alkylation (right). E-Factors shown assume solvent is recovered (c) Polymerization conditions

Conventionally, haloalcohols are used for alkylating phenols.<sup>28</sup> We chose to use cyclic carbonates as alkylating agents as they provide higher yield, excellent purity, and have the potential for biobased sourcing.<sup>36–39</sup> Conversion to the methyl ester is necessary to avoid byproducts with this approach. This adds an additional step for the cyclic carbonate route that is not necessary using the conventional

haloalcohol method. Therefore, the E-Factor and Eco-Scale were calculated for the two alkylation methods to synthesize **M1**, the monomer for PEP, to assess if ethylene carbonate is truly a greener alkylating agent than 2-chloroethanol (**Figure 2.2b**). E-Factor is simply the ratio of the mass of waste generated to the mass of the product (**Equation A1**).<sup>40</sup> An E-Factor of 0 is ideal. Conventionally, if solvents can be easily recovered simple E-Factor (sEF) is used, where the solvent contribution to E-Factor is ignored. Given that methanol and water are easily recovered, sEF was used. The E-Factor for the alkylations with ethylene carbonate is 0.97 compared to 2.26 for the haloalcohol method (**Figure 2.2b**). This demonstrates that the cyclic carbonate route produces slightly less waste, though both reactions have low E-Factors. Eco-Scale is more complex as it accounts for several factors, including yield, reagent cost, safety, lab equipment, temperature, time, and workup.<sup>41,42</sup> The Eco-Scale ranges from 0-100, where a score greater than 75 is considered excellent (**Equation A2**).<sup>42</sup> The Eco-Scale for alkylation using ethylene carbonate is 87, compared to 54 for alkylation with 2-chloroethanol (**Table A4-5**). The cyclic carbonate method has a higher Eco-Scale due to the superior yield and exclusion of the highly toxic and flammable 2-chloroethanol (**Figure 2.2b**). Thus, this route was chosen as its waste is less hazardous and the alkylating agent can be sustainably sourced, despite an additional step. It is worth noting that there are depolymerization processes that can yield the reduced methyl esters directly.<sup>14</sup> This type of process would be ideal for sustainably sourcing the monomers.

## Polymer Synthesis

**Table 2.1** Summary of polymerization results

Polymer	Yield (%)	M <sub>w</sub> (g/mol)	PDI	T <sub>g</sub> (°C)	T <sub>m</sub> (°C)	T <sub>c</sub> (°C)	T <sub>d95%</sub> (°C)
 polyethylene phloretate (PEP)	85	66400	1.78	22	128	-	356
 polyisopropyl phloretate (PiPP)	93	38790	1.70	25	-	-	349
 polypropylene phloretate (PPP)	85	54244	1.94	6	112, 120	94	365
 polyethylene dihydroferulate (PEHF)	86	85500	1.93	32	-	-	365
 polyethylene dihydrosinapate (PEHS)	91	54700	1.73	35	-	-	354

All polymers were afforded in high yield and sufficient molecular weight with Sb<sub>2</sub>O<sub>3</sub> used as a catalyst (**Figure 2.2c**). Mw values as determined by GPC ranged

from 38,790 to 85,500 g mol<sup>-1</sup> (**Table 2.1**). PiPP displayed the lowest Mw due to the lower nucleophilicity of secondary alcohols and required an increased polymerization temperature range of 160°C- 220°C. The polydispersity index (PDI) of the polymers were relatively low for condensation polymerization, with a range of 1.70-1.94. This synthetic route is feasible at large scale, and highly sustainable in terms of potential biobased carbon, except for polypropylene phloretate (PPP).

Sb<sub>2</sub>O<sub>3</sub> is less active than many other polycondensation catalysts but is less prone to side reactions.<sup>28,43,44</sup> It is important to note that a gradual temperature ramp and antioxidant is needed to produce pure polymers. 4-methoxyphenol (MEHQ) was employed as an inhibitor, as oxygen radical pathways were likely the source of degradation.<sup>45</sup> Deviance from this procedure or the use of higher activity catalyst tended to yield intractable material with high discoloration. Unfortunately, this precluded the use of a less toxic, greener earth abundant metal-based catalyst such as zinc. Organocatalyst have previously been used for polycondensation, but do not tolerate the higher temperatures required to build high molecular weight.<sup>26,46,47</sup> This is an area that requires further exploration.

### *Thermal Analysis*

All thermal transitions are reported in Table 1. Both PEP and PPP are semi-crystalline polymers exhibiting melting transitions by DSC (**Figure 2.3a**). As expected, the longer alkyl chain of PPP provided a lower glass transition temperature of 6°C compared to PEP's 22°C. This is likely due to the increased degree of flexibility imparted in the polymer backbone by a longer alkyl chain. PEP

did not crystallize upon cooling from the melt at a rate of  $10^{\circ}\text{C min}^{-1}$  and showed a significant cold crystallization peak around  $88^{\circ}\text{C}$  (**Figure A26**). PPP exhibited a  $T_c$  of  $94^{\circ}\text{C}$  and a slight cold crystallization peak before melting (**Figure A27**).

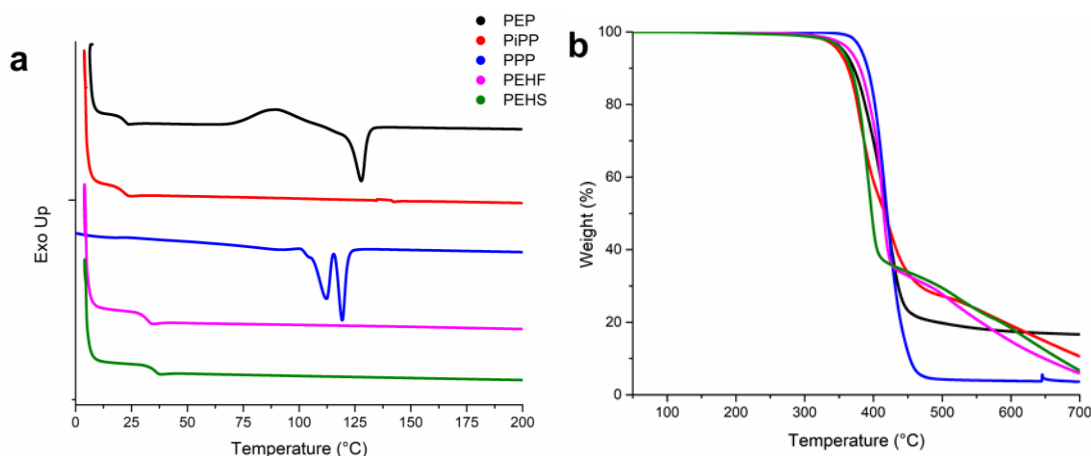


**Figure 2.3** (a) Second heating cycle from DSC after cold quenching (b) TGA curves under  $\text{N}_2$  atmosphere

The remaining three polymers were all amorphous, with glass transition temperatures ranging from  $25^{\circ}\text{C}$  to  $35^{\circ}\text{C}$ . As expected, the addition of methoxy substituents increase the glass transition temperature.<sup>19,20,28,43,48</sup> The  $T_g$  of PEHF, which contains one methoxy unit, was  $10^{\circ}\text{C}$  higher than the non-methoxy substituted PEP. However, this effect was not as pronounced with further methoxy substitution, with the additional methoxy present in polyethylene dihydrosinapate (PEHS) increasing the  $T_g$  by only  $3^{\circ}\text{C}$  above PEHF. PiPP's  $T_g$  is higher than that of its isomer PPP, likely due to steric interactions of the methylene unit restricting rotation. The lack of crystallinity in PiPP can be attributed to its chirality. Its monomer is racemic, thus the random distribution of enantiomers throughout the

polymer backbone prohibits crystal formation. All of the polymers exhibited excellent thermal stability with 5% weight loss or less up to 345°C (**Figure 2.3b**), indicating suitability for processing by extrusion and injection molding.

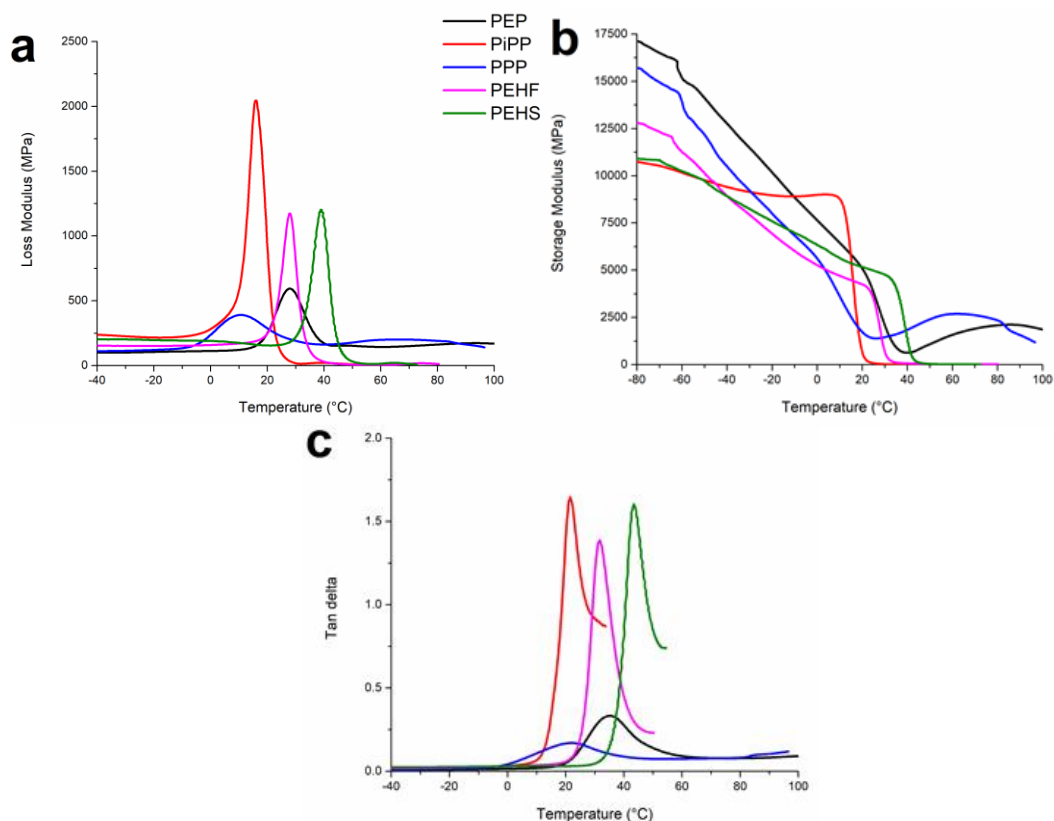


**Figure 2.6** DMA temperature sweeps of the synthesized polyesters (a) Loss modulus (b) Storage modulus (c) tan delta

Temperature sweeps were conducted by DMA to investigate the effect of temperature on the mechanical properties. The loss modulus shown in **Figure 2.4a** illustrates the presence of an  $\alpha$ -transition in each polymer that coincides with the glass transition temperatures found by DSC. PEP and PPP exhibited higher storage moduli of 17.4 and 16.0 kPa respectively at lower temperatures due to the



rigidity imparted by their crystalline domains (**Figure 2.4b**). Additionally, both polymers underwent  $T_{\alpha^*}$  transitions in which their storage moduli slightly increased between  $T_g$  and  $T_m$ . This additional  $\alpha$ -transition occurs in some semicrystalline materials and is caused by the internal friction of crystalline domains rubbing against each other as molecular mobility increases. The storage modulus of PiPP, PEHF, and PEHS dramatically decreased after their respective  $T_g$ . All polymers besides PiPP show a  $\beta$ -transition around  $-60^\circ\text{C}$  to  $-70^\circ\text{C}$ , indicating that some small-scale molecular movement is occurring. Uniquely, PiPP maintains elasticity below its  $T_g$ , shown by the plateau in the storage modulus. This phenomenon as well as the lack of  $\beta$ -transition is likely due to steric hinderance caused by the methylene unit.  $\tan \delta$  represents the dampening of a material. The temperature at which  $\tan \delta$  is at its highest value is the glass transition temperature. Thus, PiPP exhibited a lower  $T_g$  by DMA than by DSC, while PEHS showed a higher  $T_g$  by DMA (**Figure 2.4c**). This is common, as the different techniques measure the material at different frequencies and ramp rates, which will inevitably cause variation in the value as  $T_g$  is rate dependent.

### *Tensile Properties*

This class of polyesters exhibits a wide array of tensile properties. PEP showed an exceptional elongation at break of 937% along with a modest tensile strength of 21.04 MPa (**Table 2.2**). The Young's modulus is very low at 2.83 MPa. The material yields almost immediately under applied force and begins to strain harden (**Figure 2.5a**). PiPP also demonstrated strain hardening behavior along

with a low Young's modulus of 3.77 MPa. Despite its lower tensile strength of 5.40 MPa, PiPP still displayed high ductility with an elongation at break of 429%. Tensile test at higher strain rates were performed on PiPP to observe the effect of strain hardening on its tensile properties (**Figure A28**). At a rate of 50 mm min<sup>-1</sup> the modulus decreased to 2.39 MPa, and elongation at break decreased to 250% (**Table A6**). At a rate of 80 mm min<sup>-1</sup>, the Young's modulus increased to 4.76 MPa, while elongation at break was reduced to 274%. (**Table A6**). Interestingly, PiPP undergoes a more distinct yielding phenomenon at the faster rates of 50 and 80 mm min<sup>-1</sup>. There is no clear trend among the increasing rate, but the strain hardening characteristic is still present in all cases.

**Table 2.2** Summary of tensile properties

Polymer	Young's Modulus (MPa)	Tensile Strength (MPa)	Elongation at Break (%)
PEP	2.83 ± 1.87	21.04 ± 2.3	937 ± 28
PiPP	3.77 ± 1.63	5.40 ± 0.28	429 ± 57
PPP	539 ± 33	18.24 ± 0.24	4.96 ± 0.23
PEHF	2060 ± 156	58.80 ± 1.4	4.72 ± 0.65
PEHS	2345 ± 288	8.55 ± 1.3	0.51 ± 0.06

PEHF demonstrated properties similar to that of PLA, with a modulus of 2.06 GPa and tensile strength of 58.80 MPa.<sup>52</sup> PEHS had an even higher modulus but was extremely brittle with an elongation at break of 0.51% (**Table 2.2**). PEHS's low strain at break could be caused by the increased rigidity imparted by the methoxy groups. Because of this rigidity, at room temperature there is little ability for the material to flow, which inhibits plastic deformation. PPP's modulus of 539 MPa and tensile strength of 19.12 MPa are comparable to that of polybutylene

succinate. However, the high crystallinity of PPP made it significantly more brittle, with an elongation at break of 4.96%.

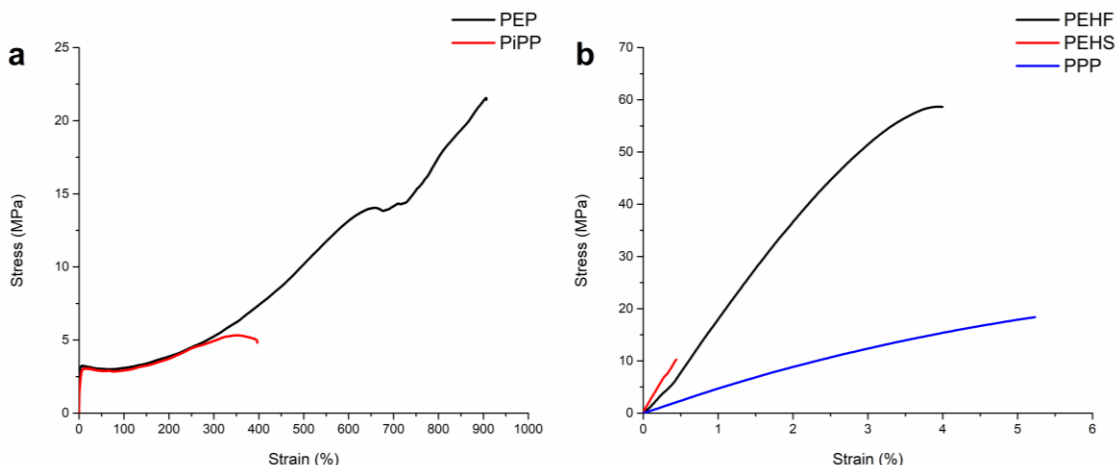


**Figure 2.9** Representative stress/strain curves from tensile testing (a) Ductile polymers (b) Brittle polymers

### *Elastomer Properties of PiPP*

PiPP exhibits characteristics of thermoplastic elastomers (TPEs), such as shape memory properties. Uniquely, PiPP is the only polymer in this study that is elastomer-like. The other polymers were all inelastic as one would expect. It has been previously demonstrated that polyesters can behave as elastomers without physical or chemical crosslinking.<sup>49–51</sup> These thermoplastic polyester elastomers (TPEEs) generally consist of a rigid, hard segment and a soft, flexible segment.<sup>52,53</sup> In the case of our AB monomer, the aromatic structure could be the hard segment, while the isopropyl group acts as a soft segment. <sup>1</sup>H NMR shows no evidence of block segments, indicating that the polymer is atactic with the enantiomers randomly distributed. Soxhlet extraction in chloroform did not yield any insoluble

fractions, suggesting that light chemical crosslinking of any kind is highly unlikely. Furthermore, the methyl unit is too short to act as a tie chain and cause physical crosslinking.<sup>54</sup> Therefore, it is unlikely that the elastomeric properties are due to any type of crosslinking phenomenon, and that PiPP is a TPEE.

The mechanical properties of PiPP were further investigated, as there are very few examples of biobased elastomers in the literature.<sup>49–52,54</sup> In stress relaxation experiments to 5% strain at ambient temperature, PiPP showed greater than 95% recovery after 2 hours (**Figure 2.6a**). At 30°C, greater than 95% recovery after 10 minutes was achieved. This correlates to the glass transition temperature of PiPP. At ambient temperatures of roughly 23°C, PiPP is just below its  $T_g$  of 25°C (**Table 2.1**), which slows the rate at which the polymer can undergo stress relief. However, the broadness of the  $T_g$ , as demonstrated by DMA, shows that there is some molecular motion that can occur below  $T_g$ , thus allowing for a slow rate of relaxation (**Figure 2.4b**). When tested in the rubbery region above its  $T_g$  at 30°C, the increased molecular motion allowed for rapid relaxation to occur. A cyclic creep test was done to further probe the elastomeric properties at ambient temperature. Under a constant force of 0.200 MPa, a significant amount of creep was observed (**Figure 2.6b**). Initially, 26% strain was reached after 10 minutes of applied force, while only 13% strain was reached in each of the 5 consecutive cycles. This suggests that some permanent deformation occurred under these conditions. However, the same conditions were not able to permanently deform the material

any further for 5 cycles. This demonstrates that PiPP has exceptional creep recovery at low stress.

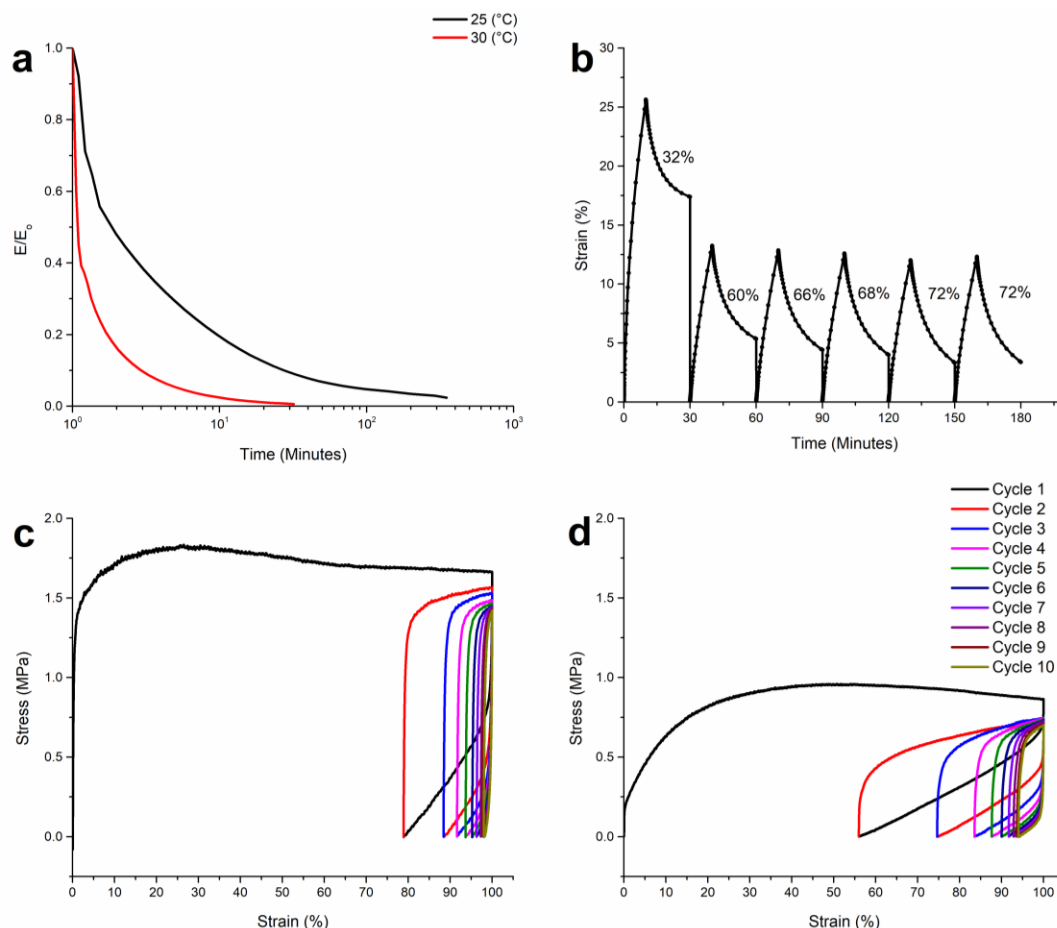


**Figure 2.12** Elastomeric properties of PiPP. (a) Stress relaxation at 5% instantaneous strain. (b) Creep cycles at a constant stress of 0.200 MPa for 10 minutes followed by a 20-minute relaxation period. Strain recovery is presented as percentage above each relaxation cycle. (c) Cyclic tensile test with a cyclic loading of 20 mm min<sup>-1</sup> for 10 cycles. (d) 10 cycles with a cyclic loading of 5 mm min<sup>-1</sup>

Shape recover ratios ( $R_r$ ) were determined by cyclic tensile test to 100% strain for 10 cycles (**Figures 2.6c-d**). The  $R_r$  data are shown in **Table 2.3**. With a

cyclic loading of 20 mm min<sup>-1</sup> the  $R_r$  of the first cycle was 21.1%. Cycles 2-10 have  $R_r$  values of 54.8 - 91% at a rate of 20 mm min<sup>-1</sup>, which is in line with other TPEEs in the literature.<sup>49–51</sup> Because of the slow shape recovery of PiPP at room temperature, a rate of 5 mm min<sup>-1</sup> was also used. At this cyclic loading rate, the  $R_r$  of the first cycle was 44.0%. Given sufficient time or temperature, the initial shape recovery may be higher. At a lower cyclic loading rate, the polymer was able to recover larger amounts strain, where the final strains at 20 and 5 mm min<sup>-1</sup> after the first cycle were 78.9 % and 56.0%, respectively.

**Table 2.3** Results from cyclic tensile testing of PiPP. Final strain is the strain at which stress is zero. Shape recovery ratio ( $R_r$ ) is the percentage of strain that was recovered in each cycle

Cycle	20 mm min <sup>-1</sup>		5 mm min <sup>-1</sup>	
	Final Strain (%)	$R_r$ (%)	Final Strain (%)	$R_r$ (%)
1	78.9	21.1	56.0	44.0
2	88.4	54.8	74.6	57.6
3	91.6	72.2	83.5	64.9
4	93.7	75.6	87.6	75.1
5	95.3	75.1	90.0	80.9
6	96.3	77.9	91.7	83.1
7	97.3	73.7	92.8	86.2
8	97.8	80.7	93.7	88.6
9	98.0	91.0	94.0	94.8
10	98.2	87.9	94.3	94.9

Under cyclic loading, an elastomer is recovered when there is no longer any stress present. A perfectly elastic material reaches zero stress when it has returned to its original shape, meaning that its strain is also zero. A material that reaches zero strain before this has been permanently deformed. So, at lower strain rates, less permanent deformation occurs to PiPP in each cycle as shape recovery

rate is dependent on strain rate and temperature. PiPP is of high significance as both a biobased and compostable elastomer. Further studies into its mechanical properties are currently underway.

#### *Respirometry*

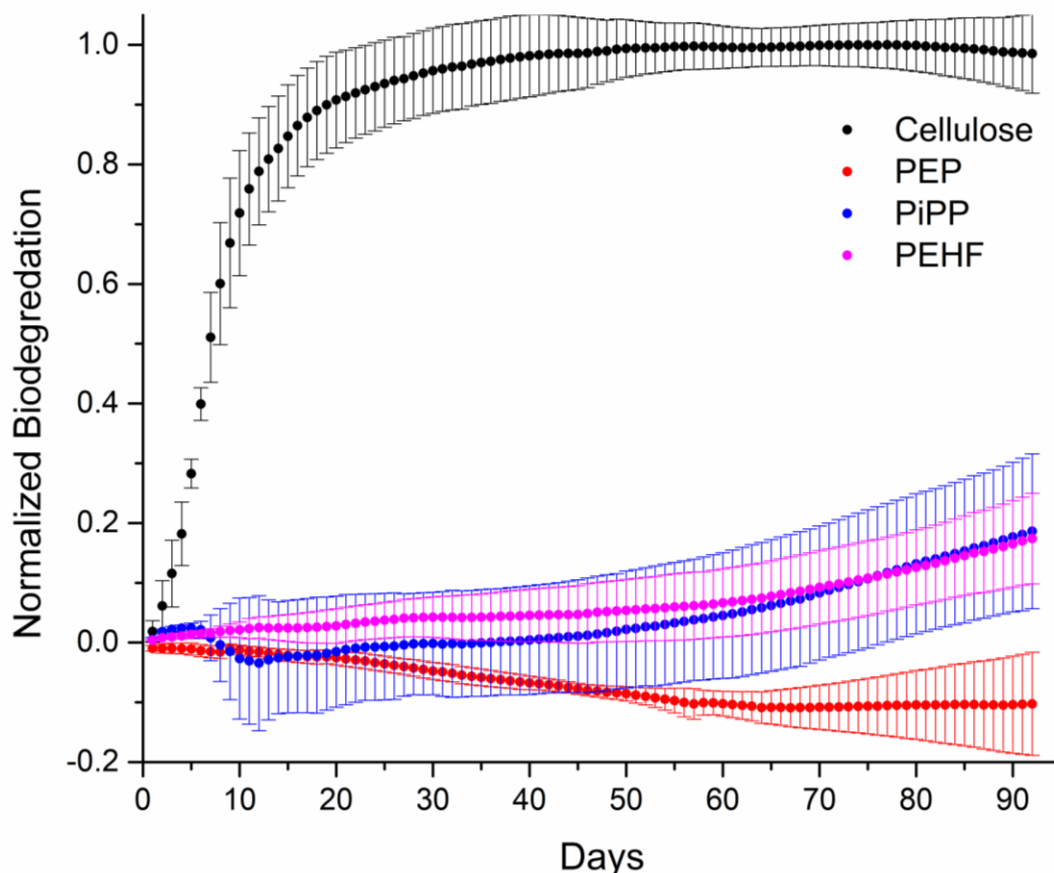


**Figure 2.15** Normalized biodegradation of PEP, PiPP, and PEHF relative to cellulose. Error bars represent one standard deviation from the mean based on triplicates

The degradation of PEP, PiPP, and PEHF was analyzed under industrial composting conditions at 58°C over 92 days by respirometry. The normalized biodegradation relative to cellulose is plotted in **Figure 2.7**. PEP showed complete stability to hydrolytic and biological degradation under these conditions. In fact, the

CO<sub>2</sub> production of compost decreased in reactors where PEP was present, which results in an overall negative normalized degradation. This could be caused by several factors ranging from the ability of the inoculum to maintain hydration to some component of the polymer having mild toxicity on the microbial community. On the other hand, PiPP and PEHF demonstrated 17.39% and 18.62% carbon mineralization relative to cellulose, respectively. This is slightly faster than polyethylene furanoate, which is one of the slower performing degraders under industrial composting conditions.<sup>57</sup> PEP's high stability is likely due to its crystalline nature along with its hydrophobicity. PEHF and PiPP are both amorphous polymers with glass transition temperatures below the temperature of the composting conditions used. Thus, the segmental motion of the polymer chains can allow for water to diffuse throughout the polymer more readily, making them susceptible to hydrolysis under these conditions. The methoxy unit present in PEHF also provides additional hydrogen bonding sites and increase the polarity of the polymer. However, based on our data it seems that crystallinity is a more significant factor as the polarity of PEP and PiPP should be very similar.

Aromatic ethers are generally not hydrolysable under these conditions. Sturgeon et al. proposed that the aromatic ethers in lignin can undergo hydrolysis through E<sub>1</sub> like mechanisms. It has been suggested that after the formation of a carbocation, subsequent rearrangement leads to an oxonium intermediate. Addition of water forms an acetal, which is hydrolytically labile.<sup>50</sup> The pendant hydroxyl and ether linkages present around lignin's aromatic ethers are not present



in the backbone of these synthetic polymers. The biological mechanisms that degrade the aromatic ether linkages in lignin are highly specific, and thus are also unlikely to be active on these derivatives.<sup>51</sup> The slow rate of degradation over 92 days suggests that there is little to no enzymatic activity occurring to the high molecular weight polymer chains. Based on this data we propose that the primary mechanism of degradation is abiotic hydrolysis of the ester bonds to low molecular weight fragments, followed metabolization of small fragments by generalist microorganisms.

## **Conclusion**

This study systematically analyzed the thermal, mechanical, and degradation characteristics of polyesters derived from reduced 4-hydroxycinamic acid and cyclic carbonates that can be potentially sourced from lignin biomass and CO<sub>2</sub>. The polymers were synthesized in a scalable fashion, easily processed by extrusion and injection molding, and characterized by thermomechanical and tensile testing. The polyesters presented could serve as sustainable replacements for a wide variety of commodity plastics. Of particular interest are the polymers PEP, PiPP, and PEHF. PEP is a highly ductile polymer that is an excellent candidate for biobased alternatives to polypropylene and polyethylene, especially in applications where high stability is needed. PiPP's TPEE properties and compostability shows promise in applications as a biodegradable elastomer. Finally, PEHF is both a high strength and compostable polymer. This work is a significant step in the characterization of these materials. Further improvement of

the sustainability of the synthesis, catalyst selection, mechanical properties, and biodegradability of these polyesters is an ongoing effort in our group.

## References

- (1) Miller, S. A. Sustainable Polymers: Opportunities for the Next Decade. *ACS Macro Lett.* **2013**, 2 (6), 550–554.
- (2) Sinha, V.; Patel, M. R.; Patel, J. V. Pet Waste Management by Chemical Recycling: A Review. *J. Polym. Environ.* **2010**, 18 (1), 8–25.
- (3) Borrelle, S. B.; Ringma, J.; Law, K. L.; Monnahan, C. C.; Lebreton, L.; McGivern, A.; Murphy, E.; Jambeck, J.; Leonard, G. H.; Hilleary, M. A.; Eriksen, M.; Possingham, H. P.; De Frond, H.; Gerber, L. R.; Polidoro, B.; Tahir, A.; Bernard, M.; Mallos, N.; Barnes, M.; Rochman, C. M. Predicted Growth in Plastic Waste Exceeds Efforts to Mitigate Plastic Pollution. *Science* **2020**, 369 (6510), 1515–1518.
- (4) Tokiwa, Y.; Calabia, B. P.; Ugwu, C. U.; Aiba, S. Biodegradability of Plastics. *Int. J. Mol. Sci.* **2009**, 10 (9), 3722–3742.
- (5) Benavides, P. T.; Dunn, J. B.; Han, J.; Biddy, M.; Markham, J. Exploring Comparative Energy and Environmental Benefits of Virgin, Recycled, and Bio-Derived PET Bottles. *ACS Sustainable Chem. Eng.* **2018**, 6 (8), 9725–9733.
- (6) Herrera, R.; Franco, L.; Rodríguez-Galán, A.; Puiggali, J. Characterization and Degradation Behavior of Poly(Butylene Adipate- Co -Terephthalate)S : Poly(Butylene Adipate- Co -Terephthalate)s. *J. Polym. Sci. A Polym. Chem.* **2002**, 40 (23), 4141–4157.

- (7) Jian, J.; Xiangbin, Z.; Xianbo, H. An Overview on Synthesis, Properties and Applications of Poly(Butylene-Adipate-Co-Terephthalate)–PBAT. *Advanced Industrial and Engineering Polymer Research* **2020**, 3 (1), 19–26.
- (8) Konstantopoulou, M.; Terzopoulou, Z.; Nerantzaki, M.; Tsagkalias, J.; Achilias, D. S.; Bikiaris, D. N.; Exarhopoulos, S.; Papageorgiou, D. G.; Papageorgiou, G. Z. Poly(Ethylene Furanoate-Co-Ethylene Terephthalate) Biobased Copolymers: Synthesis, Thermal Properties and Cocrystallization Behavior. *Eur. Polym. J.* **2017**, 89, 349–366.
- (9) Papageorgiou, G. Z.; Papageorgiou, D. G.; Terzopoulou, Z.; Bikiaris, D. N. Production of Bio-Based 2,5-Furan Dicarboxylate Polyesters: Recent Progress and Critical Aspects in Their Synthesis and Thermal Properties. *Eur. Polym. J.* **2016**, 83, 202–229.
- (10) Bozell, J. J.; Petersen, G. R. Technology Development for the Production of Biobased Products from Biorefinery Carbohydrates—the US Department of Energy’s “Top 10” Revisited. *Green Chem.* **2010**, 12 (4), 539–554.
- (11) Sonnati, M. O.; Amigoni, S.; de Givenchy, E. P. T.; Darmanin, T.; Choulet, O.; Guittard, F. Glycerol Carbonate as a Versatile Building Block for Tomorrow: Synthesis, Reactivity, Properties and Applications. *Green Chem.* **2013**, 15 (2), 283–306.
- (12) Sun, Z.; Fridrich, B.; de Santi, A.; Elangovan, S.; Barta, K. Bright Side of Lignin Depolymerization: Toward New Platform Chemicals. *Chem. Rev.* **2018**, 118 (2), 614–678.

- (13) Llevot, A.; Grau, E.; Carlotti, S.; Grelier, S.; Cramail, H. From Lignin-Derived Aromatic Compounds to Novel Biobased Polymers. *Macromol. Rapid Commun.* **2016**, *37* (1), 9–28.
- (14) Tana, T.; Zhang, Z.; Beltramini, J.; Zhu, H.; Ostrikov, K. (ken); Bartley, J.; Doherty, W. Valorization of Native Sugarcane Bagasse Lignin to Bio-Aromatic Esters/Monomers via a One Pot Oxidation–Hydrogenation Process. *Green Chem.* **2019**, *21* (4), 861–873.
- (15) Fonseca, A. C.; Lima, M. S.; Sousa, A. F.; Silvestre, A. J.; Coelho, J. F. J.; Serra, A. C. Cinnamic Acid Derivatives as Promising Building Blocks for Advanced Polymers: Synthesis, Properties and Applications. *Polym. Chem.* **2019**, *10* (14), 1696–1723.
- (16) Schijndel, J.; Molendijk, D.; Beurden, K.; Vermeulen, R.; Noël, T.; Meuldijk, J. Repeatable Molecularly Recyclable Semi-aromatic Polyesters Derived from Lignin. *J. Polym. Sci. A* **2020**, *58* (12), 1655–1663.
- (17) Lochab, B.; Shukla, S.; Varma, I. K. Naturally Occurring Phenolic Sources: Monomers and Polymers. *RSC Adv.* **2014**, *4* (42), 21712–21752.
- (18) Nguyen, H. T. H.; Suda, E. R.; Bradic, E. M.; Hvozdoch, J. A.; Miller, S. A. Polyesters from Bio-Aromatics. In *Green Polymer Chemistry: Biobased Materials and Biocatalysis*; ACS Symposium Series; American Chemical Society, 2015; Vol. 1192, pp 401–409.

- (19) Upton, B. M.; Kasko, A. M. Biodegradable Aromatic–Aliphatic Poly(Ester–Amides) from Monolignol-Based Ester Dimers. *ACS Sustainable Chem. Eng.* **2018**, 6 (3), 3659–3668.
- (20) Upton, B. M.; Kasko, A. M. Biomass-Derived Poly(Ether-Amide)s Incorporating Hydroxycinnamates. *Biomacromolecules* **2019**, 20 (2), 758–766.
- (21) Mehta, M. J.; Kulshrestha, A.; Sharma, S.; Kumar, A. Room Temperature Depolymerization of Lignin Using a Protic and Metal Based Ionic Liquid System: An Efficient Method of Catalytic Conversion and Value Addition. *Green Chem.* **2021**, 23 (3), 1240–1247.
- (22) Trejo-Machin, A.; Verge, P.; Puchot, L.; Quintana, R. Phloretic Acid as an Alternative to the Phenolation of Aliphatic Hydroxyls for the Elaboration of Polybenzoxazine. *Green Chem.* **2017**, 19 (21), 5065–5073.
- (23) Takeshima, H.; Satoh, K.; Kamigaito, M. Bio-Based Functional Styrene Monomers Derived from Naturally Occurring Ferulic Acid for Poly(Vinylcatechol) and Poly(Vinylguaiacol) via Controlled Radical Polymerization. *Macromolecules* **2017**, 50 (11), 4206–4216.
- (24) Pion, F.; Reano, A. F.; Oulame, M. Z.; Barbara, I.; Flourat, A. L.; Ducrot, P.-H.; Allais, F. Chemo-Enzymatic Synthesis, Derivatizations, and Polymerizations of Renewable Phenolic Monomers Derived from Ferulic Acid and Biobased Polyols: An Access to Sustainable Copolyesters, Poly(Ester-Urethane)s, and Poly(Ester-Alkenamer)s. In *Green Polymer Chemistry*:

*Biobased Materials and Biocatalysis*; ACS Symposium Series; American Chemical Society, 2015; Vol. 1192, pp 41–68.

- (25) Mialon, L.; Pemba, A. G.; Miller, S. A. Biorenewable Polyethylene Terephthalate Mimics Derived from Lignin and Acetic Acid. *Green Chem.* **2010**, 12 (10), 1704–1706.
- (26) Kreye, O.; Oelmann, S.; Meier, M. A. R. Renewable Aromatic-Aliphatic Copolyesters Derived from Rapeseed. *Macromol. Chem. Phys.* **2013**, 214 (13), 1452–1464.
- (27) Pang, C.; Zhang, J.; Wu, G.; Wang, Y.; Gao, H.; Ma, J. Renewable Polyesters Derived from 10-Undecenoic Acid and Vanillic Acid with Versatile Properties. *Polym. Chem.* **2014**, 5 (8), 2843–2853.
- (28) Nguyen, H. T. H.; Reis, M. H.; Qi, P.; Miller, S. A. Polyethylene Ferulate (PEF) and Congeners: Polystyrene Mimics Derived from Biorenewable Aromatics. *Green Chem.* **2015**, 17 (9), 4512–4517.
- (29) Ouimet, M. A.; Faig, J. J.; Yu, W.; Uhrich, K. E. Ferulic Acid-Based Polymers with Glycol Functionality as a Versatile Platform for Topical Applications. *Biomacromolecules* **2015**, 16 (9), 2911–2919.
- (30) Nguyen, H. T. H.; Short, G. N.; Qi, P.; Miller, S. A. Copolymerization of Lactones and Bioaromatics via Concurrent Ring-Opening Polymerization/Polycondensation. *Green Chem.* **2017**, 19 (8), 1877–1888.

- (31) Tran, H. T.; Matsusaki, M.; Akashi, M. Development of Photoreactive Degradable Branched Polyesters with High Thermal and Mechanical Properties. *Biomacromolecules* **2009**, *10* (4), 766–772.
- (32) Dong, W.; Ren, J.; Lin, L.; Shi, D.; Ni, Z.; Chen, M. Novel Photocrosslinkable and Biodegradable Polyester from Bio-Renewable Resource. *Polym. Degrad. Stab.* **2012**, *97* (4), 578–583.
- (33) Ye, J.; Ma, S.; Wang, B.; Chen, Q.; Huang, K.; Xu, X.; Li, Q.; Wang, S.; Lu, N.; Zhu, J. High-Performance Bio-Based Epoxies from Ferulic Acid and Furfuryl Alcohol: Synthesis and Properties. *Green Chem.* **2021**. <https://doi.org/10.1039/D0GC03946B>.
- (34) Carré, C.; Ecochard, Y.; Caillol, S.; Avérous, L. From the Synthesis of Biobased Cyclic Carbonate to Polyhydroxyurethanes: A Promising Route towards Renewable Non-Isocyanate Polyurethanes. *ChemSusChem* **2019**, *12* (15), 3410–3430.
- (35) Clements, J. H. Reactive Applications of Cyclic Alkylene Carbonates. *Ind. Eng. Chem. Res.* **2003**, *42* (4), 663–674.
- (36) de la Cruz-Martínez, F.; Martínez de Sarasa Buchaca, M.; Martínez, J.; Fernández-Baeza, J.; Sánchez-Barba, L. F.; Rodríguez-Diéguez, A.; Castro-Osma, J. A.; Lara-Sánchez, A. Synthesis of Bio-Derived Cyclic Carbonates from Renewable Resources. *ACS Sustainable Chem. Eng.* **2019**, *7* (24), 20126–20138.



- (37) Zhou, H.; Zhang, H.; Mu, S.; Zhang, W.-Z.; Ren, W.-M.; Lu, X.-B. Highly Regio- and Stereoselective Synthesis of Cyclic Carbonates from Biomass-Derived Polyols via Organocatalytic Cascade Reaction. *Green Chem.* **2019**, *21* (23), 6335–6341.
- (38) Zhang, F.; Bulut, S.; Shen, X.; Dong, M.; Wang, Y.; Cheng, X.; Liu, H.; Han, B. Halogen-Free Fixation of Carbon Dioxide into Cyclic Carbonates via Bifunctional Organocatalysts. *Green Chem.* **2021**, *23* (3), 1147–1153.
- (39) Fadlallah, S.; Roy, P. S.; Garnier, G.; Saito, K.; Allais, F. Are Lignin-Derived Monomers and Polymers Truly Sustainable? An in-Depth Green Metrics Calculations Approach. *Green Chem.* **2021**. <https://doi.org/10.1039/D0GC03982A>.
- (40) Charpe, V. P.; Ragupathi, A.; Sagadevan, A.; Hwang, K. C. Photoredox Synthesis of Functionalized Quinazolines via Copper-Catalyzed Aerobic Oxidative Csp<sup>2</sup>–H Annulation of Amidines with Terminal Alkynes. *Green Chem.* **2021**, *23* (14), 5024–5030.
- (41) Van Aken, K.; Strekowski, L.; Patiny, L. EcoScale, a Semi-Quantitative Tool to Select an Organic Preparation Based on Economical and Ecological Parameters. *Beilstein J. Org. Chem.* **2006**, *2* (1), 3.
- (42) Bloom, M. E.; Vicentin, J.; Honeycutt, D. S.; Marsico, J. M.; Geraci, T. S.; Miri, M. J. Highly Renewable, Thermoplastic Tetrapolyesters Based on Hydroquinone, p -Hydroxybenzoic Acid or Its Derivatives, Phloretic Acid, and

- Dodecanedioic Acid. *Journal of Polymer Science Part A: Polymer Chemistry* **2018**, 56 (14), 1498–1507.
- (43) Jacquel, N.; Freyermouth, F.; Fenouillot, F.; Rousseau, A.; Pascault, J. P.; Fuertes, P.; Saint-Loup, R. Synthesis and Properties of Poly(Butylene Succinate): Efficiency of Different Transesterification Catalysts. *J. Polym. Sci. A Polym. Chem.* **2011**, 49 (24), 5301–5312.
- (44) Scheirs, J. *Modern Polyesters: Chemistry and Technology of Polyesters and Copolyesters (Wiley Series in Polymer Science)*; Wiley, 2003.
- (45) Flores, I.; Demarteau, J.; Müller, A. J.; Etxeberria, A.; Irusta, L.; Bergman, F.; Koning, C.; Sardon, H. Screening of Different Organocatalysts for the Sustainable Synthesis of PET. *Eur. Polym. J.* **2018**, 104, 170–176.
- (46) Basterretxea, A.; Jehanno, C.; Mecerreyes, D.; Sardon, H. Dual Organocatalysts Based on Ionic Mixtures of Acids and Bases: A Step Toward High Temperature Polymerizations. *ACS Macro Lett.* **2019**, 8 (8), 1055–1062.
- (47) Mialon, L.; Vanderhenst, R.; Pemba, A. G.; Miller, S. A. Polyalkylenehydroxybenzoates (PAHBs): Biorenewable Aromatic/Aliphatic Polyesters from Lignin. *Macromol. Rapid Commun.* **2011**, 32 (17), 1386–1392.
- (48) Holt, A.; Ke, Y.; Bramhall, J. A.; Crane, G.; Grubbs, J. B., III; White, E. M.; Horn, J.; Locklin, J. Blends of Poly(Butylene Glutarate) and Poly(Lactic Acid) with Enhanced Ductility and Composting Performance. *ACS Appl. Polym. Mater.* **2021**, 3 (3), 1652–1663.

- (49) Liu, F.; Zhang, J.; Wang, J.; Na, H.; Zhu, J. Incorporation of 1,4-Cyclohexanedicarboxylic Acid into Poly(Butylene Terephthalate)-b-Poly(Tetramethylene Glycol) to Alter Thermal Properties without Compromising Tensile and Elastic Properties. *RSC Adv.* **2015**, 5 (114), 94091–94098.
- (50) Liu, F.; Qiu, J.; Wang, J.; Zhang, J.; Na, H.; Zhu, J. Role of Cis-1,4-Cyclohexanedicarboxylic Acid in the Regulation of the Structure and Properties of a Poly(Butylene Adipate-Co-Butylene 1,4-Cyclohexanedicarboxylate) Copolymer. *RSC Adv.* **2016**, 6 (70), 65889–65897.
- (51) Jia, Z.; Wang, J.; Sun, L.; Zhu, J.; Liu, X. Fully Bio-Based Polyesters Derived from 2,5-Furandicarboxylic Acid (2,5-FDCA) and Dodecanedioic Acid (DDCA): From Semicrystalline Thermoplastic to Amorphous Elastomer. *J. Appl. Polym. Sci.* **2018**, 135 (14), 46076.
- (52) Watts, A.; Kurokawa, N.; Hillmyer, M. A. Strong, Resilient, and Sustainable Aliphatic Polyester Thermoplastic Elastomers. *Biomacromolecules* **2017**, 18 (6), 1845–1854.
- (53) Biemond, G. J. E.; Gaymans, R. J. Elastic Properties of Thermoplastic Elastomers Based on Poly(Tetramethylene Oxide) and Monodisperse Amide Segments. *J. Mater. Sci.* **2010**, 45 (1), 158–167.
- (54) Nurhamiyah, Y.; Amir, A.; Finnegan, M.; Themistou, E.; Edirisinghe, M.; Chen, B. Wholly Biobased, Highly Stretchable, Hydrophobic, and Self-Healing

Thermoplastic Elastomer. *ACS Appl. Mater. Interfaces* **2021**, 13 (5), 6720–6730.

- (55) Lead products - Avantium <https://www.avantium.com/lead-products/#pef&fdca/> (accessed Jul 7, 2021).
- (56) Sturgeon, M. R.; Kim, S.; Lawrence, K.; Paton, R. S.; Chmely, S. C.; Nimlos, M.; Foust, T. D.; Beckham, G. T. A Mechanistic Investigation of Acid-Catalyzed Cleavage of Aryl-Ether Linkages: Implications for Lignin Depolymerization in Acidic Environments. *ACS Sustainable Chem. Eng.* **2014**, 2 (3), 472–485.
- (57) Buswell, J. A.; Odier, E.; Kirk, T. K. Lignin Biodegradation. *Crit. Rev. Biotechnol.* **1987**, 6 (1), 1–60.

CHAPTER 3:  
PROPERTIES OF BRANCHED THERMOPLASTIC POLYESTER ELASTOMER  
POLY(ISOPROPYL PHLORETATE) BY EPOXY CHAIN EXTENDER<sup>2</sup>

---

<sup>2</sup>DeMichael Winfield, Jason Locklin, To be submitted to Journal of Applied Polymer Science.

## **Abstract**

Thermoplastic polyester elastomers (TPEEs) are a unique class of non-crosslinked polymers that have elastomer-like properties seen in crosslinked materials. Previously, we have reported the synthesis and properties of poly(isopropyl phloretate) (PiPP), a ductile homopolymer TPEE with shape memory. To improve its mechanical properties, we used reactive extrusion with epoxy modifier Joncryl 4368 to create branched PiPP. Gel permeation chromatography (GPC), tensile testing, differential scanning calorimetry (DSC), and rheology were used to characterize the epoxy modified PiPP.  $M_w$  values of up to 171,287 and branching of up to 4.6 were achieved without the formation of crosslinking or gel fractions. The elastic modulus was increased by up to 3 orders with increased Joncryl loading, while ductility decreased. The modulus increased in a linear fashion, allowing for the tensile properties of PiPP to be easily tuned. Additionally, the rheological properties were enhanced, showing improved storage modulus, loss modulus, viscosity, and shear modulus. Shape memory was retained at all Joncryl loadings. This work demonstrates PiPPs potential for both soft and hard rubber applications.

## Introduction

Thermoplastic elastomers (TPEs) are viscoelastic materials that share properties of conventional elastomers and thermoplastics.<sup>1</sup> Conventional elastomers have robust mechanical and thermal properties due to their crosslinking by irreversible covalent bonds.<sup>1</sup> Consequently, this also renders them nondegradable and extremely difficult to recycle.<sup>1,2</sup> As thermosets, these materials are also unable to be reprocessed.<sup>1,3</sup> TPEs on the other hand, can be processed as thermoplastics by conventional melt processing methods, allowing for recycling.<sup>1</sup> TPEs can also potentially be made up of biodegradable structures.

TPEs achieve rubbery-like elastomeric properties through their unique architecture. Typically, these materials are biphasic in nature, having a hard, rigid segment and a soft, flexible segment.<sup>1</sup> Under applied force, the hard segment will mostly remain in place while the soft segment can flow to dissipate energy.<sup>1–3</sup> When the force is released, the hard segments act as ‘knots’ pulling the soft segments back into place.<sup>6</sup> The hard segments can be made by a variety of interactions, both chemical and physical. Hydrogen bonding networks can provide hard segments and are commonly employed as such in thermoplastic urethanes (TPU).<sup>7,8</sup> Physical crosslinks can come from block copolymers or side groups acting as tie chains.<sup>7</sup>

A particularly interesting subclass of TPEs are thermoplastic polyester elastomers (TPEEs). These polymers are unique in that they do not have any crosslinking but behave like elastomers.<sup>4,6–8</sup> These materials’ properties still arise

from hard and soft segments along the polymer backbone. When force is applied to a TPEE, segmental motion occurs at the soft segments, while motion in the hard segments remains minimal up to a certain point.<sup>4,6,8</sup> In 1972, DuPont's Hytrel became the first commercialized TPEE.<sup>6</sup> Despite being known for 5 decades, TPEEs are exceptionally rare.<sup>1,4,6–8</sup>

Previously, we reported the synthesis of poly(isopropyl phloretate) (PiPP), which has TPEE properties (**Figure 3.1**). PiPP exhibits remarkable shape memory properties while also being both biobased and industrially compostable. Because there are few examples of biobased and biodegradable elastomers, as well as very few examples of TPEEs, we decided to further explore PiPP's properties. PiPP is a ductile polymer with an elongation at break of 429% and a low elastic modulus of 3.77 MPa. Low elastic moduli are common in TPEs, which largely limits their applications to soft rubbers or foams.<sup>1</sup>

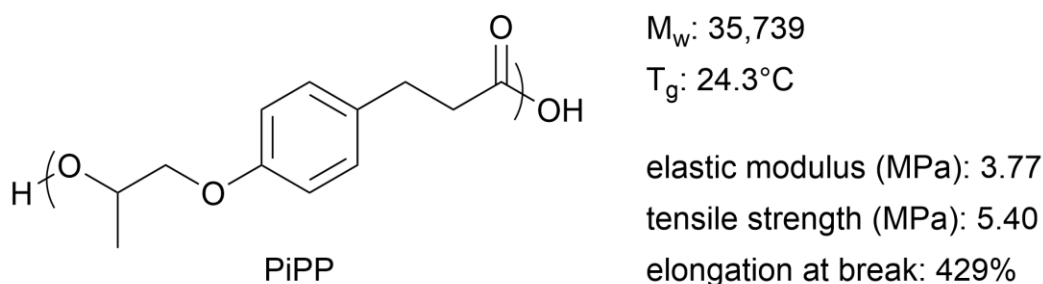


**Figure 3.1** Summary of PiPP properties

One method for modulating the properties of a polymer is reactive extrusion (REX). Chain extenders employed in reactive extrusion allows for the reactive end groups of polyesters to further react.<sup>10</sup> These chain extenders can be utilized to



both increase the molecular weight and impart specific molecular architectures.<sup>10–12</sup> Due to the high shear, pressure, and temperature of extrusion, short residence times are needed to prevent degradation. This necessitates the need for click or click-like chemistry in REX.<sup>13,14</sup> Some commonly used chemistry in REX includes isocyanates, peroxides, and epoxides.<sup>15–17</sup>

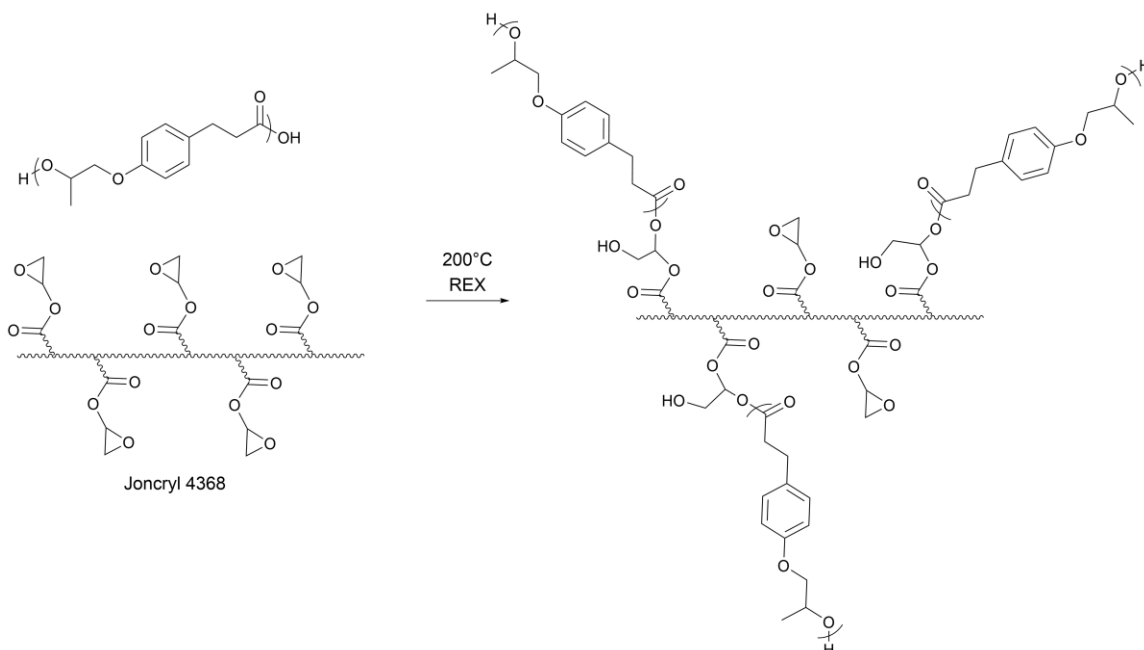


**Figure 3.2** Branched PiPP structures obtained by REX using Joncryl 4368. Joncryl 4368 is a multifunctional chain extender that has a linear backbone with epoxide side chains

In this work, Joncryl 4368, a multifunctional epoxide, was utilized to create branched PiPP structures (**Figure 3.2**). It has been demonstrated that branching can improve a material's elastic modulus.<sup>18,19</sup> Without catalyst, epoxides react selectively with carboxylic acid end groups below 220°C.<sup>18</sup> This allows for exclusive formation of ester bonds, which are generally hydrolytically labile under industrial composting conditions.<sup>20–22</sup> This may prove advantageous in maintaining

the compostability of PiPP. A series of Joncryl modified PiPP (JPiPP) was prepared with 0.1 to 15 weight percent Joncryl. This epoxy modified TPEE demonstrated improved molecular weight and elastic modulus. Additionally, the nonlinear branched structures also enhanced the rheological properties of PiPP.

## Experimental

### Materials

Phloretic Acid (98%) was purchased from Oakwood Chemical. 4-methoxyphenol (97%) and propylene carbonate (98%) were purchased from TCI Chemical. Sodium hydroxide (97%) was purchased from Fisher Scientific. Antimony oxide (99%), Joncryl 4368, and potassium carbonate (99%) were purchased from Sigma Aldrich.

### Synthesis of PiPP

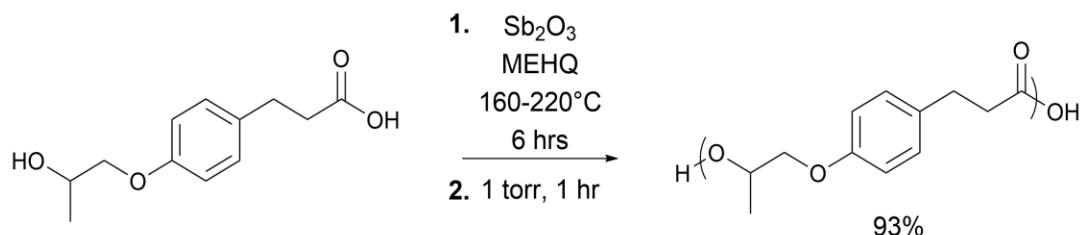


**Figure 3.3** Synthesis of PiPP by polycondensation

PiPP and its monomer were synthesized via our previous procedure (**Figure 3.3**). Briefly, 285 g of monomer, 3.71 g of  $\text{Sb}_2\text{O}_3$ , and 285 mg of MEHQ were added in a 500 mL glass reactor fitted with an overhead stirrer, short path distillation, and temperature probe. After backfilling with  $\text{N}_2$  3 times, the internal

temperature was raised to 160°C and the melt was stirred at 150 rpm. The temperature was ramped to 220°C over 6 hours. Vacuum was then gradually applied over 30 minutes until a pressure of less than 1 torr was achieved, and the melt was stirred for an additional hour. The reaction was cooled to room temperature, and crude PiPP was melted from the flask resulting in 93% crude yield. The polymer was used without further purification.

### *Characterization*

Molecular weight was determined by gel permeation chromatography (GPC), equipped with two pumps (Shimadzu, LC-20AD) and a column oven (Shimadzu, CTO-20A) set to 40°C. Samples were analyzed at a concentration of 1 mg mL<sup>-1</sup> in CHCl<sub>3</sub> and a flow rate of 1 mL min<sup>-1</sup>. Molecular weight is reported according to polystyrene standards.

Thermal properties were measured by differential scanning calorimetry (DSC) on a DSC 250 (TA Instruments). Approximately 5-10 mg of sample was heated at a rate of 10 °C min<sup>-1</sup> from 0°C to 200°C for two cycles. All data reported was taken from the second scans.

### *Compounding and Extrusion*

PiPP and Joncryl 4368 were dry blended in selected ratios. Samples were extruded using a HAAKE Minilab 2 twin screw extruder and injection molded using a HAAKE Minijet Pro Piston Injection Molding System. REX was done at 200°C at 100 RPM under N<sub>2</sub>. A residence time of 3 minutes was used, followed by cooling to 120°C. After the temperature reached 120°C (approximately 5 minutes), the

material was extruded into the injection molding barrel, set at 120°C, then injection molded into an ASTM Type 5 dog bone mold at 500 bar. The mold was set to 40°C. In all cases, magnesium stearate powder was applied to the mold as a mold release agent.

Residual material from the extrusion process was collected from the back channel. This material (roughly 2.5 g) was pressed into thin films using a Carver Press. A temperature of 120°C with minimal pressure was used for a few seconds, resulting in films of 250-300 microns. Tensile bars were cut from the films using a micro tensile punch.

#### *Mechanical Testing*

Tensile properties were measured using a Shimadzu AGS-X series tensile tester. In standard tests, samples were tested at ambient conditions (23.2°C) at a rate of 20 mm min<sup>-1</sup> to failure. In cyclic tests, micro tensile bars were tested at a rate of 20% min<sup>-1</sup> to 150% for 10 cycles.

#### *Rheology*

Rheological experiments were conducted on a TA Discover Rheometer. A circular geometry with a diameter of 40 mm was used. All experiments were conducted at 120°C. Amplitude sweeps at an angular frequency of 10 rad/s were used to determine the linear viscoelastic range. All oscillatory tests were conducted at 1% strain, and all flow tests were conducted with a logarithmically sweeping shear rate.

## Results and Discussion

### *Molecular Weight*

**Table 3.1** Results of REX. Molecular weights of epoxy modified PiPP determined by GPC. Degrees of branching (DB) determined by equation 1.  $T_g$  was determined by DSC.

Sample	$M_w$ (g/mol)	$M_n$ (g/mol)	PDI	DB	$T_g$ (°C)
PiPP	35,739	18,624	1.92	-	24.3
JPiPP.1	31,781	17,644	1.80	-	24.8
JPiPP.5	43,214	19,704	2.19	1	24.7
JPiPP1	54,175	23,992	2.26	1.3	24.9
JPiPP5	130,332	41,333	3.15	3.6	25.6
JPiPP10	156,908	60,590	2.59	4.2	27.4
JPiPP15	171,287	92,641	1.85	4.6	27.6

A high temperature of 200°C was used to facilitate the reaction of the carboxylic acid groups with the epoxides. However, at this temperature the viscosity of PiPP was too low for injection molding. The temperature was lowered to PiPP's typical processing temperature of 120°C so that the material could be handled.

The molecular weights obtained from REX with Joncryl 4368 are shown in **Table 3.1**. All epoxy modified samples were obtained without any discernable gel formation. Upon low loadings of 0.1 and 0.5 weight percent, little change in  $M_w$  was seen. In fact, JPiPP.1 underwent a small degree of degradation at with  $M_w$  decreasing from 35,739 g mol<sup>-1</sup> to 31,781 g mol<sup>-1</sup>. At 0.5 weight percent a small increase to 43,214 g mol<sup>-1</sup> was achieved. At 1 weight percent, a modest increase to 54,175 g mol<sup>-1</sup> was observed, however significant increases were achieved at 5

to 15 weight percent.  $M_w$  was increased to 130,332 to 171,287 g mol<sup>-1</sup> in these cases, providing high molecular weight PiPP. These high loadings were needed due to the low molecular weight of the synthesized PiPP. Typical loadings of Joncryn 4368 usually range from 0.1 to 5 weight percent. However, the low molecular weight of PiPP leads to a high concentration of carboxylic acid end groups being present. Thus, high loadings are needed for a sufficient number of epoxide groups to be present. A substantial excess of epoxide groups must be present, as all epoxides cannot react. Experimental data has suggested that a maximum of 5 of the 9-10 epoxides present on each Joncryn molecule can react.<sup>18</sup>

The degree of branching, based on the average number of PiPP chains per Joncryn, can be determined by **equation 3.1**:

$$M_w \text{PiPP} = DB * M_{wo} \text{PiPP} - M_w \text{Joncryn} \quad (\text{equation 3.1})$$

Where  $M_w$  PiPP is the molecular weight after REX, DB is the degrees of branching,  $M_{wo}$  PiPP is the molecular weight of PiPP before REX, and  $M_w$  Joncryn is the molecular weight of Joncryn 4368. With the Joncryn loading presented in this study, a degree of branching of 1-4.6 was achieved (**Table 3.1**). At 15 weight percent, the  $M_w$  is close to the supposed maximum of 5 chains. While 0.5 and 1 weight percent exhibit the  $M_w$  that corresponds to an average of 1 and 1.3 PiPP chains, the GPC curves illustrate that this is not the case (**Figure 3.4**). At these two loadings, the distribution from  $10^3$  to  $10^5$  log( $M_w$ ) is very similar to that of the unmodified PiPP. However, high molecular weight fractions were formed. This suggests that the

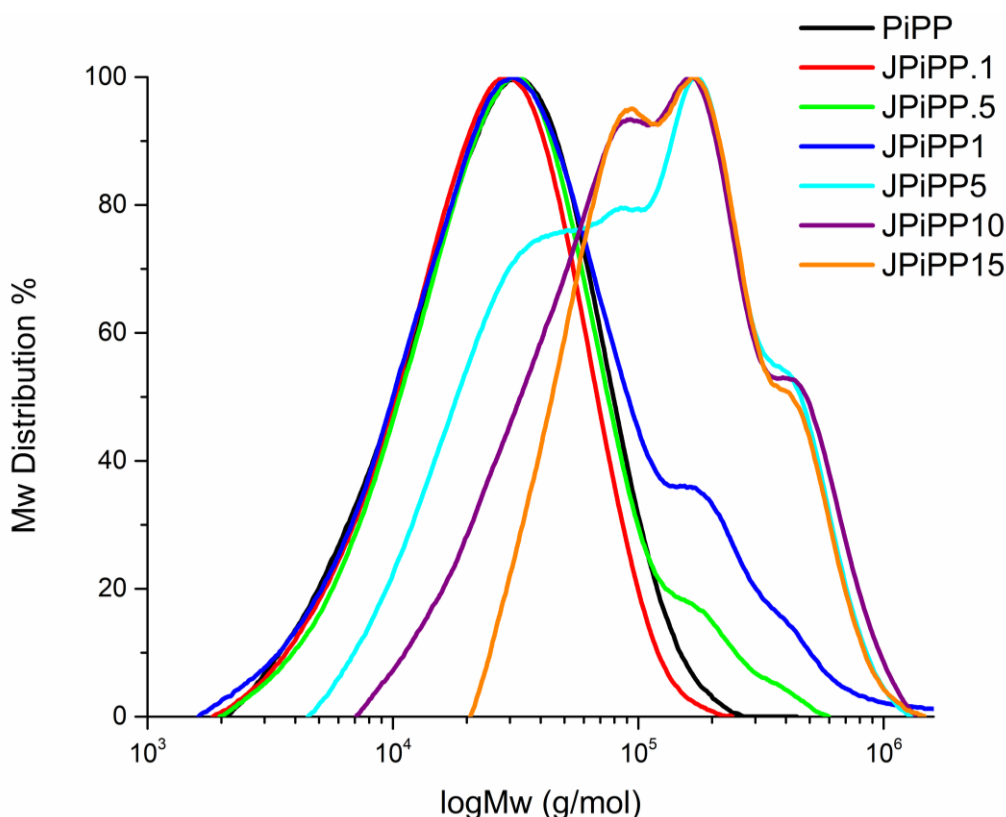


**Figure 3.6** GPC traces of PiPP and epoxy modified polymers

PiPP chains are not evenly distributed among the epoxy modifier, but rather that there are many Joncryl chains with a high number of reacted PiPP chains and several PiPP chains that underwent no reaction. This is also demonstrated by the higher PDI and  $M_n$  values that have only marginally increased. JPiPP5 still shows a significant high molecular weight fraction, but the increased  $M_n$  of 41,333 indicates better distribution of epoxy modifier. At 5 weight percent and higher, it is likely that a majority of PiPP molecules have reacted with an epoxide. The distribution continues to become more even as the concentration of Joncryl is increased to 10 and 15 weight percent. At the highest loading, JPiPP15 had a low

PDI of 1.85 and an  $M_n$  of 92,641 indicates excellent distribution. Thus, at higher loadings the average number of chains per Joncryl reported in **Table 3.1** are reflective of the actual structures of the Joncryl modified PiPP.

#### *Thermal Properties*

A small increase in  $T_g$  was seen with increasing epoxy content (**Table 3.1**). As the degree of branching increases, it becomes more difficult for segmental motion to occur along the PiPP chains. However, this effect is minimal as the glass transition temperature increases from 24.3°C to 27.6°C with the highest loading of epoxy content. With increasing molecular weight, PiPP still remained amorphous. This is due to the atactic nature of the polymer that is imparted by the racemic methylene group.

#### *Tensile Properties*

A clear trend in the tensile properties is seen with increasing Joncryl loading (**Figure 3.5a**). As epoxy modifier is increased, PiPP becomes substantially stronger and loses ductility. The elastic modulus increased by up to 3 orders of magnitude, from 3.77 MPa to 1.267 GPa for PiPP and JPiPP15 (**Figure 3.5a,c**). This was accompanied by a significant decrease in elongation at break, from 429% to 52% (**Figure 3.5a,d**). The ultimate tensile strength is shown in **Figure 3.5c**, which increased up to 27.73 MPa. These changes are well fitted by linear



regression. For the elastic modulus, an  $R^2$  value of 0.95 was obtained for the fitting (**Figure 3.6a**). The elongation at break was comparable with an  $R^2$  value of 0.93, while tensile strength was more moderately correlated with an  $R^2$  of 0.72 (**Figure 3.6b,c**). With these fittings, an elastomer with a specific elastic modulus or elongation at break could be targeted by varying Joncryl loading. The change in tensile properties can be explained by the branched structure of the modified PiPP. Joncryl 4368 itself has a branched structure, with the main chain having side chains with epoxide groups. Therefore, when the acid end groups of PiPP react with Joncryl, a highly branched structure is formed as opposed to a linear structure. When tensile stress is applied to unmodified PiPP, the chain entanglements can

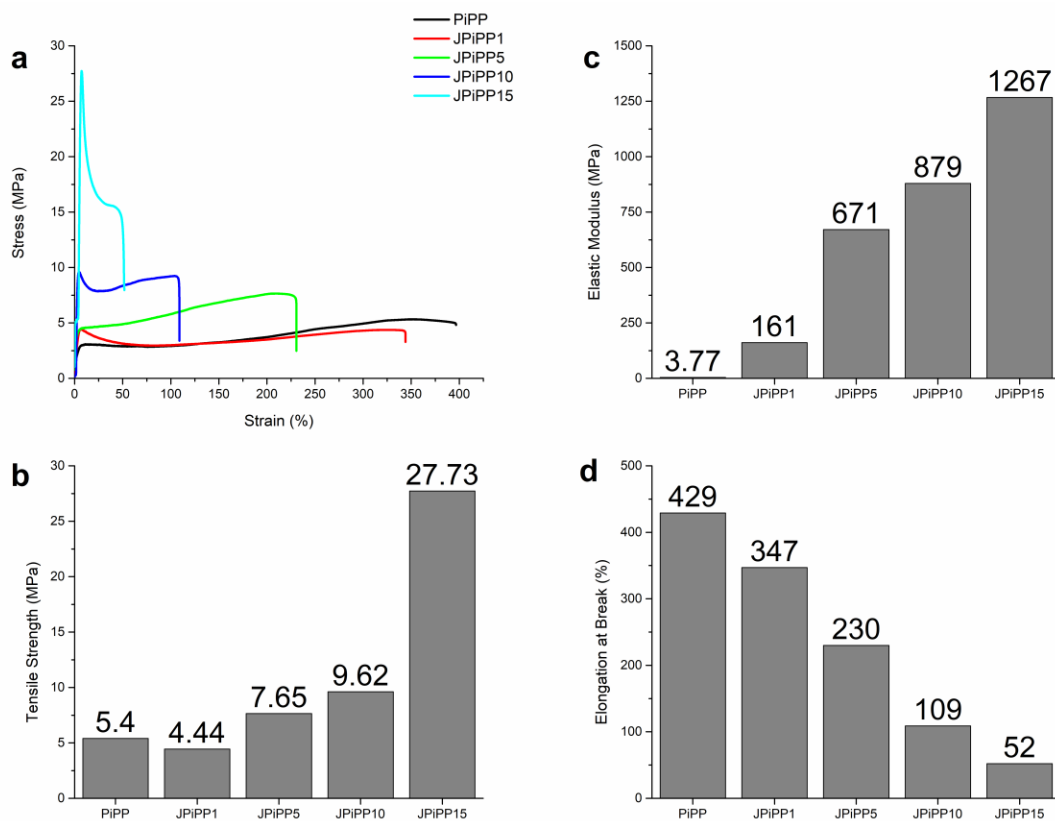


**Figure 3.7** Tensile properties of polymers in this study (a) Stress/Strain curves (b) Ultimate tensile strength (c) Elastic modulus (d) Elongation at break

easily slip past one another and uncoil. This is demonstrated by its low elastic modulus and the fact that it begins strain hardening almost immediately under an applied load. The epoxy modified PiPP is more compact due to the branching, so untangling of the chains is more difficult. Consequently, a greater degree of stress is needed for the material to yield. Concurrently, this branching limits the strain. In branched PiPP, the chains are bound to a central Joncryl molecule, and this branching region along the Joncryl backbone is less flexible. This causes carbon-carbon bond cleavage to occur sooner, as stretching is limited. Cyclic tensile testing was performed on the samples to investigate the TPEE properties. The

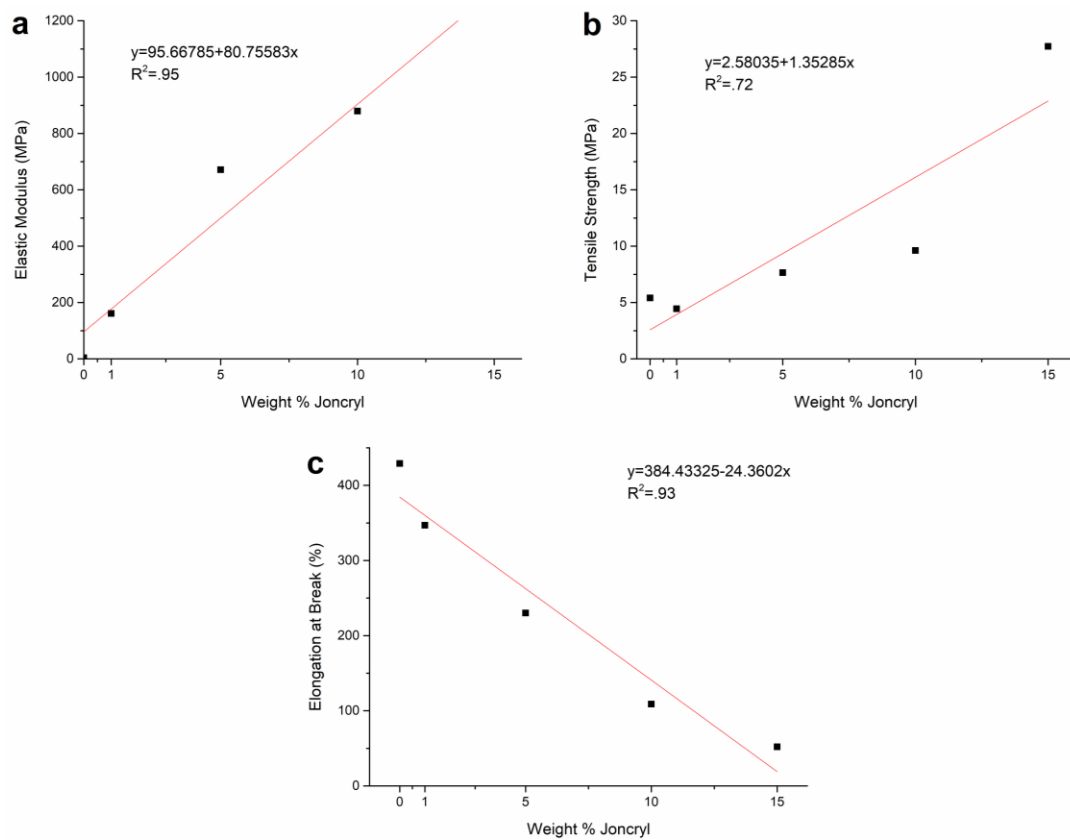


**Figure 3.10** Linear regressions and adjusted  $R^2$  values for tensile properties

materials were tested at a low strain rate to allow for sufficient strain to be achieved in the samples. The ability to undergo elastic deformation was maintained at each loading tested (**Table 3.2**). When subjected to a cyclic loading of 20% min<sup>-1</sup> to 150% strain for 10 cycles, several cycles among the tested specimens had a R<sub>r</sub> (recovery ratio) of greater than 100%. This is due to the fact that PiPP is very slow to return to its original shape under ambient conditions (23.2°C). Because of this, there are likely relaxation phenomena occurring over multiple cycles that could lead to greater than 100% recovery. In fact, qualitatively, PiPP and its epoxy modified tested samples can be observed returning close to their original shape over several hours. These materials also maintained reprocessability, as the highly branched extrudate was easily pressed into films.

**Table 3.2** Tensile test with cyclic loading rate 20% min<sup>-1</sup> of to 150% strain for 10 cycles

Cycle	PiPP		JPiPP1		JPiPP5		JPiPP10		JPiPP15	
	Final Strain (%)	R <sub>r</sub> (%)	Final Strain (%)	R <sub>r</sub> (%)	Final Strain (%)	R <sub>r</sub> (%)	Final Strain (%)	R <sub>r</sub> (%)	Final Strain (%)	R <sub>r</sub> (%)
1	94.9	36.7	88.5	41.0	113.5	24.3	120.1	20.0	122.4	18.4
2	98.1	94.2	118.5	51.3	128.8	58.0	123.7	87.8	141.4	31.1
3	112.4	72.5	124.8	79.8	123.3	126.1	131.7	69.5	128.7	247.9
4	123.7	69.8	129.1	83.1	124.4	95.9	135.2	80.8	145.1	22.8
5	123.1	102.4	135.1	71.1	129.2	81.0	132.5	118.8	146.5	72.6
6	124.8	93.6	125.4	165.4	129.3	99.5	147.1	16.4	147.0	86.3
7	117.9	127.7	131.5	75.1	118.8	150.9	147.8	77.8	147.2	91.3
8	127.1	71.1	130.9	103.7	128.8	68.0	148.0	87.9	147.5	89.2
9	121.5	124.8	133.7	85.0	129.4	96.9	148.1	95.4	147.7	93.3
10	128.0	77.0	126.3	145.5	130.0	97.1	148.2	93.6	147.8	94.4

## Rheology

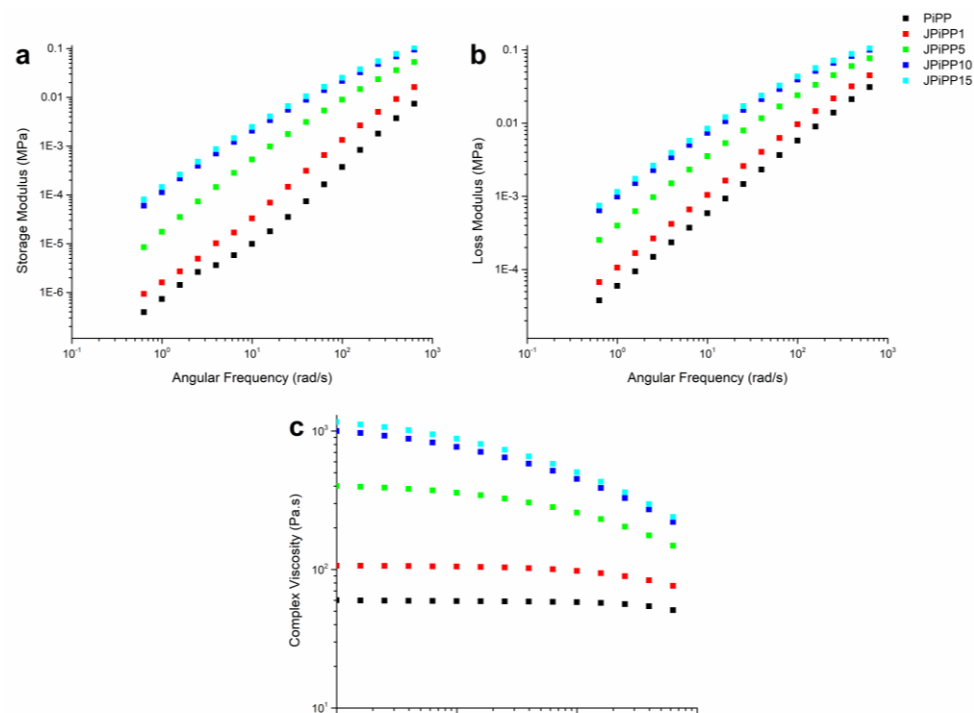


**Figure 3.11** Rheological data of polymers from oscillatory experiments. All experiments were conducted at 1% strain at 120°C. Data is plotted as a function of angular frequency.

Rheological properties were measured at relevant processing temperature (120°C) at 1% strain in oscillatory tests and at a logarithmic shear rate sweep with 30 second intervals for flow tests. Properties of note are shown in **Figure 3.7**. At any given frequency, the loss modulus ( $G''$ ) is 1-2 orders of magnitude higher than the storage modulus ( $G'$ ) (**Figure 3.7ab**).  $G'$  increases with Joncryl loading due to branching (**Figure 3.7a**). The enhanced  $G'$  value suggests that melt elasticity and melt strength were improved with branching.<sup>23</sup> As shown in **Figure 3.7b**,  $G''$  also increased with Joncryl loading. Additionally, the slope decreases slightly with increasing epoxy content. This is indicative of a higher degree of chain

entanglement.<sup>23</sup> This is due to the increasing branching making it more difficult for the PiPP chains to relax under strain. **Figure 3.7c** shows the material's shear thinning behavior. Higher loadings have a larger downward slope. As with the  $G''$ , the PiPP chains are slower to relax at higher frequencies. This causes the complex viscosity to decrease more sharply, as the polymer chains cannot re-entangle themselves fast enough to maintain their viscosity.

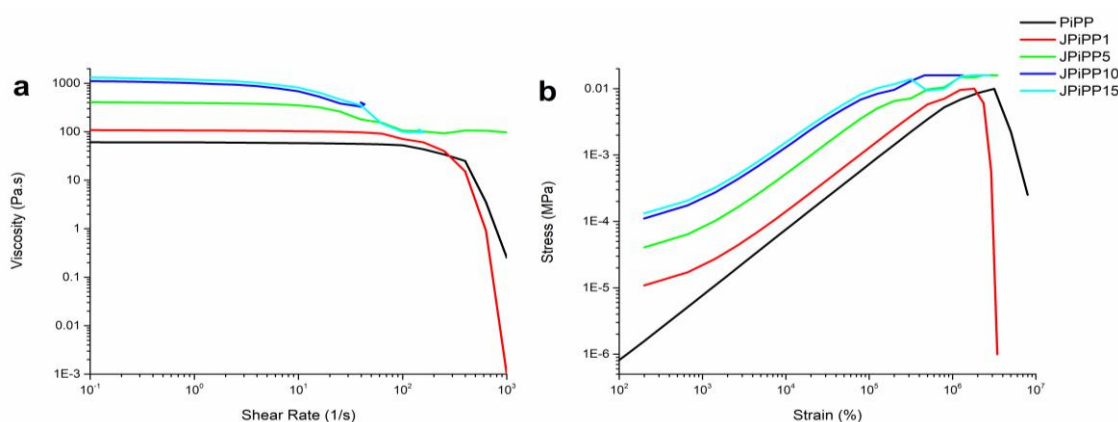


**Figure 3.12** Rheological data of polymers from shear sweep experiments. Shear rate was ramped in a logarithmic fashion. (a) Viscosity of polymers over different shear rates. (b) Shear Stress/Strain curve

During shear sweep experiments, the viscosity plateaued during the duration of the experiment (**Figure 3.8a**). This is typical of pseudoplastic materials.<sup>24</sup> At low shear rates, these materials show a constant viscosity, referred to as zero shear viscosity. At a critical shear rate, a shear thinning region begins. The beginning of the shear thinning region of PiPP and JPiPP1 can be seen when approaching a shear rate of 10<sup>3</sup> s<sup>-1</sup>. Both materials failed when the shear rate was increased any further. This failure occurs when the shear force overcomes the self-adhesion of the material. Due to the low viscosity, the melt can no longer adhere

to itself and breaks into smaller droplets. JPiPP515 began to see a decline in viscosity at  $10 \text{ s}^{-1}$  shear, but the force limit of the rheometer was reached shortly after impeding testing at higher shear rates.

All of the epoxy modified materials are shear strain hardening, an important property for blown films, blow molding, thermoforming, and foams (**Figure 3.8b**).<sup>7,18</sup> The curve of unmodified PiPP is effectively linear, demonstrating very little shear strain hardening. Incorporation of epoxy modifier modestly increased the shear strain hardening. The shape of the curves present in **Figure 3.8b** are characteristic of pseudoplastic fluids.<sup>24</sup> Pseudoplastic behavior occurs when a material rheologically behaves in a manner in between that of a Newtonian liquid and a plastic.<sup>24</sup> The shear modulus of PiPP was increased from 0.781 Pa to 31.1 Pa with 15 weight percent epoxy modifier (**Table 3.3**).

**Table 3.3** Shear Modulus of polymers based on shear rate sweeps

Sample	Shear Modulus (Pa)
Control	.781
JPiPP1	1.49
JPiPP5	5.13
JPiPP10	19.4
JPiPP15	31.1

## Conclusion

In this work, we investigated Joncryl 4368 as a branching agent for PiPP, our novel TPEE. High molecular weights were achieved by REX without the formation of any insoluble gel fractions, and the shape memory properties were retained. While uniform distribution of epoxy content is hard to achieve, high loadings of Joncryl gave sufficient distribution with low PDI and higher  $M_n$  values. The elastic modulus of PiPP could be tuned over 3 orders of magnitude, allowing for the preparation of soft and hard elastomers. Finally, the rheological properties were studied. An expected increase in viscosity and shear modulus with higher branching was observed. Further studies into the degradation, thermoforming, and shape memory of PiPP materials are currently underway.

## References

- (1) Spontak, R. J.; Patel, N. P. Thermoplastic Elastomers: Fundamentals and Applications. *Curr. Opin. Colloid Interface Sci.* **2000**, 5 (5), 333–340.
- (2) Nurhamiyah, Y.; Amir, A.; Finnegan, M.; Themistou, E.; Edirisinghe, M.; Chen, B. Wholly Biobased, Highly Stretchable, Hydrophobic, and Self-Healing Thermoplastic Elastomer. *ACS Appl. Mater. Interfaces* **2021**, 13 (5), 6720–6730.
- (3) Watts, A.; Kurokawa, N.; Hillmyer, M. A. Strong, Resilient, and Sustainable Aliphatic Polyester Thermoplastic Elastomers. *Biomacromolecules* **2017**, 18 (6), 1845–1854.
- (4) Liu, F.; Zhang, J.; Wang, J.; Liu, X.; Zhang, R.; Hu, G.; Na, H.; Zhu, J. Soft Segment Free Thermoplastic Polyester Elastomers with High Performance. *J. Mater. Chem. A Mater. Energy Sustain.* **2015**, 3 (26), 13637–13641.
- (5) Biemond, G. J. E.; Gaymans, R. J. Elastic Properties of Thermoplastic Elastomers Based on Poly(Tetramethylene Oxide) and Monodisperse Amide Segments. *J. Mater. Sci.* **2010**, 45 (1), 158–167.
- (6) Jia, Z.; Wang, J.; Sun, L.; Zhu, J.; Liu, X. Fully Bio-Based Polyesters Derived from 2,5-Furandicarboxylic Acid (2,5-FDCA) and Dodecanedioic Acid (DDCA): From Semicrystalline Thermoplastic to Amorphous Elastomer. *J. Appl. Polym. Sci.* **2018**, 135 (14), 46076.
- (7) Jiang, R.; Chen, Y.; Yao, S.; Liu, T.; Xu, Z.; Park, C. B.; Zhao, L. Preparation and Characterization of High Melt Strength Thermoplastic Polyester



- Elastomer with Different Topological Structure Using a Two-Step Functional Group Reaction. *Polymer* **2019**, 179, 121628.
- (8) Liu, F.; Zhang, J.; Wang, J.; Na, H.; Zhu, J. Incorporation of 1,4-Cyclohexanedicarboxylic Acid into Poly(Butylene Terephthalate)-b-Poly(Tetramethylene Glycol) to Alter Thermal Properties without Compromising Tensile and Elastic Properties. *RSC Adv.* **2015**, 5 (114), 94091–94098.
  - (9) Frenz, V.; Scherzer, D.; Villalobos, M. Multifunctional Polymers as Chain Extenders and Compatibilizers for Polycondensates and Biopolymers. *Tech. Pap. Reg. Tech* **2008**, 3.
  - (10) Beyer, G.; Hopmann, C. *Reactive Extrusion: Principles and Applications*; Wiley-VCH, 2018.
  - (11) Tzoganakis, C. Reactive Extrusion of Polymers: A Review. *Adv. Polym. Technol.* **1989**, 9 (4), 321–330.
  - (12) Formela, K.; Zedler, Ł.; Hejna, A.; Tercjak, A. Reactive Extrusion of Bio-Based Polymer Blends and Composites – Current Trends and Future Developments. *eXPRESS Polymer Letters* **2018**, 12 (1), 24–57.
  - (13) Giri, P.; Tambe, C.; Narayan, R. Using Reactive Extrusion To Manufacture Greener Products: From Laboratory Fundamentals to Commercial Scale. *ACS Symposium Series*. 2018, pp 1–23. <https://doi.org/10.1021/bk-2018-1304.ch001>.

- (14) Devaraj, N. K.; Finn, M. G. Introduction: Click Chemistry. *Chem. Rev.* **2021**, *121* (12), 6697–6698.
- (15) Meng, Q.; Heuzey, M.-C.; Carreau, P. J. Control of Thermal Degradation of Polylactide/Clay Nanocomposites during Melt Processing by Chain Extension Reaction. *Polym. Degrad. Stab.* **2012**, *97* (10), 2010–2020.
- (16) Liu, C.; Jia, Y.; He, A. Preparation of Higher Molecular Weight Poly (L-Lactic Acid) by Chain Extension. *Int. J. Polym. Sci.* **2013**, *2013*. <https://doi.org/10.1155/2013/315917>.
- (17) Przybysz-Romatowska, M.; Haponiuk, J.; Formela, K. Reactive Extrusion of Biodegradable Aliphatic Polyesters in the Presence of Free-Radical-Initiators: A Review. *Polym. Degrad. Stab.* **2020**, *182*, 109383.
- (18) Schneider, J.; Shi, X.; Manjure, S.; Gravier, D.; Narayan, R. Epoxy Functionalized Poly(Lactide) Reactive Modifier for Blown Film Applications. *J. Appl. Polym. Sci.* **2015**, *132* (28). <https://doi.org/10.1002/app.42243>.
- (19) Schneider, J.; Manjure, S.; Narayan, R. Reactive Modification and Compatibilization of Poly(Lactide) and Poly(Butylene Adipate-Co-Terephthalate) Blends with Epoxy Functionalized-Poly(Lactide) for Blown Film Applications. *Journal of Applied Polymer Science* **2016**, *133* (16). <https://doi.org/10.1002/app.43310>.
- (20) Tokiwa, Y.; Calabia, B. P.; Ugwu, C. U.; Aiba, S. Biodegradability of Plastics. *Int. J. Mol. Sci.* **2009**, *10* (9), 3722–3742.

- (21) Emadian, S. M.; Onay, T. T.; Demirel, B. Biodegradation of Bioplastics in Natural Environments. *Waste Manag.* **2017**, *59*, 526–536.
- (22) Scaffaro, R.; Maio, A.; Sutura, F.; Gulino, E. F.; Morreale, M. Degradation and Recycling of Films Based on Biodegradable Polymers: A Short Review. *Polymers* **2019**, *11* (4). <https://doi.org/10.3390/polym11040651>.
- (23) Liu, Z.-Y.; Weng, Y.-X.; Huang, Z.-G.; Wang, L.; Qiu, D.; Shao, S.-X. Effect of epoxy chain extender on the properties of polylactic acid <https://opastonline.com/wp-content/uploads/2018/05/effect-of-epoxy-chain-extender-on-the-properties-of-polylactic-acid-amse-18.pdf> (accessed Sep 22, 2021).
- (24) Boger, D. V. Demonstration of Upper and Lower Newtonian Fluid Behaviour in a Pseudoplastic Fluid. *Nature* **1977**, *265* (5590), 126–128.

CHAPTER 4:  
ENHANCEMENT OF POLY(BUTYLENE SUCCINATE'S) CRYSTALLINITY,  
STIFFNESS, AND TOUGHNESS BY BLENDING WITH SEMI-AROMATIC  
LIGNOPOLYESTERS<sup>3</sup>

---

<sup>3</sup>DeMichael Winfield, Jason Locklin. To be submitted to Journal of Applied Polymer Science.

## **Abstract**

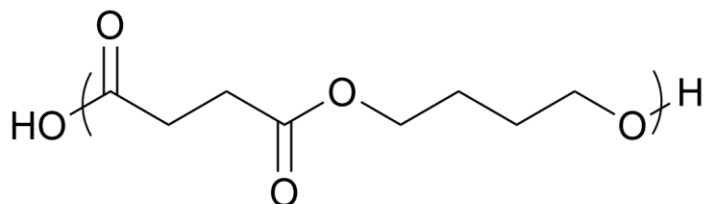
Biobased aliphatic polyesters are an attractive class of materials for replacing petroleum derived plastics. Poly(butylene succinate) (PBS) is a potentially biobased polyester with moderate properties and excellent compatibility. In this study, we blended PBS with our previously synthesized class of lignopolyesters. Blends were prepared with and without epoxy based Joncryl 4368 (J4368) compatibilizer through hot melt extrusion. The thermal and tensile properties were investigated. Despite little change in  $M_w$ , crystallinity was increased by both introduction of J4368 and the semi-aromatic polyesters. In all cases, blends showed a modest improvement to PBS's toughness. Of particular interest are the blends of PBS/PEHF, which not only showed improved toughness, but also improved stiffness as well. This work shows the utility of PEHF as an additive for PBS.

## Introduction

In addition to the aromatic small molecules discussed in Chapter 1, there are numerous other platform chemicals that can be derived from lignocellulosic biomass. Two that are of particular interest for polymer synthesis are diacids and diols, which are used to synthesize a variety of polyesters.<sup>1,2</sup> C<sub>2</sub>-C<sub>5</sub> diols and diacids can be obtained biosynthetically from lignocellulosic biomass or through fermentation.<sup>3-6</sup> C<sub>6</sub>-C<sub>10</sub> analogues can also be readily obtained from other biological sources with varying levels of cost effectiveness.<sup>7</sup> Most notably, C<sub>6</sub> based adipic acid and hexanediol are particularly difficult to produce from biosources.<sup>1,7</sup> Generally speaking, short chain linear aliphatic polyesters are biodegradable.<sup>2</sup> Due to this, aliphatic polyesters are of interest to addressing the plastics crisis.

PBS is a particularly interesting aliphatic polyester due to its moderate thermomechanical properties.<sup>8</sup> PBS has multiple biobased routes to its monomers and high biomass utilization efficiency.<sup>6</sup> The properties of PBS are shown in **figure 4.1**. With an elastic modulus of roughly 0.6 GPa and an elongation at break of 148%, PBS sits at the interface of strength and flexibility. Additionally, its T<sub>m</sub> is greater than 100°C, rendering it with sufficient thermal properties for a variety of applications. Several reports in the literature have demonstrated that PBS has excellent compatibility in blends with other materials. Blending with poly(lactic acid) (PLA) for improved ductility and other applications has been an extensive topic of research.<sup>9-13</sup> PBS also shows high compatibility with naturally occurring

biopolymers and additives.<sup>14,15</sup> This has led to it having a wide array of applications, ranging from single use plastics, agricultural materials, fibers, and automotive parts.<sup>16</sup>



PBS

$M_w$ : 193,400 g/mol	E (MPa): 587
$T_g$ : -32°C	$\sigma_{ult}$ (MPa): 40.70
$T_m$ : 114°C	$\epsilon$ : 148%

**Figure 4.1** Properties of PBS FZ91 used in this study

In our ongoing efforts to explore the applications of our lignopolyesters, we sought to use PBS as a platform for blending. As we previously reported, this class of polyesters has a wide array of properties. Thus, we envisioned that they would be well suited to augment PBS's moderate mechanical properties. In our approach, we elected to use both neat blends and blends with epoxy based compatibilizer Joncryl 4368. Herein, we report the thermal and tensile properties of said blends.

## Experimental

### Materials

PBS FZ91 was purchased from Mitsubishi Chemical. Joncryl 4368 was purchased from Sigma Aldrich. Precursors for other polymers were obtained as previously disclosed. All solvents were purchased from Sigma Aldrich in high purity.

### Synthesis of Lignopolyesters

The lignopolyesters shown in **Figure 4.2** below were synthesized by our previously reported procedure.

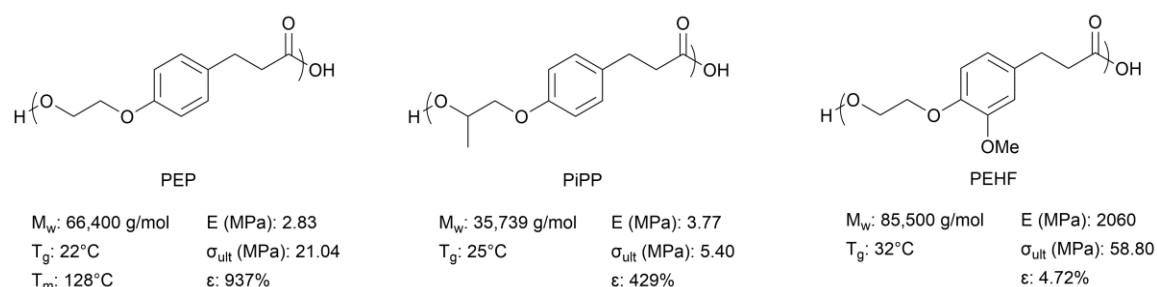


**Figure 4.2** Structure of lignopolyesters used in this work

### Characterization

Molecular weight was determined by gel permeation chromatography (GPC), equipped with two pumps (Shimadzu, LC-20AD) and a column oven (Shimadzu, CTO-20A) set to 40°C. Samples were analyzed at a concentration of 1 mg mL<sup>-1</sup> in CHCl<sub>3</sub> and a flow rate of 1 mL min<sup>-1</sup>. Molecular weight is reported according to polystyrene standards.

Thermal properties were measured by differential scanning calorimetry (DSC) on a DSC 250 (TA Instruments). Approximately 5-10 mg of sample was



heated at a rate of 10°C min<sup>-1</sup> from 0°C to 200°C for two cycles. All data reported was taken from the second scans. Crystallinity was determined by **equation 4.1**. The theoretical enthalpy of 100% crystallization was assumed to be the same value as pure PBS polymer, 210 J g<sup>-1</sup>.<sup>17</sup>

$$X = \frac{\Delta H_c}{\Delta H_c^\circ \phi} \quad (\text{equation 4.1})$$

#### *Compounding and Extrusion*

PBS was dried in a vacuum oven at 70°C overnight before use. All blends contained 90 weight percent PBS and 10 weight percent of selected lignopolyester. Blends with Joncryl 4368 contained 1 weight percent of the epoxy resin. Samples were extruded using a HAAKE Minilab 2 twin screw extruder and injection molded using a HAAKE Minijet Pro Piston Injection Molding System. Blends were extruded at 150°C at 100 RPM under N<sub>2</sub>. A residence time of 3 minutes was used, followed by extrusion into the injection molding barrel and injection molded into an ASTM Type 5 dog bone mold at 500 bar. The mold was set to 40°C. For blends with Joncryl 4368, an extruder temperature of 200°C was used.

#### *Mechanical Testing*

Tensile properties were measured using a Shimadzu AGS-X series tensile tester. In standard tests, samples were tested at ambient conditions (23.2°C) at a rate of 20 mm min<sup>-1</sup> to failure.

## Results and Discussion

### *Thermal Properties*

The cooling and heating curves from DSC are shown in **Figure 4.3**. Virgin PBS resin shows a broad  $T_c$ , while other samples displayed a sharper crystallization peak. While all PBS blends showed a narrowed  $T_c$  at a higher temperature compared to the PBS control, it is apparent that simple melt processing of PBS

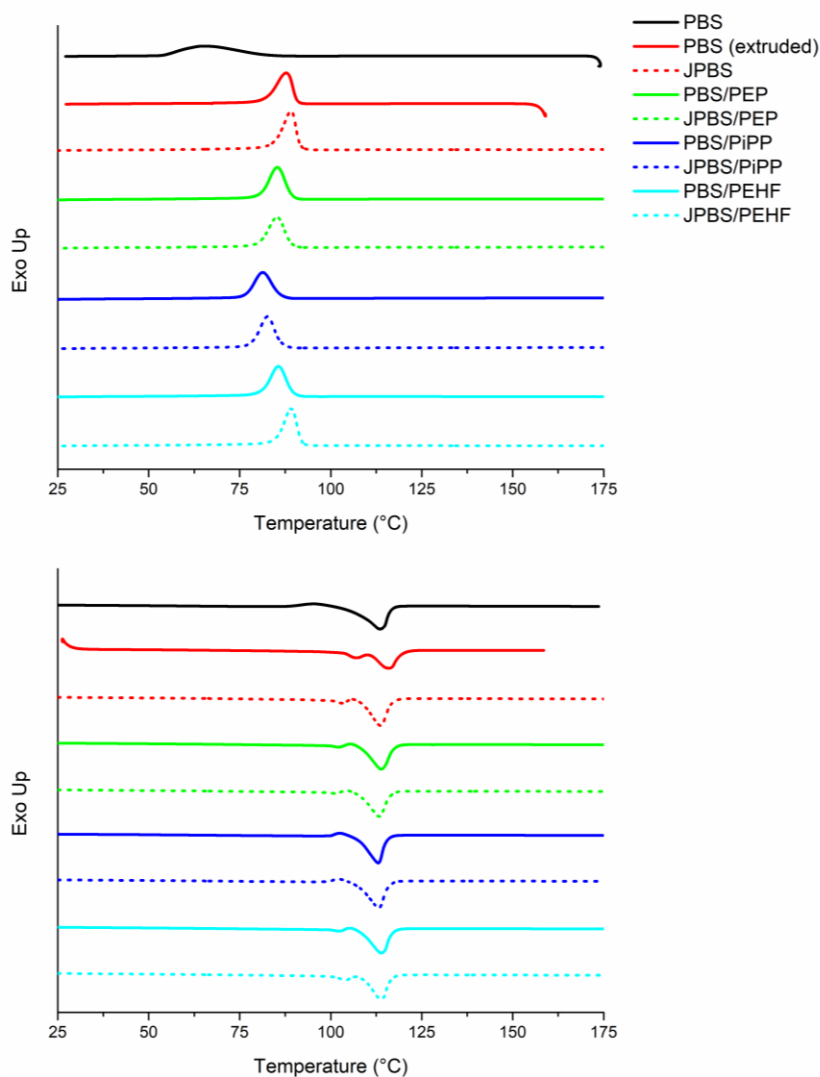


**Figure 4.3** DSC overlays of PBS and blends. Second cycle of cooling scan (top) and heating scan (bottom) is shown

changed its crystallization phenomenon. It has been shown in the literature that PBS undergoes a significant degree of shear-induced crystallization.<sup>18–20</sup> While this effect is highly pronounced in PBS, the thermal and mechanical history of polymers effects their crystallization.<sup>21</sup> In fact, orientation of the crystalline domains during melt processing can be significantly different than the orientation of crystals in bulk.<sup>21</sup> As shown in **Table 4.1**, a slight increase in crystallinity is observed from extruding PBS. The introduction of J4368 enhances this effect, with crystallinity increasing from 32% to 37%. Of the three lignopolymers blended with PBS in this study, PEHF appears to enhance this effect. The crystallinity of PBS/PEHF with and without J4368 increased to 41% and 38% respectively. The  $T_m$  in all cases was largely unaffected.

**Table 4.1** Thermal properties from second cycle of DSC. X is the fraction of crystallinity, calculated by **eq. 4.1**. PBSe referrers to neat PBS that has been hot melt extruded.

Sample	$M_w$ (g/mol)	$M_n$ (g/mol)	PDI	$\Delta H_c$ (J/g)	Peak (°C)	X
PBS	193.4	101.2	1.91	64.92	64.78	.309
PBSe				66.78	87.76	.318
JPBS	254.8	124.5	2.05	77.74	89.11	.370
PBS/PEP				71.43	85.43	.378
JPBS/PEP	224.0	101.4	2.21	68.33	85.21	.362
PBS/PiPP				60.84	81.30	.322
JPBS/PiPP	191.3	72.4	2.64	66.52	82.67	.352
PBS/PEHF				71.56	85.63	.379
JPBS/PEHF	345.8	101.3	3.41	76.54	89.11	.405

### *Tensile Properties*

The tensile properties of the blends are shown in **Figure 4.4**. A modest increase in ductility was observed with each blend. PBS blended with PiPP and

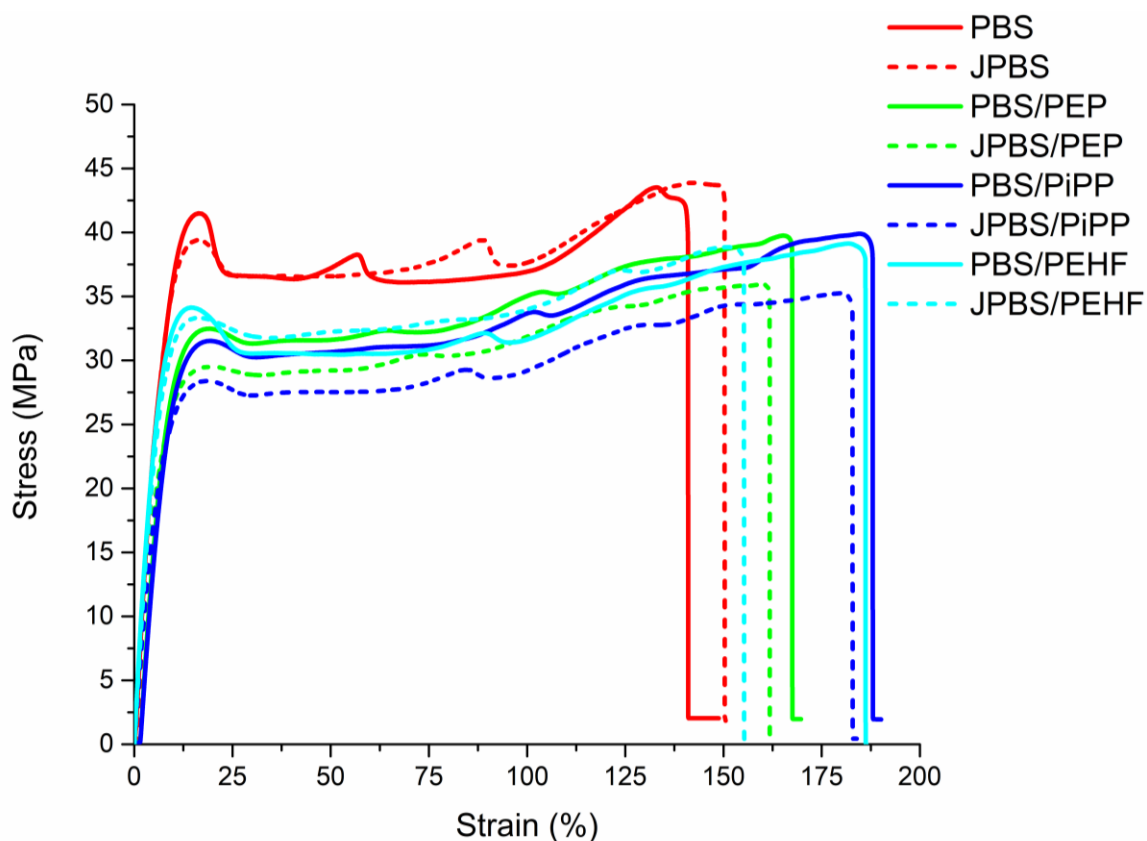


**Figure 4.6** Stress/Strain curves of polymer blends at 20 mm min<sup>-1</sup>

PEHF showed the greatest improvement, with strain at break increasing from 148% to 188% and 186% respectively (**Table 4.2**). Generally, increases in toughness are accompanied by decreases in modulus, but in the case of PEHF the modulus increased. With and without J4368, modulus increased from 654 MPa to 691 and 756 MPa respectively with minimal decrease in ultimate tensile strength. Both PEP and PiPP blends reduced elastic modulus.

From our study, it seems that the inclusion of a compatibilizer had a negative effect on the tensile properties. This may be due to the increased

temperature needed for the reactivity of epoxides without the addition of a catalyst. Observationally, slight yellowing was present in all samples processed with J4368 at 200°C, which is around the  $T_{d95\%}$  of PBS.<sup>16</sup> In fact, other than the PEHF blend, increases in  $M_w$  were small (**Table 4.1**). Therefore, the better performance of the non-compatible blends may be due to the lack of thermal degradation occurring at lower temperatures. Equivalent loading of epoxy resin may mitigate this issue.

**Table 4.2** Tensile data of PBS and blends

Sample	Elastic Modulus (MPa)	Ultimate Tensile Strength (MPa)	% $\epsilon$
PBS	653.93	40.70	148.10
JPBS	577.38	42.77	150.20
PBS/PEP	542.36	38.86	167.42
JPBS/PEP	551.31	35.18	161.69
PBS/PiPP	476.49	38.42	187.92
JPBS/PiPP	503.04	33.91	182.76
PBS/PEHF	755.63	38.00	186.08
JPBS/PEHF	690.81	37.58	155.15

With the data presented, PEHF is a highly advantageous additive for PBS. When blended with 10% PEHF, PBS's strain at break is increased 26% and its elastic modulus is increased 16%. With only a marginal decrease in ultimate tensile strength, both stiffness and ductility of PBS were improved. Furthermore, the crystallinity was significantly increased, with an increase of 6% in blends without compatibilizer. Thus, this work may prove to be a significant step in PBS processing, as it offers a simple solution to the improvement of stiffness, ductility, and crystallization with one polyester additive. Further studies into blends of our

novel lignopolyesters with other commodity biopolyesters is an ongoing topic of research.

## **Conclusion**

Blends of PBS and semi-aromatic lignopolyesters were prepared by hot melt extrusion. The lignopolyesters acted as toughening agents in every case. Furthermore, the crystallinity of PBS was increased by the blends as well as simple melt processing. Stiffness was significantly improved by blending PEHF with PBS. We have demonstrated that PEHF is an excellent blending additive for PBS with little to no downsides along with the improved tensile properties. This work shows the potential of PEHF in polyester blends. Further studies into the utility of our lignopolyesters in polymer blends is an ongoing effort in our group.

## References

- (1) Isikgor, F. H.; Remzi Becer, C. Lignocellulosic Biomass: A Sustainable Platform for the Production of Bio-Based Chemicals and Polymers. *Polym. Chem.* **2015**, 6 (25), 4497–4559.
- (2) Díaz, A.; Katsarava, R.; Puiggalí, J. Synthesis, Properties and Applications of Biodegradable Polymers Derived from Diols and Dicarboxylic Acids: From Polyesters to Poly(Ester Amide)s. *Int. J. Mol. Sci.* **2014**, 15 (5), 7064–7123.
- (3) Nguyen, H. T. H.; Suda, E. R.; Bradic, E. M.; Hvozdoch, J. A.; Miller, S. A. Polyesters from Bio-Aromatics. In *Green Polymer Chemistry: Biobased Materials and Biocatalysis*; ACS Symposium Series; American Chemical Society, 2015; Vol. 1192, pp 401–409.
- (4) Arnaud, S. P.; Wu, L.; Wong Chang, M.-A.; Comerford, J. W.; Farmer, T. J.; Schmid, M.; Chang, F.; Li, Z.; Mascal, M. New Bio-Based Monomers: Tuneable Polyester Properties Using Branched Diols from Biomass. *Faraday Discuss.* **2017**, 202, 61–77.
- (5) DeRosa, C. A.; Kua, X. Q.; Bates, F. S.; Hillmyer, M. A. Step-Growth Polyesters with Biobased (R)-1,3-Butanediol. *Ind. Eng. Chem. Res.* **2020**, 59 (35), 15598–15613.
- (6) Dai, Z.; Guo, F.; Zhang, S.; Zhang, W.; Yang, Q.; Dong, W.; Jiang, M.; Ma, J.; Xin, F. Bio-based Succinic Acid: An Overview of Strain Development, Substrate Utilization, and Downstream Purification. *Biofuels Bioprod. Biorefin.* **2020**, 14 (5), 965–985.

- (7) Steinbüchel, A. *Biopolymers*; Wiley-VCH, 2001.
- (8) Tokiwa, Y.; Calabia, B. P.; Ugwu, C. U.; Aiba, S. Biodegradability of Plastics. *Int. J. Mol. Sci.* **2009**, *10* (9), 3722–3742.
- (9) Shibata, M.; Inoue, Y.; Miyoshi, M. Mechanical Properties, Morphology, and Crystallization Behavior of Blends of Poly(l-Lactide) with Poly(Butylene Succinate-Co-l-Lactate) and Poly(Butylene Succinate). *Polymer* **2006**, *47* (10), 3557–3564.
- (10) Ganesh Saratale, R.; Cho, S.-K.; Dattatraya Saratale, G.; Kadam, A. A.; Ghodake, G. S.; Kumar, M.; Naresh Bharagava, R.; Kumar, G.; Su Kim, D.; Mulla, S. I.; Seung Shin, H. A Comprehensive Overview and Recent Advances on Polyhydroxyalkanoates (PHA) Production Using Various Organic Waste Streams. *Bioresour. Technol.* **2021**, *325*, 124685.
- (11) Chen, G.-X.; Kim, H.-S.; Kim, E.-S.; Yoon, J.-S. Compatibilization-like Effect of Reactive Organoclay on the Poly(l-Lactide)/Poly(Butylene Succinate) Blends. *Polymer* **2005**, *46* (25), 11829–11836.
- (12) Muhuo, Y. Dynamic Mechanical Properties and Thermal Stability of Poly(Lactic Acid) and Poly(Butylene Succinate) Blends Composites. *J. fiber bioeng. inform.* **2013**, *6* (1), 85–94.
- (13) Deng, Y.; Thomas, N. L. Blending Poly(Butylene Succinate) with Poly(Lactic Acid): Ductility and Phase Inversion Effects. *Eur. Polym. J.* **2015**, *71*, 534–546.



- (14) Li, Y.-D.; Zeng, J.-B.; Wang, X.-L.; Yang, K.-K.; Wang, Y.-Z. Structure and Properties of Soy Protein/Poly(Butylene Succinate) Blends with Improved Compatibility. *Biomacromolecules* **2008**, 9 (11), 3157–3164.
- (15) Uesaka, T.; Nakane, K.; Maeda, S.; Ogihara, T.; Ogata, N. Structure and Physical Properties of Poly(Butylene Succinate)/Cellulose Acetate Blends. *Polymer* **2000**, 41 (23), 8449–8454.
- (16) Rafiqah, S. A.; Khalina, A.; Harmaen, A. S.; Tawakkal, I. A.; Zaman, K.; Asim, M.; Nurrazi, M. N.; Lee, C. H. A Review on Properties and Application of Bio-Based Poly(Butylene Succinate). *Polymers* **2021**, 13 (9). <https://doi.org/10.3390/polym13091436>.
- (17) Ye, H.-M.; Tang, Y.-R.; Xu, J.; Guo, B.-H. Role of Poly(Butylene Fumarate) on Crystallization Behavior of Poly(Butylene Succinate). *Ind. Eng. Chem. Res.* **2013**, 52 (31), 10682–10689.
- (18) Xie, X.-L.; Li, Y.; Xu, J.-Z.; Yan, Z.; Zhong, G.-J.; Li, Z.-M. Largely Enhanced Mechanical Performance of Poly(Butylene Succinate) Multiple System via Shear Stress-Induced Orientation of the Hierarchical Structure. *J. Mater. Chem. A Mater. Energy Sustain.* **2018**, 6 (27), 13373–13385.
- (19) Zhou, W.; Shi, J.; Yuan, S.; Chen, Y. Crystallization and Shear-Induced Formation of Organogels in Novel Poly[(Butylene Succinate)-Co - Diol(isobutyl)-[Polyhedral Oligomeric Silsesquioxane] Copolyesters. *Polym. Int.* **2014**, 63 (4), 626–632.

- (20) Chae, D. W.; Kim, B. C.; Kim, D. K. Effects of Shearing and Comonomer Content on the Crystallization Behavior of Poly(Butylene Succinate-Co-Butylene 2-Ethyl-2-Methyl Succinate). *Polym. Int.* **2004**, 53 (9), 1266–1273.
- (21) Vleeshouwers, S.; Meijer, H. E. H. A Rheological Study of Shear Induced Crystallization. *Rheol. Acta* **1996**, 35 (5), 391–399.

CHAPTER 5:  
POLYESTERS AS DUAL TOUGHENING AGENTS AND PROCESSING AIDS IN  
POLY(HYDROXYL ALKANOATE) BLENDS<sup>4</sup>

---

<sup>4</sup>DeMichael Winfield, Apisata Holt, Grant Crane, Jason Locklin, To be submitted to Journal of Applied Polymer Science.

**Abstract**

Poly(hydroxyl alkanate) (PHA) is an attractive biobased polymer for replacing conventional plastics. It boasts a wide array of thermomechanical properties and has excellent compostability and biodegradability. Melt processing of PHA by extrusion is challenging due to thermal decomposition. Previously, our group has demonstrated that poly(butylene glutarate) (PBG) can act as an effective processing aid for PHA. Since polymer blends have the added benefit of modulating tensile properties, we decided to investigate the effects of other polyester blends on the ductility of PHA. Semi-aromatic lignin-based polyesters as well as aliphatic polyesters were synthesized and blended with PHA for tensile testing. In all cases, PHA's strain at break of 18% was improved. Our novel lignopolyester PEHF resulted in the largest increase in strain at break at 136% while also maintaining PHA's moderately high elastic modulus. Aliphatic polyester PBSA also showed a significant increase to 122% strain at break, but slightly decreased the modulus. This work is of practical importance to the formulation of PHA for melt processing.

## Introduction

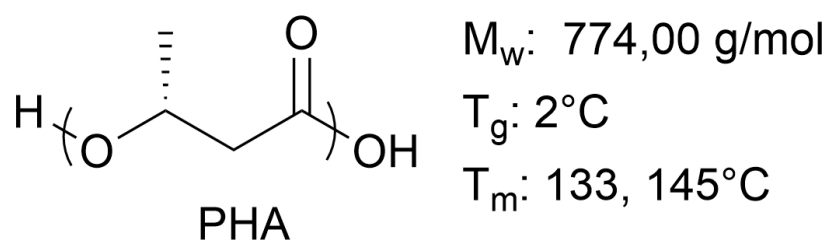
Recently, interest in using PHA as a biobased and biodegradable polymer for plastic applications has grown. PHAs are a highly abundant class of biopolymers produced by bacteria.<sup>1,2</sup> Microorganisms produce PHA as a form of energy storage when nutrient content is low.<sup>1,2</sup> Compared to other bioplastics produced from biosynthetic routes such as PLA or PBS, PHA is truly a naturally occurring biopolymer.<sup>3</sup> PHA also shows excellent biodegradability in a variety of environmentally relevant conditions.<sup>4–8</sup> Bacteria can produce hundreds of different comonomers, allowing for PHA to have a wide array of properties.<sup>3</sup> Due to this, PHA has been touted as a key material in replacing conventional plastics.<sup>9</sup>

The most commonly produced PHA by biological organisms is polyhydroxybutyrate (PHB). Pure PHB is a highly crystalline polyester with a melting transition of 170-175°C.<sup>10,11</sup> This range can be dramatically changed by comonomer content, with some PHAs having a  $T_m$  as low as 40°C.<sup>3</sup> PHB has a low glass transition temperature of 5°C, but this can also be tuned with comonomer content.<sup>3</sup> Likewise, the mechanical properties can be readily varied by comonomer content. PHB is a highly brittle polymer, but incorporation of comonomers with longer alkyl units can afford ductile PHAs. Because of their tunable properties, PHAs are a useful platform for different applications as bioplastics. PHA comonomers can be tuned in industrial fermentation processes through advantageous use of genetic engineering and controlling the bacteria's food inputs.<sup>12,13</sup>

Despite its advantages, there are numerous technical challenges in working with PHAs. Particularly, the extrusion of PHA is challenging. PHA undergoes a significant degree of melt fracturing during extrusion, ruining the finish of the material. Additionally, PHB degrades at its melting point, necessitating the need to either lower its melting point or improve its thermal stability.<sup>2</sup> Even with lowered melting transitions, PHAs are still highly susceptible to thermal degradation during extrusion.<sup>14</sup> Many polyesters undergo thermal degradation during extrusion, but this problem is exacerbated in PHA, as it also readily undergoes  $\beta$ -elimination.<sup>15</sup> The carbonyl oxygen of the ester and the adjacent monomers  $\alpha$ -proton in PHA can readily form a six membered transition state. The high temperature and shear conditions of extrusion are highly conducive for promoting  $\beta$ -elimination in PHA by both ionic and radical based mechanisms.<sup>16</sup> This is problematic given that more than half of plastic products are processed by extrusion.<sup>17</sup>

One simple way to mitigate this issue is by adding processing aids to the polymer being extruded. Generally, processing aids improve melt stability by reducing shear stress and increasing flowability.<sup>18</sup> Of the many processing aids that can be employed, we are interested in using polymer blends. Polymer blends are advantageous as processing aids since they can also be used to modulate the tensile properties. Polyesters can act as a lubricant through adhesive mechanisms inside the extruder. This alleviates melt fracturing and degradation, as the interface between the polyesters can dissipate shear stress.<sup>18</sup> Our group has extensively investigated the extrusion and thermomechanical properties of our PHA shown in

**Figure 5.1.** Previously, we have shown that poly(butylene glutarate) (PBG) is an effective processing aid for both PLA and PHA.<sup>19,20</sup> At 10 weight percent, PBG completely eliminates melt fracturing in PHA.<sup>20</sup> Interestingly, when using the optimized extrusion conditions developed by Holt, we have found that the blending of most polyesters with PHA has the same effect. Since the improvement in ductility with PBG was minimal, we sought to investigate the use of other polyesters to further improve the tensile properties during extrusion (**Figure 5.1**). In this study, we synthesized a library of polyesters including our novel semi-aromatic lignopolyesters as well as other aliphatic polyesters. Herein, the tensile properties of these blends are discussed.



PHA neat	PHA with 10 wt% PBG
E (MPa): 966	E (MPa): 778
$\sigma_{ult}$ (MPa): 32.57	$\sigma_{ult}$ (MPa): 23.59
$\epsilon$ : 18%	$\epsilon$ : 43%

**Figure 5.1** Properties of the PHA used in this study

## Experimental

### Materials

PHA was provided by the New Materials Institute at the University of Georgia. Butanediol (98%), succinic acid (97%), glutaric acid (96%), adipic acid (97%), and zirconium tertbutoxide (80% in BuOH solution) were purchased from Sigma Aldrich. 4-methoxyphenol (97%) was purchased from TCI Chemical. PBS FZ91 was purchased from Mitsubishi Chemical. Precursors for other polymers were obtained as previously disclosed. All solvents were purchased from Sigma Aldrich in high purity. Glutaric acid was recrystallized from methanol before use. All other reagents were used as received.

### Synthesis of lignopolyesters

The lignopolyesters shown in **Figure 5.2** below were synthesized by our previously reported procedure.

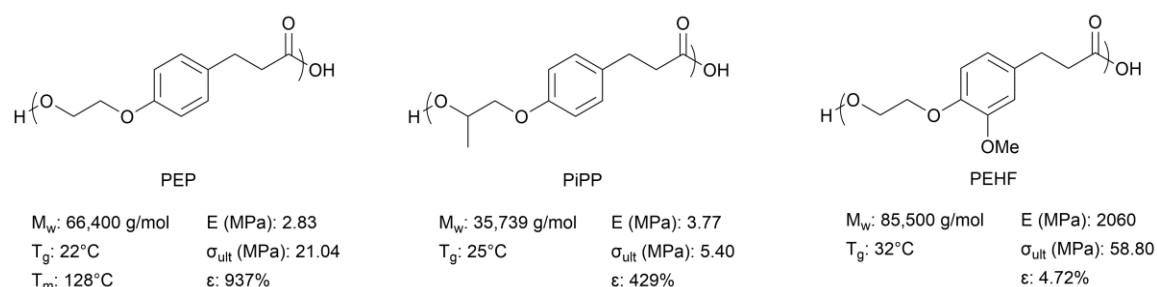


**Figure 5.2** Properties of lignopolyesters used in this study

### Synthesis of poly(butylene glutarate) (PBG)

Glutaric acid (1 equiv) and butanediol (1.03 equivs) were added into a flask. After backfilling with N<sub>2</sub> three times, the mixture was heated to 180°C and slowly



ramped to 200°C over 4 hours. The reaction vessel was then evacuated until a pressure of less than 1 torr was achieved. Temperature and vacuum were maintained overnight. The flask was then brought to atmospheric pressure with N<sub>2</sub>, and zirconium catalyst was injected. Vacuum was immediately restored (less than 1 torr), and the polymerization was allowed to continue for 4 hours. Afterwards, the melt was allowed to cool to room temperature. The crude polymer was taken up in CHCl<sub>3</sub> and precipitated in excess cold MeOH. The solids were collected by vacuum filtration and dried in vacuum overnight before use. M<sub>w</sub>: 53,300 g/mol

#### *Synthesis of poly(butylene adipate) (PBA)*

PBA was synthesized by the aforementioned procedure. M<sub>w</sub>: 41,719 g/mol

#### *Synthesis of poly(butylene succinate co-adipate) (PBSA)*

PBS was synthesized by the aforementioned procedure. M<sub>w</sub>: 31,400 g/mol

#### *Characterization*

All NMR spectra were collected on a Varian Mercury 300 MHz or 500 MHz spectrometer in appropriate deuterated solvent. Molecular weight was determined by gel permeation chromatography (GPC), equipped with two pumps (Shimadzu, LC-20AD) and a column oven (Shimadzu, CTO-20A) set to 40°C. Samples were analyzed at a concentration of 1 mg mL<sup>-1</sup> in CHCl<sub>3</sub> and a flow rate of 1 mL min<sup>-1</sup>. Molecular weight is reported according to polystyrene standards.

Thermal properties were measured by differential scanning calorimetry (DSC) on a DSC 250 (TA Instruments). Approximately 5-10 mg of sample was heated at a rate of 10°C min<sup>-1</sup> from 0°C to 180°C, then cold quenched to 0°C at a

rate of 100°C min<sup>-1</sup>, followed by an additional heating and cooling scan at 10°C min<sup>-1</sup>. All data reported was taken from the second scans. Crystallinity was determined by **Equation 5.1**. The theoretical enthalpy of 100% crystallization was assumed to be the same value as PHB homopolymer, 146 J g<sup>-1</sup>.<sup>10</sup>

$$X = \frac{\Delta H_c}{\Delta H_c^\circ \phi} \quad (\text{equation 5.1})$$

### *Compounding and Extrusion*

Prior to blending, PHA was dried in a vacuum oven at 60°C for 48 hours. All blends contained 90 weight percent of PHA and 10 weight percent of the second polyester. After careful weighing, polymers were cooled by liquid N<sub>2</sub> and dry mixed in a domestic coffee blender. Afterwards, blends were then melt mixed in a HAAKE Minilab 2 twin screw extruder following the previously developed procedure.<sup>19</sup> Briefly, samples were subjected to a 6-minute residence time at 150°C and 30 RPM to ensure homogeneity. ASTM Type 5 Tensile bar were prepared by injection molding. The cylinder and mold were heated to 155°C and 40°C respectively. A pressure of 650 bar for 5 seconds followed by a post pressure of 400 bar for 2 seconds was used. Samples were allowed to age for 10 days before testing.

### *Tensile Testing*

Tensile properties were measured using a Shimadzu AGS-X series tensile tester. In standard tests, samples were tested at ambient conditions (23.2°C) at a rate of 5 mm min<sup>-1</sup> to failure.

## Results and Discussion

### Thermal Properties

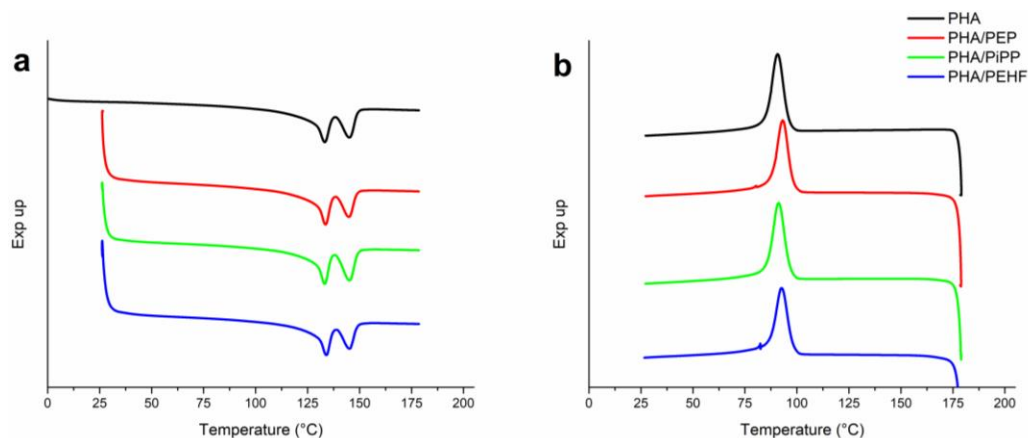


**Figure 5.3** Second scans from DSC of polymer blends. (a) second heating cycle (b) second cooling cycle

As expected, all polyesters blends were able to mitigate melt fracturing of the PHA. Melt blending of the polymers had no effect on PHA's ability to crystallize from the melt (**Figure 5.3b**). The control PHA and each blend had crystallinities ranging from 33-35% by DSC (**Table 5.1**). This is advantageous, as one of the primary challenges facing PHA is its crystallization.<sup>11</sup> The melting transitions were largely unchanged (**Figure 5.3a**).

**Table 5.1** Thermal properties from second cycle of DSC. X is the fraction of crystallinity, calculated by **eq. 5.1**

Sample	$\Delta H_c$ (J/g)	Peak (°C)	X
PHA	47.82	90.75	.328
PHA/PEP	45.72	93.11	.348
PHA/PiPP	47.24	91.08	.344
PHA/PEHF	45.02	92.65	.343

### *Tensile Properties*

All lignopolyesters blends improved the toughness of PHA (**Figure 5.4**). PHA blends with PEP and PBG were comparable in elongation at break with values of 39% and 43% respectively. The 10% blend with PEHF showed the largest increase in toughness with an elongation at break of 136% (**Table 5.2**). When blended with PiPP, the increase in toughness was less stark, but still significantly improved with a strain at break of 77%. As shown in **Figure 5.4**, the lignopolyesters yielded PHA blends with slight strain hardening properties. This

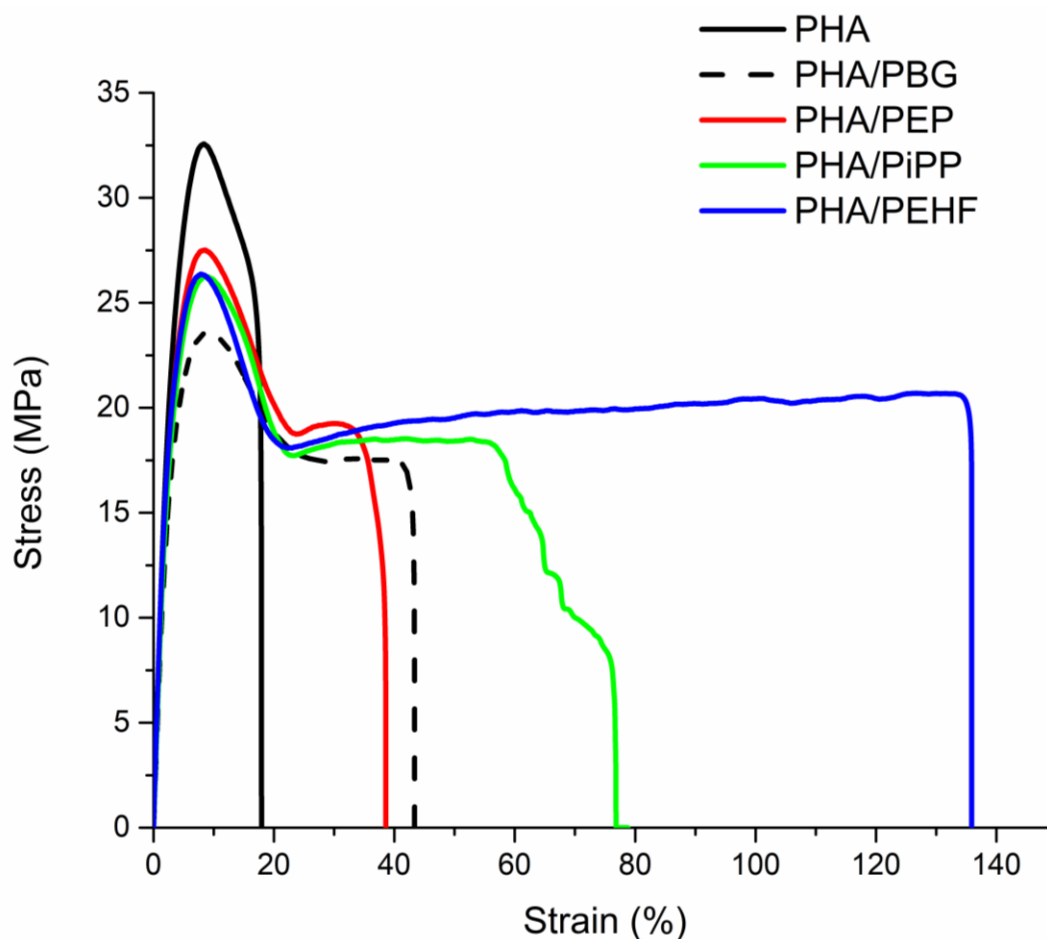


**Figure 5.6** Stress/Strain curves of PHA, PBG, and lignopolyester blends

suggests that the PHA component still undergoes brittle failure in a similar fashion, but afterwards the blended component can dissipate strain allowing for ductile failure to occur at higher strains. This also occurs with PBG, but strain hardening does not.

**Table 5.2** Tensile properties of PHA and PHA blends

Sample	Tensile Strength (MPa)	Elastic Modulus (MPa)	% $\epsilon$
PHA	32.57	966.26	17.88
PHA/PBG	23.59	778.27	43.32
PHA/PEP	27.51	908.78	38.56
PHA/PiPP	26.24	846.88	76.79
PHA/PEHF	26.37	956.36	135.89

Remarkably, the highly ductile blend with PEHF showed virtually no decrease in modulus, with PHA's modulus being 966 MPa and the blends 956 MPa. Compared to PBG blends modulus of 778, all of the lignopolyesters had a higher modulus. Blending with PEP saw a minor decrease in modulus to 909 MPa, while the PiPP blend showed a larger decrease in elastic modulus to 847 MPa. All lignopolyester blends showed a modest decrease in ultimate tensile strength, decreasing from 33 MPa to 26-28 MPa, but still remained higher than the PBG blend at 24 MPa. Speculatively, the high performance of the PEHF blend could be due to it having higher stiffness. The  $t_g$  of PEHF is 32°C, thus at ambient conditions

the PEHF component of the blend is in its hard, glassy state (**Figure 5.2**). At a low testing rate of  $5 \text{ mm min}^{-1}$ , there may not be enough stress in the system to induce the typical brittle failure of PEHF.

#### *Blends with commodity polyesters*

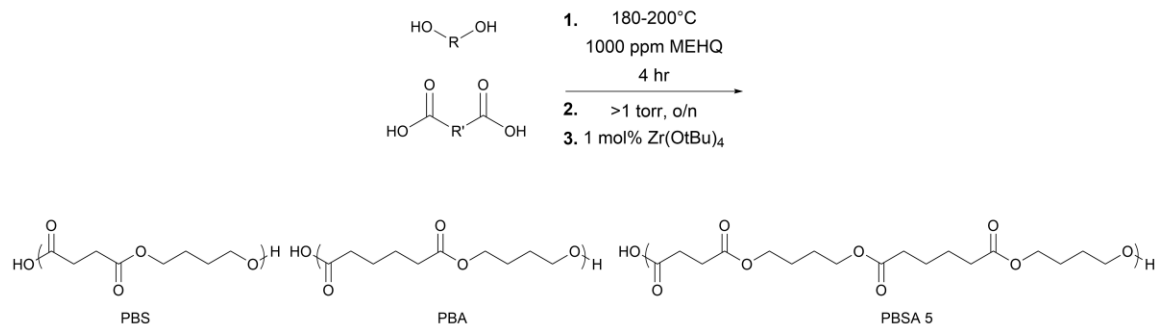


**Figure 5.7** Generalized scheme for the synthesis of aliphatic polyesters and their structures. PBSA 5 refers to PBA copolymer content of 5%

In addition to our novel polyesters, we also investigated the properties of blends of PHA with different aliphatic polyesters. PBS was purchased from Mitsubishi chemical, while PBA and PBSA were synthesized according to **Figure 5.5**. Of these polyesters blends, all resulted in a decrease in elastic modulus (**Table 5.3**). Like the lignopolyesters, a modest decrease in ultimate tensile strength was also observed. Similar to PEP and PBG, blends of PBS and PBA exhibited a slight increase in toughness. However, PBSA showed a significant increase in toughness, with strain at break increasing from 18% to 122%.

Compared to the other aliphatic polyesters, PBSA is waxy at ambient conditions, potentially allowing for better homogeneity when blended with PHA. The addition of the adipic acid comonomer reduces its  $T_g$ , allowing for a higher

degree of molecular motion and thus miscibility with PHA. Uniquely, the PBSA blend exhibited slight strain hardening character like the semi-aromatic polyester blends (**Figure 5.6**).

**Table 5.3** Tensile properties of all blends evaluated in this study

Sample	Tensile Strength (MPa)	Elastic Modulus (MPa)	% $\epsilon$
PHA	32.57	966.26	17.88
PHA/PBG	23.59	778.27	43.32
PHA/PEP	27.51	908.78	38.56
PHA/PiPP	26.24	846.88	76.79
PHA/PEHF	26.37	956.36	135.89
PHA/PBS	28.75	898.95	35.11
PHA/PBA	24.33	769.42	51.65
PHA/PBSA	25.77	829.09	121.82

Of all the polyesters examined in this study, PEHF appeared to be the best for blending with PHA to increase its toughness (**Figure 5.6**). While the 10% blend of PHA/PEHF showed the same decrease in tensile strength as the other blends, its elastic modulus was practically unchanged while the toughness increased by a factor of 7.6. PBSA also showed a significant increase in toughness, albeit at a higher expense of elastic modulus. PEHF can potentially be 100% biobased, while

PBSA currently cannot.<sup>21–24</sup> Thus, as a biobased additive, PEHF is the superior additive for PHA.

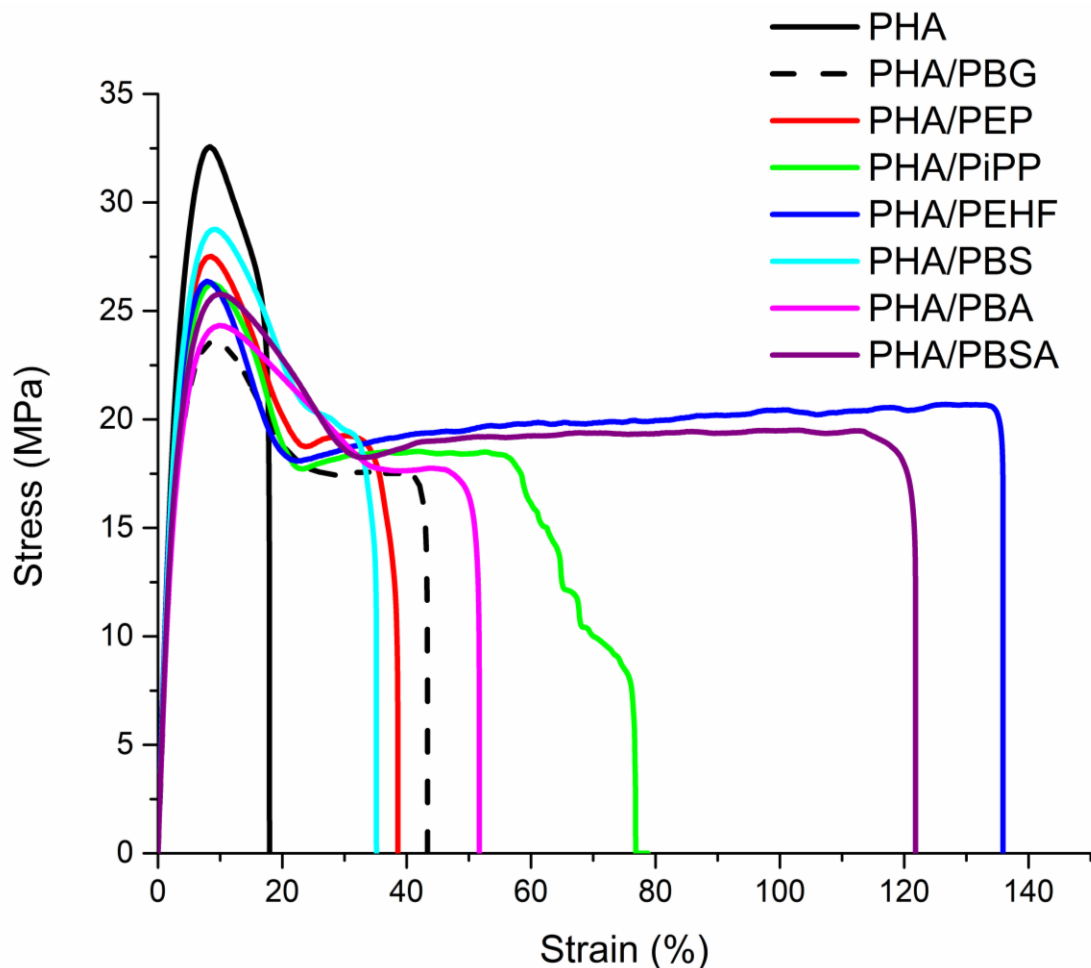


**Figure 5.10** Stress/Strain curves of PHA and all blends evaluated in this study

Based on the data presented, there is no clear trend on the effect of polyesters containing aromatic groups and those that are wholly aliphatic. There are several factors affecting the performance and morphology of polymer blends. The two amorphous polyesters, PiPP and PEHF both show a significant increase in ductility. PBSA is semi-crystalline, but its crystallinity is relatively low.



Incorporation of the adipic acid unit into PBS significantly reduces the degree of crystallinity.<sup>25</sup> Thus, amorphicity seems to improve the ductility of PHA in our case. Further investigation into other polyesters is underway.

## **Conclusion**

In this work we have investigated the effect of various polyester blends on the ductility of PHA based on PBG's ability to act as an effective processing aid for PHA. As polyesters generally tend to act as an effective processing aid for PHA, the choice of polyester can be optimized for desired tensile properties. Of our lignopolyesters, PiPP and PEHF showed significant improvement in ductility, while PEP only showed a small increase. Of the aliphatic polyesters used in this study, PBSA showed a substantial increase in ductility while the others showed a small increase. PEHF was the optimal polyester for blending, as it gave the largest increase in ductility while also maintaining the elastic modulus. Further studies into the mechanical properties of these blends and use of other polyesters are underway.

## References

- (1) Anderson, A. J.; Dawes, E. A. Occurrence, Metabolism, Metabolic Role, and Industrial Uses of Bacterial Polyhydroxyalkanoates. *Microbiol. Rev.* **1990**, *54* (4), 450–472.
- (2) Możejko-Ciesielska, J.; Kiewisz, R. Bacterial Polyhydroxyalkanoates: Still Fabulous? *Microbiol. Res.* **2016**, *192*, 271–282.
- (3) Steinbüchel, A. *Biopolymers*; Wiley-VCH, 2001.
- (4) Lott, C.; Eich, A.; Unger, B.; Makarow, D.; Battagliarin, G.; Schlegel, K.; Lasut, M. T.; Weber, M. Field and Mesocosm Methods to Test Biodegradable Plastic Film under Marine Conditions. *PLoS One* **2020**, *15* (7), e0236579.
- (5) Wang, G.-X.; Huang, D.; Ji, J.-H.; Völker, C.; Wurm, F. R. Seawater-Degradable Polymers-Fighting the Marine Plastic Pollution. *Adv. Sci.* **2020**, *8* (1), 2001121.
- (6) Dilkes-Hoffman, L. S.; Lant, P. A.; Laycock, B.; Pratt, S. The Rate of Biodegradation of PHA Bioplastics in the Marine Environment: A Meta-Study. *Mar. Pollut. Bull.* **2019**, *142*, 15–24.
- (7) Emadian, S. M.; Onay, T. T.; Demirel, B. Biodegradation of Bioplastics in Natural Environments. *Waste Manag.* **2017**, *59*, 526–536.
- (8) Mergaert, J.; Webb, A.; Anderson, C.; Wouters, A.; Swings, J. Microbial Degradation of Poly(3-Hydroxybutyrate) and Poly(3-Hydroxybutyrate-Co-3-Hydroxyvalerate) in Soils. *Appl. Environ. Microbiol.* **1993**, *59* (10), 3233–3238.

- (9) Muneer, F.; Rasul, I.; Azeem, F.; Siddique, M. H.; Zubair, M.; Nadeem, H. Microbial Polyhydroxyalkanoates (PHAs): Efficient Replacement of Synthetic Polymers. *J. Polym. Environ.* **2020**, *28* (9), 2301–2323.
- (10) Barham, P. J.; Keller, A.; Otun, E. L.; Holmes, P. A. Crystallization and Morphology of a Bacterial Thermoplastic: Poly-3-Hydroxybutyrate. *J. Mater. Sci.* **1984**, *19* (9), 2781–2794.
- (11) Domínguez-Díaz, M.; Flores, A.; Romo-Urbe, A.; Cruz-Silva, R. Kinetics of Crystallization of Biodegradable PHA Copolymers: A Combined X-Ray Scattering and Micro-Indentation Study. *Mater. Res. Soc. Symp. Proc.* **2011**, *1301* (mrsf10-1301-pp11-14). <https://doi.org/10.1557/opl.2011.555>.
- (12) Ganesh Saratale, R.; Cho, S.-K.; Dattatraya Saratale, G.; Kadam, A. A.; Ghodake, G. S.; Kumar, M.; Naresh Bharagava, R.; Kumar, G.; Su Kim, D.; Mulla, S. I.; Seung Shin, H. A Comprehensive Overview and Recent Advances on Polyhydroxyalkanoates (PHA) Production Using Various Organic Waste Streams. *Bioresour. Technol.* **2021**, *325*, 124685.
- (13) Nomura, C. T.; Taguchi, S. PHA Synthase Engineering toward Superbiocatalysts for Custom-Made Biopolymers. *Appl. Microbiol. Biotechnol.* **2007**, *73* (5), 969–979.
- (14) Montano-Herrera, L.; Pratt, S.; Arcos-Hernandez, M. V.; Halley, P. J.; Lant, P. A.; Werker, A.; Laycock, B. In-Line Monitoring of Thermal Degradation of PHA during Melt-Processing by Near-Infrared Spectroscopy. *N. Biotechnol.* **2014**, *31* (4), 357–363.

- (15) Xiang, H.; Wen, X.; Miu, X.; Li, Y.; Zhou, Z.; Zhu, M. Thermal Depolymerization Mechanisms of Poly(3-Hydroxybutyrate-Co-3-Hydroxyvalerate). *Progress in Natural Science: Materials International* **2016**, 26 (1), 58–64.
- (16) Determination of Multiple Thermal Degradation Mechanisms of Poly(3-Hydroxybutyrate). *Polym. Degrad. Stab.* **2008**, 93 (8), 1433–1439.
- (17) Beyer, G.; Hopmann, C. *Reactive Extrusion: Principles and Applications*; Wiley-VCH, 2018.
- (18) Achilleos, E. C.; Georgiou, G.; Hatzikiriakos, S. G. Role of Processing Aids in the Extrusion of Molten Polymers. *J. Vinyl Addit. Technol.* **2002**, 8 (1), 7–24.
- (19) Holt, A.; Ke, Y.; Bramhall, J. A.; Crane, G.; Grubbs, J. B., III; White, E. M.; Horn, J.; Locklin, J. Blends of Poly(Butylene Glutarate) and Poly(Lactic Acid) with Enhanced Ductility and Composting Performance. *ACS Appl. Polym. Mater.* **2021**, 3 (3), 1652–1663.
- (20) Holt, A. The Modification of Bio-Based Polyesters with Additives by Means of Solution Casting and Extrusion. PhD, University of Georgia, 2021.
- (21) Subbotina, E.; Rukkijakan, T.; Marquez-Medina, M. D.; Yu, X.; Johnsson, M.; Samec, J. S. M. Oxidative Cleavage of C-C Bonds in Lignin. *Nat. Chem.* **2021**. <https://doi.org/10.1038/s41557-021-00783-2>.
- (22) Nguyen, H. T. H.; Suda, E. R.; Bradic, E. M.; Hvozdoch, J. A.; Miller, S. A. Polyesters from Bio-Aromatics. In *Green Polymer Chemistry: Biobased*

*Materials and Biocatalysis*; ACS Symposium Series; American Chemical Society, 2015; Vol. 1192, pp 401–409.

- (23) Miller, S. A. Sustainable Polymers: Opportunities for the Next Decade. *ACS Macro Lett.* **2013**, 2 (6), 550–554.
- (24) Fadlallah, S.; Roy, P. S.; Garnier, G.; Saito, K.; Allais, F. Are Lignin-Derived Monomers and Polymers Truly Sustainable? An in-Depth Green Metrics Calculations Approach. *Green Chem.* **2021**.  
<https://doi.org/10.1039/D0GC03982A>.
- (25) Rafiqah, S. A.; Khalina, A.; Harmaen, A. S.; Tawakkal, I. A.; Zaman, K.; Asim, M.; Nurrazi, M. N.; Lee, C. H. A Review on Properties and Application of Bio-Based Poly(Butylene Succinate). *Polymers* **2021**, 13 (9).  
<https://doi.org/10.3390/polym13091436>.

CHAPTER 6:  
SCREENING AND OPTIMIZATION OF BASE CATALYST FOR THE  
SYNTHESIS OF HIGH TM BIOBASED POLYESTERS FROM  
HYDROXYCINNAMIC ACIDS<sup>5</sup>

---

<sup>5</sup>DeMichael Winfield, Jason Locklin. To be submitted to Macromolecules.

## Abstract

Development of high  $T_m$  polyesters from biobased sources has proven to be difficult. One potentially viable polyester for this application is poly(phloretic acid) (PPA) based on lignin derived hydroxycinnamic acids. Typically synthesized by acidolysis polymerizations, achieving high yield and molecular weight is difficult due to the sluggish reactivity and competitive side reactions. PPA and its derivatives also suffer from poor thermal stability. One strategy to combat this is to use base catalysts to form anionic end groups, increasing their nucleophilicity. In this work we screened several base catalysts by DSC to assess their feasibility for this polymerization. Hydroxide salts proved to be the most effective catalyst, with tetramethylammonium hydroxide (TMAH) performing the best. Upon optimization with this catalyst PPA molecular weights of up to  $49,903 \text{ g mol}^{-1}$ . The resultant polymer had a  $T_m$  of  $247^\circ\text{C}$  and  $T_g$  of  $53^\circ\text{C}$ . This synthesis produces higher molecular weight in a faster, greener fashion than what has been previously reported. Further investigation revealed that thermal stability of PPA was still quite poor, even with higher molecular weight and less catalyst residue. Further studies into improvement of PPA's thermal stability are needed to make full use of our optimized synthesis.

## Introduction

Despite the numerous examples of biobased polyesters in the literature, high  $T_m$  polyesters have remained uncommon.<sup>1</sup> Several research efforts have been made to find biobased alternatives to poly(ethylene terephthalate) (PET), a widely produced commodity thermoplastic with a melting transition of approximately 260°C.<sup>2–4</sup> A class of biobased polyesters with potential to fill this role are the homopolymers of hydroxycinnamic acid derivatives. Its precursors, phloretic acid, ferulic acid, and sinapic acid can all be sourced from lignocellulose.<sup>5–8</sup> In particular, poly(phloretic acid) (PPA) is an attractive derivative due to its precursor's high abundance and its relative stability compared to its methoxy containing derivatives.<sup>9,10</sup> A generalized polymerization scheme of PPA is shown in **Figure 6.1**.

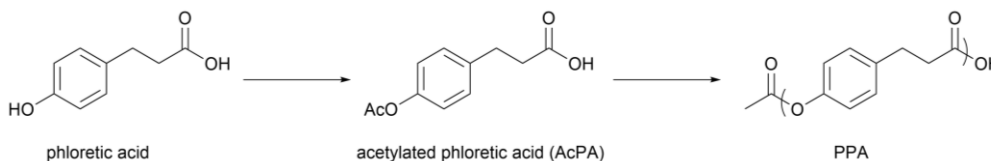


**Figure 6.1** General synthetic scheme for acidolysis polymerization of PPA

Synthesis of PPA and its derivatives is challenging for a multitude of reasons. First, homopolymerization of hydroxycinnamic acids directly does not yield polymer due to the poor nucleophilicity of phenolic groups.<sup>2,11</sup> Because of this, the phenolic group is usually acetylated to allow for an acidolysis polymerization (**Figure 6.1**). Despite being a more efficient synthesis than traditional



polycondensation, acidolysis is still difficult to achieve in high yield and purity.<sup>2,11,12</sup> As shown in the mechanism in **Figure 6.2**, the productive pathway requires the leaving of a phenoxy group over a carboxylate, a better leaving group, in step **2**. Thus, driving acidolysis polymerizations forward is difficult. Secondly, activated aromatics can undergo a variety of competitive side reactions under the reaction conditions, including electrophilic aromatic substitution, decarboxylation, and fries rearrangements.<sup>12</sup> These reactions lead to degradation and crosslinking that yields intractable material.<sup>2</sup>

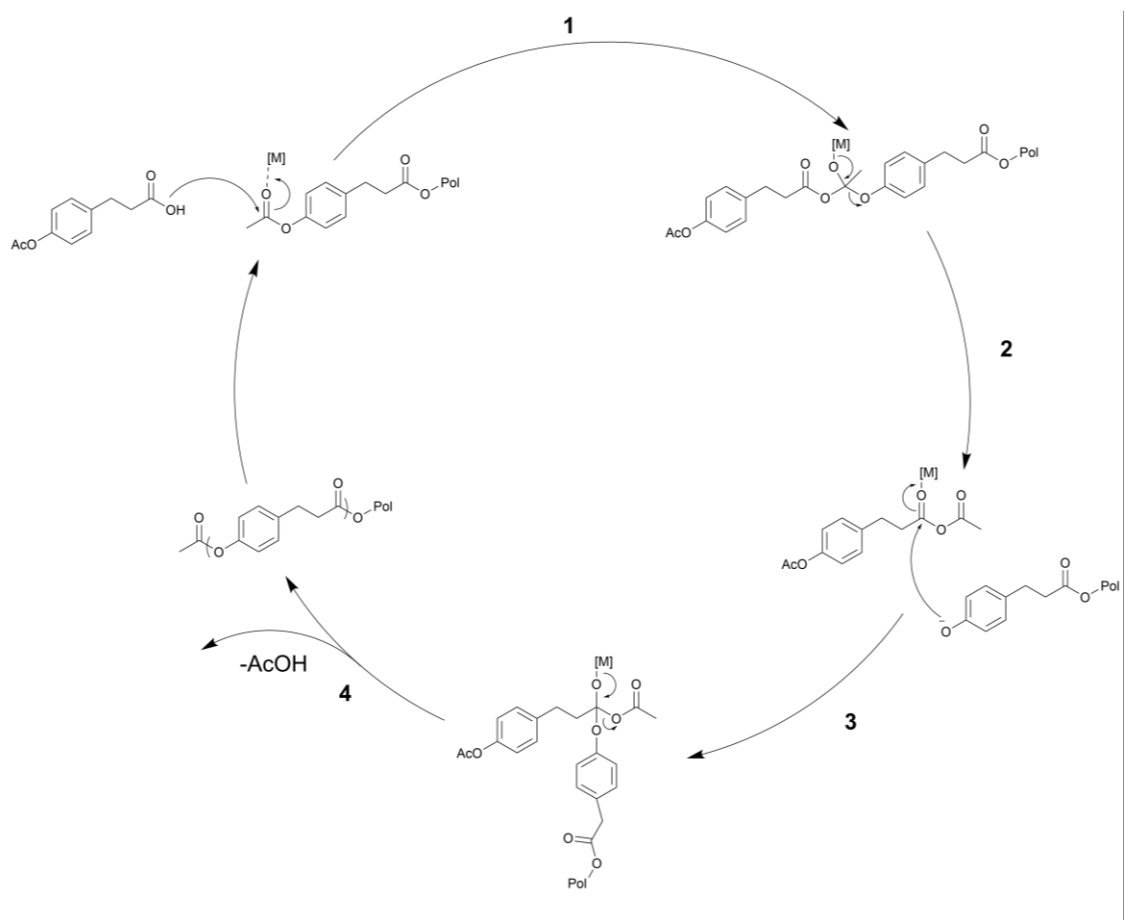


**Figure 6.4** Generalized mechanism for the polymerization of AcPA to PPA by metal-based Lewis acid catalyst

Mialon et al. reported the synthesis of poly(dihydroferulic acid) with  $\text{Zn}(\text{OAc})_2 \cdot 2\text{H}_2\text{O}$  in 68% yield.<sup>2</sup>  $M_n$  determined by  $^1\text{H}$  NMR was  $17,800 \text{ g mol}^{-1}$ , but polymer produced by this method is impure and has a high degree of discoloration and poor thermal stability. Other reports in the literature have also had poor molecular weights and/or yields with this route.<sup>11</sup> In the interest of optimizing this synthesis, we preliminarily screened a few acid based catalysts shown in **Table 6.1**. With  $\text{Zn}(\text{OAc})_2 \cdot 2\text{H}_2\text{O}$ , lower temperatures and longer reaction times only gave oligomers with a  $^1\text{H}$  NMR  $M_n$  of  $889.23 \text{ g mol}^{-1}$ . Increasing the temperature yielded intractable material, leaving us unsuccessful in improving the synthesis with  $\text{Zn}(\text{OAc})_2 \cdot 2\text{H}_2\text{O}$ . A significantly higher reactivity catalyst in  $\text{Zr}(\text{OtBu})_4$  was used to try and build molecular weight at moderate temperatures but was also unsuccessful. Likewise, organoacid catalyst also yielded intractable material.

**Table 6.1** Preliminary acid catalyst screening for PPA synthesis. AcPA was melted under  $\text{N}_2$  at  $180^\circ\text{C}$ , then ramped to the final temperature, followed by 4 hours of vacuum

Catalyst	Temperature ( $^\circ\text{C}$ )	$^1\text{H}$ NMR $M_n$ (g/mol)	Solubility
$\text{Zn}(\text{OAc})_2 \cdot 2\text{H}_2\text{O}$	220	889.23	$\text{CHCl}_3/\text{TFA}$
$\text{Zn}(\text{OAc})_2 \cdot 2\text{H}_2\text{O}$	260	-	-
$\text{Zr}(\text{OtBu})_4$	200	-	-
MSA	220	-	-
p-TSA	220	-	-

Recently, it has been demonstrated that forming anionic carboxylate end groups can increase the reactivity of AcPA towards oligomers at low temperatures (**Figure 6.3**).<sup>13</sup> Given the lack of success with acid catalysts, we decided to investigate this strategy further. In this work, a variety of base catalysts and their

activity for PPA were screened by DSC. DSC allows for high throughput catalyst screening that traditionally takes long periods of time to perform.<sup>14–16</sup> Herein, we report the catalyst screening and optimization of PPA synthesis by different base catalysts.

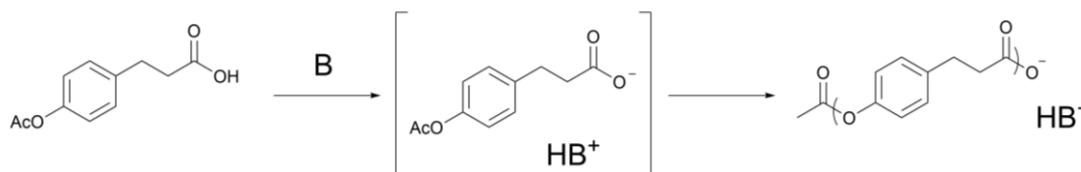


**Figure 6.5** Generalized scheme for the synthesis of PPA from AcPA with carboxylate end groups

## Experimental

### Materials

Phloretic Acid (98%), sodium acetate (anhydrous), and acetic anhydride (acs grade) were purchased from Oakwood Chemical. Sodium hydroxide (97%) was purchased from Fisher Scientific. Antimony oxide (99%), sodium carbonate (acs grade), 25% tetramethylammonium hydroxide solution in water, 8-Diazabicyclo[5.4.0]undec-7-ene (DBU), zirconium tertbutoxide (80% in BuOH), and 4-Dimethylaminopyridine (DMAP) were purchased from Sigma Aldrich. Methanesulfonic acid (MSA), p-toluenesulfonic acid (PTSA), and zinc acetate dihydrate (98%) were purchased from Arcos Organic.

### Monomer Synthesis

Phloretic acid (1 equiv) and NaOH (2.5 equivs) were dissolved in water (1M). Using an addition funnel, acetic anhydride (1.5 equivs) was added dropwise.

The reaction was allowed to stir overnight at room temperature. The solution was acidified to a pH of 1, and the resultant precipitate filtered and washed extensively with cold water. The product was used without further purification. 93% yield.  $^1\text{H}$  NMR (500 MHz,  $\text{cdcl}_3$ )  $\delta$  7.23, 7.20, 7.02, 7.00 (aromatic H), 2.96, 2.68 (t, 4H), 2.29 (s, 3H).

### *Polymerizations*

PPA was polymerized in a 3 neck round bottom flask equipped with an overhead stirrer, temperature probe, and short path distillation apparatus. In a typical example, monomer and 10 mol% of catalyst were added and heated to 140°C under  $\text{N}_2$  for 4 hours, followed by 1 hour at 160°C, 1 hour at 180°C, then 2 hours at either 200 or 240°C under vacuum. The resultant polymer was cooled and crushed to remove from flask. 85% yield.  $M_n$  was determined by  $^1\text{H}$  NMR in  $\text{CDCl}_3$ /trifluoroacetic acid by end group analysis. Spectra can be seen in text below.

### *Characterization*

All NMR spectra were collected on a Varian Mercury 500 MHz spectrometer in appropriate deuterated solvent. Thermal properties were measured by differential scanning calorimetry (DSC) on a DSC 250 (TA Instruments). Approximately 5-10 mg of sample was heated at a rate of 10°C  $\text{min}^{-1}$  from 0°C to 300°C, then cold quenched to 0°C at a rate of 100°C  $\text{min}^{-1}$ , followed by an additional heating and cooling scan at 10°C  $\text{min}^{-1}$ . All data reported was taken from the second scans. Degradation temperature was measured using

thermogravimetric analysis (TGA) on a Discovery TGA (TA Instruments). Approximately 10-15 mg of sample was heated from ambient temperature to 700°C at 10°C min<sup>-1</sup> under N<sub>2</sub> atmosphere.

### *Catalyst Screening*

Catalyst screening was performed by DSC in high pressure pans. Monomer and 10 mol% of catalyst were carefully measured by analytical balance and/or micropipette, then added into the sealed high-pressure pans. DSC reactions were performed at a ramp rate of 5°C min<sup>-1</sup> from 25-250°C.

## **Results and Discussion**

### *Monomer Synthesis*

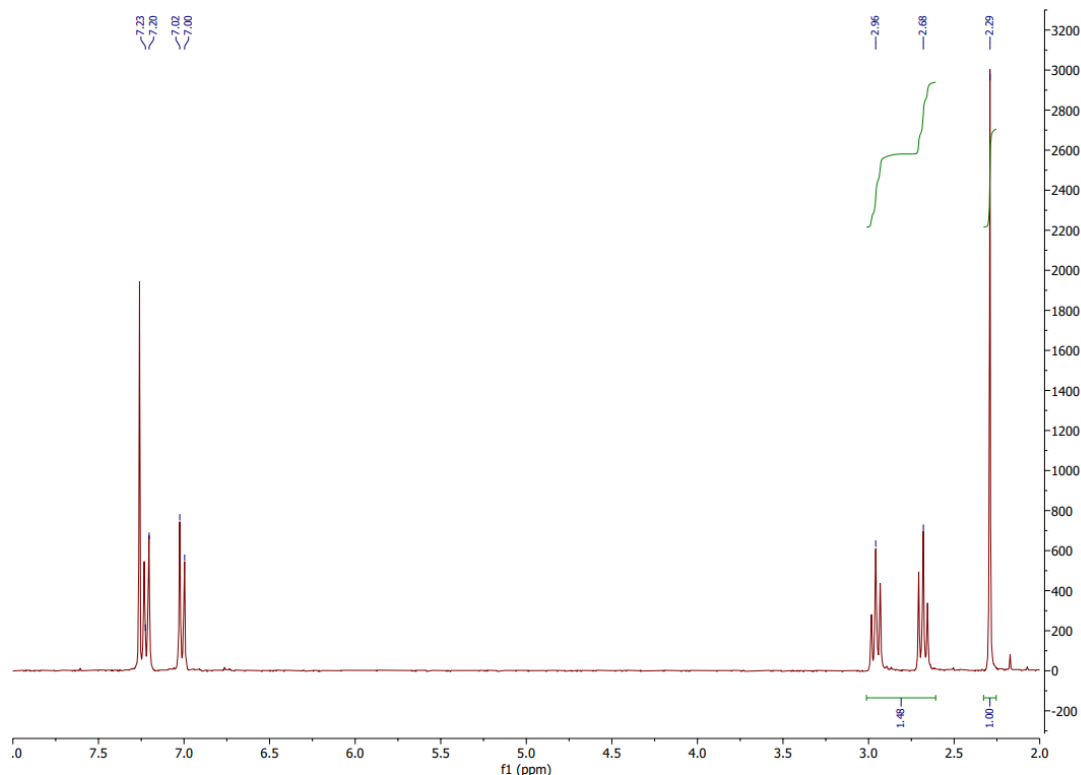


**Figure 6.8** <sup>1</sup>H NMR of AcPA. The integrations of the protons at 2.96 and 2.68 ppm are compared to the integration of methyl end group at 2.29 to calculate D<sub>p</sub>

Acetylation of phloretic acid was achieved in high yield with acetic anhydride. A slight degree of dimerization occurred during synthesis (**Figure 6.4**). In order to obtain high yield, the pure monomer was not isolated. A  $D_p$  of 1.11 was obtained by  $^1\text{H}$  NMR, which was inconsequential for the purposes of this study. The synthesized AcPA had a melting point of  $96^\circ\text{C}$  with a broad range, likely due to the product mixture broadening the melting point (**Figure 6.5a**).

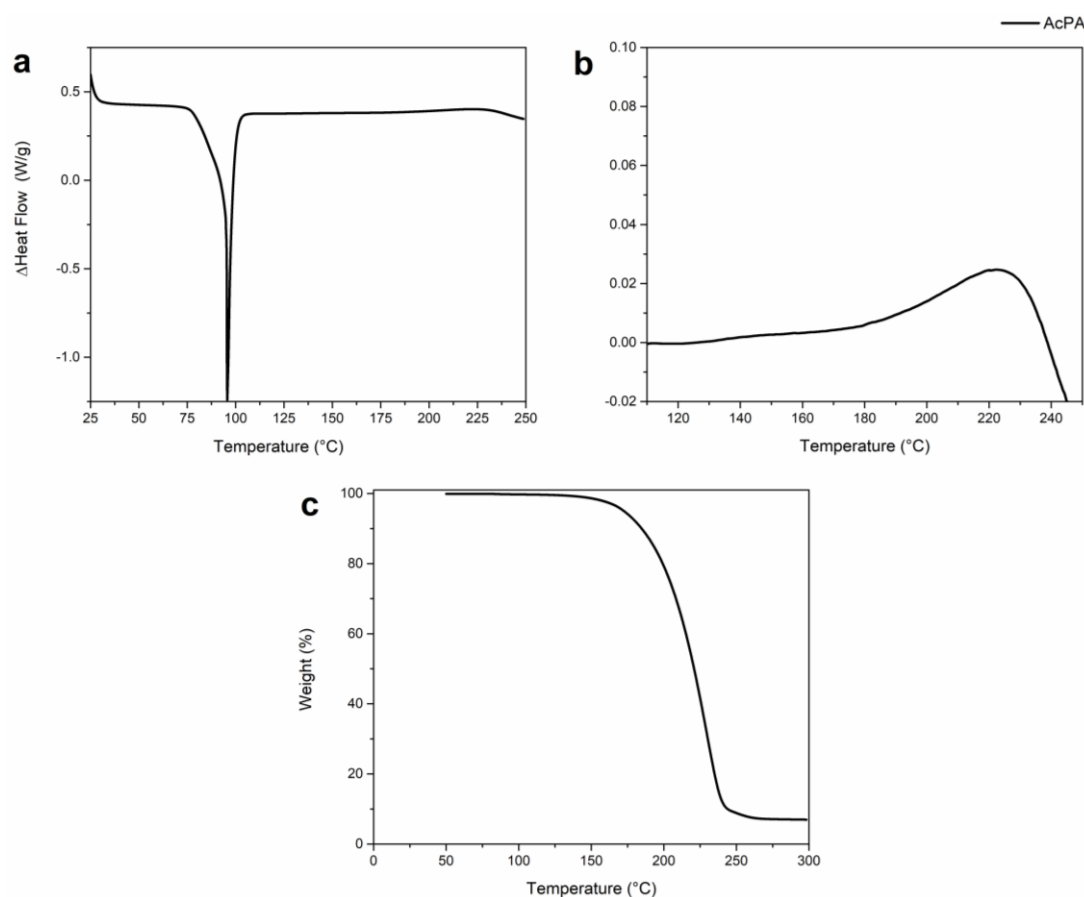


**Figure 6.11** Thermal analysis of AcPA for polymerization optimization. (a) Heating scan by high pressure DSC (b) Zoom in of heating scan in **a** showing the slight exotherm resulting from homopolymerization of AcPA (c) TGA of AcPA at  $10^\circ\text{C min}^{-1}$  under  $\text{N}_2$  atmosphere

## Catalyst Screening

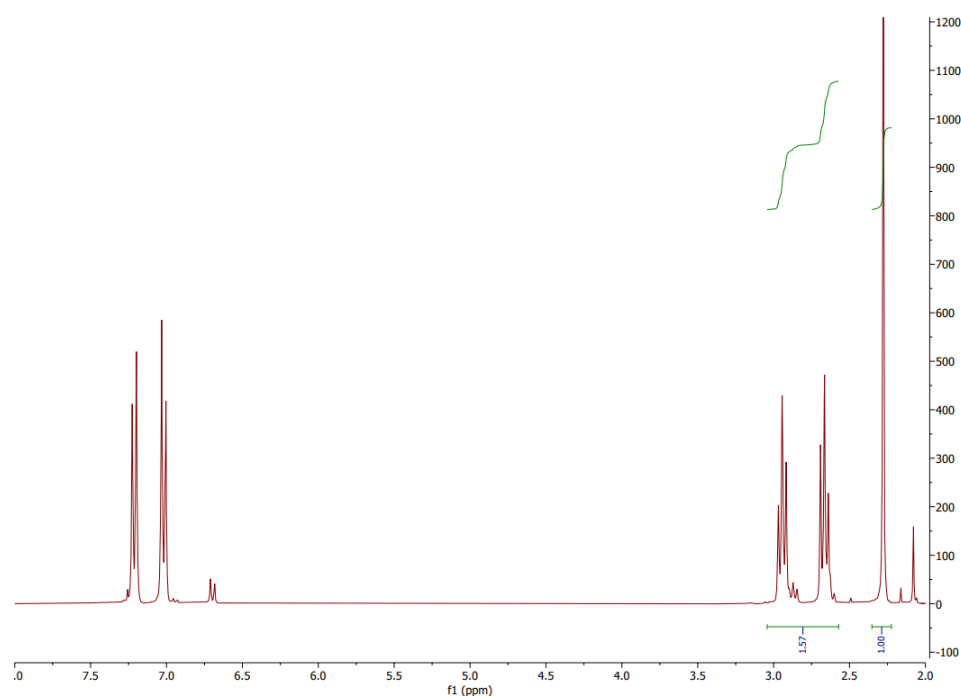


**Figure 6.14**  $^1\text{H}$  NMR of AcPA polymerization after 3 hours at 140°C

The homopolymerization of AcPA with and without catalyst was investigated by DSC. Based on the exotherm that occurs after the melting transition, AcPA begins to react around 117°C, with an exothermic peak max of 239°C (**Figure 6.5b**). Based off TGA, the AcPA monomer appears to begin degrading around 145-150°C (**Figure 6.5c**). Thus, the polymerization procedure began at a temperature of 140°C to avoid degradation reactions discussed earlier. As expected, almost no change was seen without catalyst at 140°C by  $^1\text{H}$  NMR.  $D_p$  increased from 1.11 to 1.12 after one hour, and to 1.18 after 3 hours (**Figure 6.6**).

A variety of base catalysts were screened by DSC. We postulated that bases that could facilitate the formation of anionic end groups and act as effective

phenoxide transfer catalyst in their conjugate acid form would perform the best. Three classes of catalyst were screened; carbonyl based, hydroxide based, and organobase. Thermograms of each class of base as well as the prototypical zinc catalyst at 10 mol% loading are shown in **Figure 6.7**. A loading of 10 mol% was used to ensure accurate weighting of each catalyst used at the micromolar scale. All of the shown DSC's are normalized to AcPA, meaning that positive values correspond with increased reactivity and negative values indicate lesser reactivity than catalyst-free conditions.

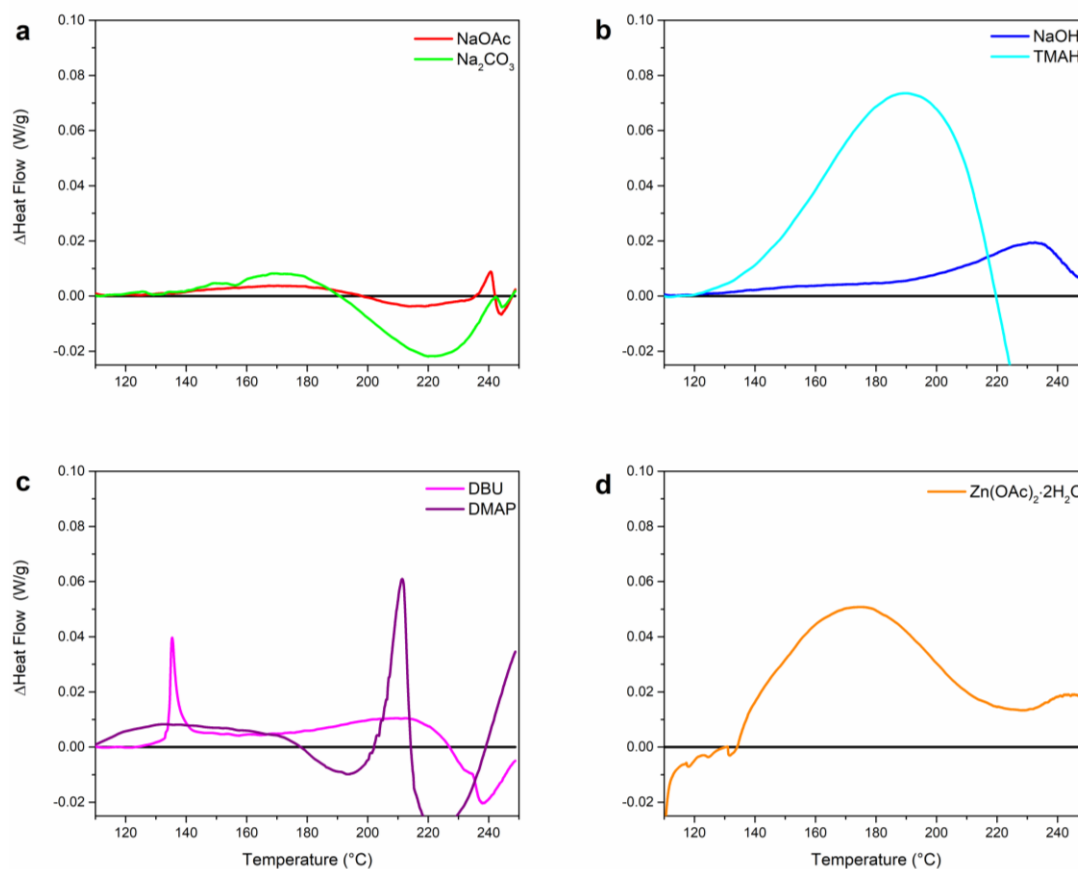


**Figure 6.15** High pressure DSC runs of AcPA with 10% of selected catalyst. Traces shown are the change in heat flow from AcPA run with no catalyst. (a) Carboxyl catalyst (b) Hydroxide based catalyst (c) Organobase catalyst (d) Traditionally used zinc catalyst for reference



Both NaOAc and Na<sub>2</sub>CO<sub>3</sub> were poor catalysts, with only a marginal increase in reactivity at lower temperatures of 140-180°C and lower reactivity above 200°C (**Figure 6.7a**). Both bases have similar pKa's to AcPA, likely resulting in poor formation of the carboxylate end group.<sup>17</sup> It is more likely that these bases promoted the polymerization through deprotonation of the protonated carboxylic acid group after nucleophilic attack. Hydroxide bases shown in **Figure 6.7b** were far more effective at catalyzing the reaction, with TMAH showing the largest exotherm of all catalyst screening. With TMAH and NaOH having pKa's of 14 and 15.7 respectively, they are effective at forming anionic carboxylate end groups. Both sodium and tetramethyl ammonium counter cations are hard Lewis acids, affording an increased propensity for activating the phenoxy nucleophile.<sup>17</sup> Organobase catalyst shown in **Figure 6.7c** also showed decent activity, though the higher temperatures required are much higher than their onset of oxidative degradation.<sup>18-23</sup> Thus, these catalysts were excluded from further consideration. The activity of the commonly employed Zn(OAc)<sub>2</sub>·2H<sub>2</sub>O is shown in **Figure 6.7d**. The zinc centered catalyst shows high activity, but also appears to catalyze a secondary reaction around 220-230°C. With the data presented in this study, TMAH appears to be the superior catalyst.

Utilizing 2.5 mol% TMAH, optimized conditions were developed based on the exotherm onset by DSC and <sup>1</sup>H NMR monitoring. After 3 and 4 hours at 140°C, degrees of polymerization of AcPA were 4.37 and 6.83 respectively. Given the D<sub>p</sub> of 6.00 obtained with Zn(OAc)<sub>2</sub>·2H<sub>2</sub>O after longer polymerization times and

vacuum at 200°C, TMAH is significantly more effective at catalyzing the polymerization of PPA. After 4 hours, the temperature was increase to 160°C, and a  $^1\text{H}$  NMR  $D_p$  of 21.69 was achieved. After increasing the temperature to 200°C, vacuum was pulled for 2 hours, resulting in a  $D_p$  of 70.19. After the vacuum step, PPA was no longer soluble in chloroform and had to be taken up in chloroform/trifluoroacetic acid mixture for analysis. While affording significantly higher  $M_n$  than the results of the initial screening with zinc catalyst, this still resulted in a low  $^1\text{H}$  NMR  $M_n$  of only 10,402 g mol $^{-1}$  (**Table 6.2**). Thus, TMAH loading was increased to 10 mol% utilizing the same conditions. At this loading, a substantially increased  $D_p$  of 268.89 and  $M_n$  of 39,853 g mol $^{-1}$  was obtained. To the best of our knowledge, this is a slight improvement to the highest reported PPA  $^1\text{H}$  NMR  $M_n$  reported of 38,400 g mol $^{-1}$ .<sup>13</sup> This reported method utilizes a three step cocatalyst system in which the first step employs NaOH, sequential solvent assisted polymerization and addition of metal catalyst, followed by removal of solvent and 3 hours of polymerization under vacuum at 240°C.<sup>13</sup> Our polymerization conditions with 2.5 mol% TMAH provide the same molecular weight with a shorter reaction time, lower temperature, and without the use of solvent. By increasing the temperature of the final step to 240°C  $M_n$  was further increased to 49,903 g mol $^{-1}$ , still utilizing shorter reaction time (9 hours vs 8 hours), no solvent, and without the use of two catalysts. It is worth noting that the referenced conditions also require additional time for solvent removal in between the second and final step.<sup>13</sup> TMAH can also be obtained from biological sources.<sup>24–26</sup> Thus, our continuous batch

conditions are substantially greener than what is currently reported in the literature.<sup>2,11,13</sup>

**Table 6.2** Results of optimization of PPA synthesis with hydroxide based catalyst. All polymerizations were conducted under N<sub>2</sub> at 140°C for 4 hours, 160°C for 1 hour, 200°C for 1 hour, then 2 hours at the final temperature under vacuum for 2 hours.

Catalyst	Final Temperature (°C)	D <sub>p</sub>	<sup>1</sup> H NMR M <sub>n</sub> (g/mol)	T <sub>d95%</sub> (°C)
2.5% TMAH	200	70.19	10,402	227
10% TMAH	200	268.89	39,853	211
10% TMAH	240	366.70	49,903	214
10% NaOH	240	48.08	7,125	202

In order to further understand the mechanism, we synthesized PPA using our optimized conditions with 10 mol% NaOH. In doing this, we were able to compare our conditions with TMAH and NaOH to the reported conditions using both NaOH and Zn(OAc)<sub>2</sub>·2H<sub>2</sub>O. With 10 mol% NaOH, a M<sub>n</sub> of only 7,125 g mol<sup>-1</sup> was obtained (**Table 6.2**). Therefore, it is clear that the activity of the 3 catalysts follows the trend TMAH>Zn(OAc)<sub>2</sub>·2H<sub>2</sub>O>NaOH. Additionally, the ability of the base to form anionic carboxylate end groups helps to form PPA oligomers at significantly lower temperatures than metal catalyst, but high molecular weight appears to be dependent on the Lewis acid. Na<sup>+</sup> is known to be a poor polycondensation catalyst, limiting NaOH to predominantly acting as a deprotonating agent. TMA<sup>+</sup> may perform as a better catalyst due to its small size and high charge density compared to Zn<sup>2+</sup>. Per hard/soft acid and base theory, Zn<sup>2+</sup> is classified as an intermediate acid while TMA<sup>+</sup> is a hard acid.<sup>17</sup> Given that phenolates and the carbonyl oxygens of carboxylic acids and esters are hard

bases, TMA<sup>+</sup> may simply be more effective at the stabilization on the phenoxy anion and/or the polarization of the carbonyl centers. Additionally, hydroxides are far more effective at forming carboxylate end groups than acetates, making TMAH more effective in both regards. TMAH is also homogenous in the melt, potentially allowing for higher reactivity. Due to the complexity of coordination complexes formed during polycondensations, computational studies would be useful in fully elucidating the roles of the catalyst.

### *Thermal Properties of PPA*

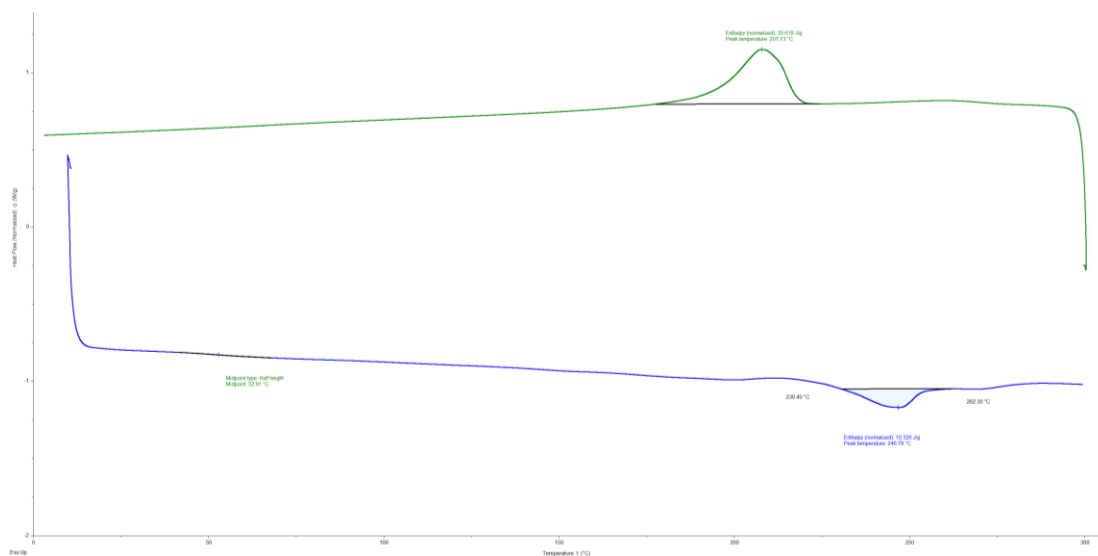


**Figure 6.16** Second heating cooling scan of PPA synthesized from optimized conditions.

The synthesized PPA was a high melting semi-crystalline polymer with a  $T_m$  of 247°C and a  $T_g$  of 53°C (**Figure 6.8**). With high  $M_n$  PPA in hand, we attempted to extrude the material to assess its tensile properties. However, PPA appears to be highly susceptible to thermal degradation, as extrusion at PPA's  $T_m$  endset of

265°C led to the liquification of the extrudate. The  $T_{d95\%}$  with 10 mol% TMAH was 214°C by TGA, with 22 weight percent being lost at the minimum extrusion temperature of 265°C (**Table 6.2**). This was far below the thermal stability needed for hot melt extrusion. Thermal stability with 2.5 mol% TMAH was better with 12 weight percent lost at extrusion temperature, but still poor. Because of the poor solubility of PPA, removal of catalyst residue by precipitation could not be achieved. Despite our significant improvement of PPA's molecular weight, its thermal stability was poor as previous literature has reported.<sup>2,11,13</sup> PPA may innately have poor thermal stability due to its aromatic ester bonds. The phenoxy structure present is a better leaving group than aliphatic counterparts by roughly 5 orders of magnitude. Despite this, the improvement of the molecular weight presented is still a significant step in improving PPA synthesis. Current studies into the degradation mechanism and improvement of the thermal stability are underway.

## Conclusion

PPA is a promising biobased polyester due to having a high  $T_m$  comparable to PET and PEF. Synthesis of high molecular weight PPA has been challenging due to its monomer's low reactivity towards polymerization compared to side reactions and decomposition. In this study, we employed base catalysts to form anionic end groups so that the polymerization could proceed at lower temperature. DSC was utilized as a high-throughput screening method for catalyst screening. With optimized conditions a  $^1\text{H}$  NMR  $M_n$  of up to 49,903 g mol<sup>-1</sup> was achieved. Solubility

was improved but still require a small amount of trifluoroacetic acid for analysis. The resulting polyester exhibited a melting transition of 247°C but poor thermal stability remained an issue. Investigation into other catalysts, blending, and additives for modulating the thermal stability is currently underway.

## References

- (1) Miller, S. A. Sustainable Polymers: Opportunities for the Next Decade. *ACS Macro Lett.* **2013**, 2 (6), 550–554.
- (2) Mialon, L.; Pemba, A. G.; Miller, S. A. Biorenewable Polyethylene Terephthalate Mimics Derived from Lignin and Acetic Acid. *Green Chem.* **2010**, 12 (10), 1704–1706.
- (3) Papadopoulos, L.; Zamboulis, A.; Kasmi, N.; Wahbi, M.; Nannou, C.; Lambropoulou, D. A.; Kostoglou, M.; Papageorgiou, G. Z.; Bikiaris, D. N. Investigation of the Catalytic Activity and Reaction Kinetic Modeling of Two Antimony Catalysts in the Synthesis of Poly(Ethylene Furanoate). *Green Chem.* **2021**, 23 (6), 2507–2524.
- (4) Konstantopoulou, M.; Terzopoulou, Z.; Nerantzaki, M.; Tsagkalias, J.; Achilias, D. S.; Bikiaris, D. N.; Exarhopoulos, S.; Papageorgiou, D. G.; Papageorgiou, G. Z. Poly(Ethylene Furanoate-Co-Ethylene Terephthalate) Biobased Copolymers: Synthesis, Thermal Properties and Cocrystallization Behavior. *Eur. Polym. J.* **2017**, 89, 349–366.
- (5) Isikgor, F. H.; Remzi Becer, C. Lignocellulosic Biomass: A Sustainable Platform for the Production of Bio-Based Chemicals and Polymers. *Polym. Chem.* **2015**, 6 (25), 4497–4559.
- (6) Pion, F.; Reano, A. F.; Oulame, M. Z.; Barbara, I.; Flourat, A. L.; Ducrot, P.-H.; Allais, F. Chemo-Enzymatic Synthesis, Derivatizations, and

- Polymerizations of Renewable Phenolic Monomers Derived from Ferulic Acid and Biobased Polyols: An Access to Sustainable Copolyesters, Poly(Ester-Urethane)s, and Poly(Ester-Alkenamer)s. In *Green Polymer Chemistry: Biobased Materials and Biocatalysis*; ACS Symposium Series; American Chemical Society, 2015; Vol. 1192, pp 41–68.
- (7) Nguyen, H. T. H.; Suda, E. R.; Bradic, E. M.; Hvozdoch, J. A.; Miller, S. A. Polyesters from Bio-Aromatics. In *Green Polymer Chemistry: Biobased Materials and Biocatalysis*; ACS Symposium Series; American Chemical Society, 2015; Vol. 1192, pp 401–409.
- (8) Lochab, B.; Shukla, S.; Varma, I. K. Naturally Occurring Phenolic Sources: Monomers and Polymers. *RSC Adv.* **2014**, *4* (42), 21712–21752.
- (9) Lancefield, C. S.; Westwood, N. J. The Synthesis and Analysis of Advanced Lignin Model Polymers. *Green Chem.* **2015**, *17* (11), 4980–4990.
- (10) Kaneko, T.; Thi, T. H.; Shi, D. J.; Akashi, M. Environmentally Degradable, High-Performance Thermoplastics from Phenolic Phytomonomers. *Nat. Mater.* **2006**, *5* (12), 966–970.
- (11) Bloom, M. E.; Vicentin, J.; Honeycutt, D. S.; Marsico, J. M.; Geraci, T. S.; Miri, M. J. Highly Renewable, Thermoplastic Tetrapolyesters Based on Hydroquinone, p -Hydroxybenzoic Acid or Its Derivatives, Phloretic Acid, and Dodecanedioic Acid. *Journal of Polymer Science Part A: Polymer Chemistry* **2018**, *56* (14), 1498–1507.



- (12) Buyle Padias, A.; Hall, H. K., Jr. Mechanism Studies of LCP Synthesis. *Polymers* **2011**, 3 (2), 833–845.
- (13) Schijndel, J.; Molendijk, D.; Beurden, K.; Vermeulen, R.; Noël, T.; Meuldijk, J. Repeatable Molecularly Recyclable Semi-aromatic Polyesters Derived from Lignin. *J. Polym. Sci. A* **2020**, 58 (12), 1655–1663.
- (14) Kinnertová, E.; Slovák, V. Kinetics of Resorcinol–Formaldehyde Polycondensation by DSC. *J. Therm. Anal. Calorim.* **2018**, 134 (2), 1215–1222.
- (15) Achilias, D. S. Investigation of the Radical Polymerization Kinetics Using DSC and Mechanistic or Isoconversional Methods. *J. Therm. Anal. Calorim.* **2014**, 116 (3), 1379–1386.
- (16) Achilias, D. S.; Siafaka, P. I. Polymerization Kinetics of Poly(2-Hydroxyethyl Methacrylate) Hydrogels and Nanocomposite Materials. *Processes* **2017**, 5 (2), 21.
- (17) Atkins, P.; de Paula, J. *Atkins' Physical Chemistry*; OUP Oxford, 2010.
- (18) Flores, I.; Demarteau, J.; Müller, A. J.; Etxeberria, A.; Irusta, L.; Bergman, F.; Koning, C.; Sardon, H. Screening of Different Organocatalysts for the Sustainable Synthesis of PET. *Eur. Polym. J.* **2018**, 104, 170–176.
- (19) Jehanno, C.; Flores, I.; Dove, A. P.; Müller, A. J.; Ruipérez, F.; Sardon, H. Organocatalysed Depolymerisation of PET in a Fully Sustainable Cycle Using Thermally Stable Protic Ionic Salt. *Green Chem.* **2018**, 20 (6), 1205–1212.

- (20) Basterretxea, A.; Jehanno, C.; Mecerreyes, D.; Sardon, H. Dual Organocatalysts Based on Ionic Mixtures of Acids and Bases: A Step Toward High Temperature Polymerizations. *ACS Macro Lett.* **2019**, 8 (8), 1055–1062.
- (21) Bossion, A.; Heifferon, K. V.; Meabe, L.; Zivic, N.; Taton, D.; Hedrick, J. L.; Long, T. E.; Sardon, H. Opportunities for Organocatalysis in Polymer Synthesis via Step-Growth Methods. *Prog. Polym. Sci.* **2019**, 90, 164–210.
- (22) Coady, D. J.; Fukushima, K.; Horn, H. W.; Rice, J. E.; Hedrick, J. L. Catalytic Insights into Acid/Base Conjugates: Highly Selective Bifunctional Catalysts for the Ring-Opening Polymerization of Lactide. *Chem. Commun.* **2011**, 47 (11), 3105–3107.
- (23) Procuranti, B.; Connon, S. J. Unexpected Catalysis: Aprotic Pyridinium Ions as Active and Recyclable Brønsted Acid Catalysts in Protic Media. *Org. Lett.* **2008**, 10 (21), 4935–4938.
- (24) Anthoni, U.; Bohlin, L.; Larsen, C.; Nielsen, P.; Nielsen, N. H.; Christophersen, C. Tetramine: Occurrence in Marine Organisms and Pharmacology. *Toxicon* **1989**, 27 (7), 707–716.
- (25) Dolan, L. C.; Matulka, R. A.; Burdock, G. A. Naturally Occurring Food Toxins. *Toxins* **2010**, 2 (9), 2289–2332.
- (26) Henry, A. J. The Toxic Principle of Courbonia Virgata; Its Isolation and Identification as a Tetramethylammonium Salt. *Br. J. Pharmacol. Chemother.* **1948**, 3 (3), 187.

## CHAPTER 7:

### Outlook

#### **Conclusion**

In this dissertation, the synthesis, characterization, blending, and optimization of lignopolyesters has been described. Our work also demonstrates the high potential of these materials. In Chapter 2, a synthetically simple platform from lignin derivatives is utilized to generate a diverse array of materials. Chapter 3 describes the modification of what may be the most interesting material from this class, a non-crosslinked shape memory elastomer. In this chapter we describe the tuning of its properties for different applications. Chapters 4 and 5 describe the use of these polyesters as additives for PBS and PHA, improving their tensile properties. Finally, Chapter 6 represents a significant step in the future application of PPA and derivatives, a desperately needed class of biopolyesters.

#### **Future Work**

Formulation of PEP, PiPP, and PEHF with various additives and performance enhancers need to be explored so that they can be utilized in different applications. Degradation additives for the accelerated degradation of these derivatives are of particular interest. There are also several copolymers that should be explored among the monomers reported in this dissertation. Further studies on the thermomechanical properties of PiPP are needed to fully understand its shape

memory properties. Further derivatization and analysis of similar linkers with iso groups is currently underway. Additionally, modification of PiPP via reactive extrusion with other chain extenders is an area that should be explored. Furthermore, application of the described polyesters in blends is of interest given their high performance. Investigation of the morphology of these blends is needed to fully understand their properties. Finally, continued catalyst optimization of PPA synthesis and improvement of its thermal properties could lead to a highly valuable material. PPA's performance in blends and compostability also needs to be investigated.

### **Final Remarks**

This contribution to the scalable synthesis and extensive characterization of lignopolyesters demonstrates their potential to replace petrol-based polymers. The research detailed within is a significant step in the advancement of this field of study. Further investigation into the structure-property relationships of these materials could aid in developing new generations of lignopolyesters for different applications.

## Appendix

### Supporting Information for Semi-Aromatic Biobased Polyesters Derived From Lignin and Cyclic Carbonates

## NMR Spectra

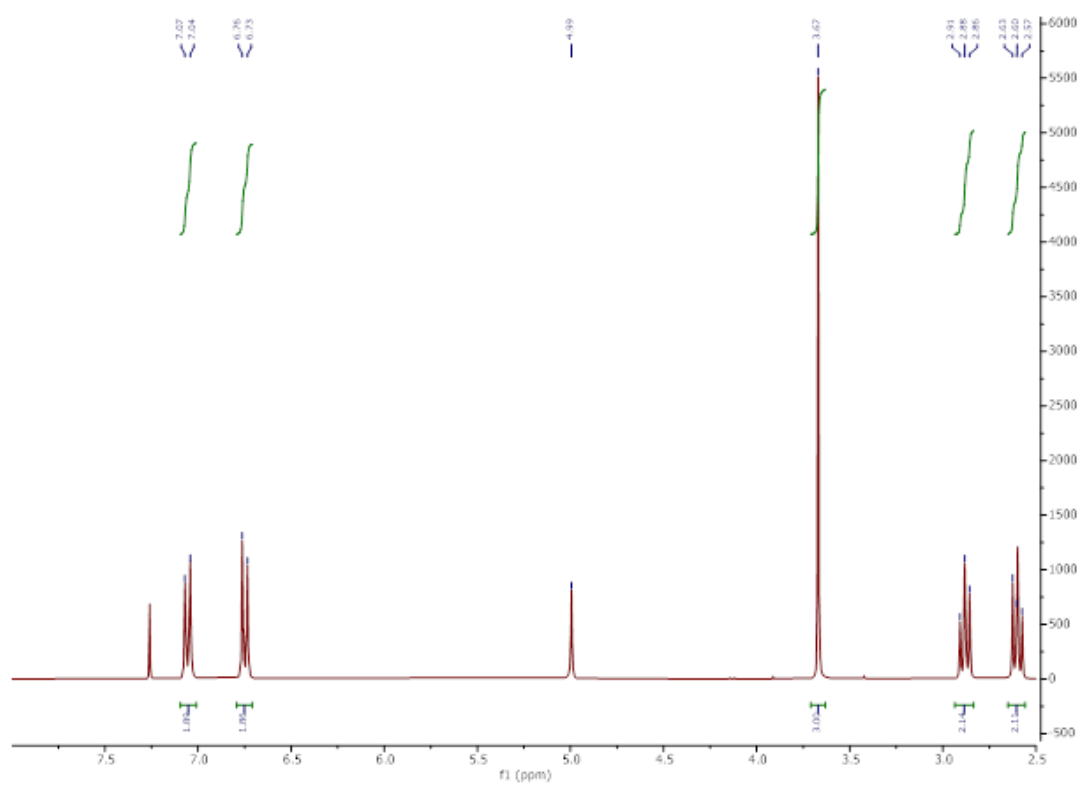


**Figure A.1**  $^1\text{H}$  NMR spectrum of methyl 3-(4-hydroxyphenyl)propanoate

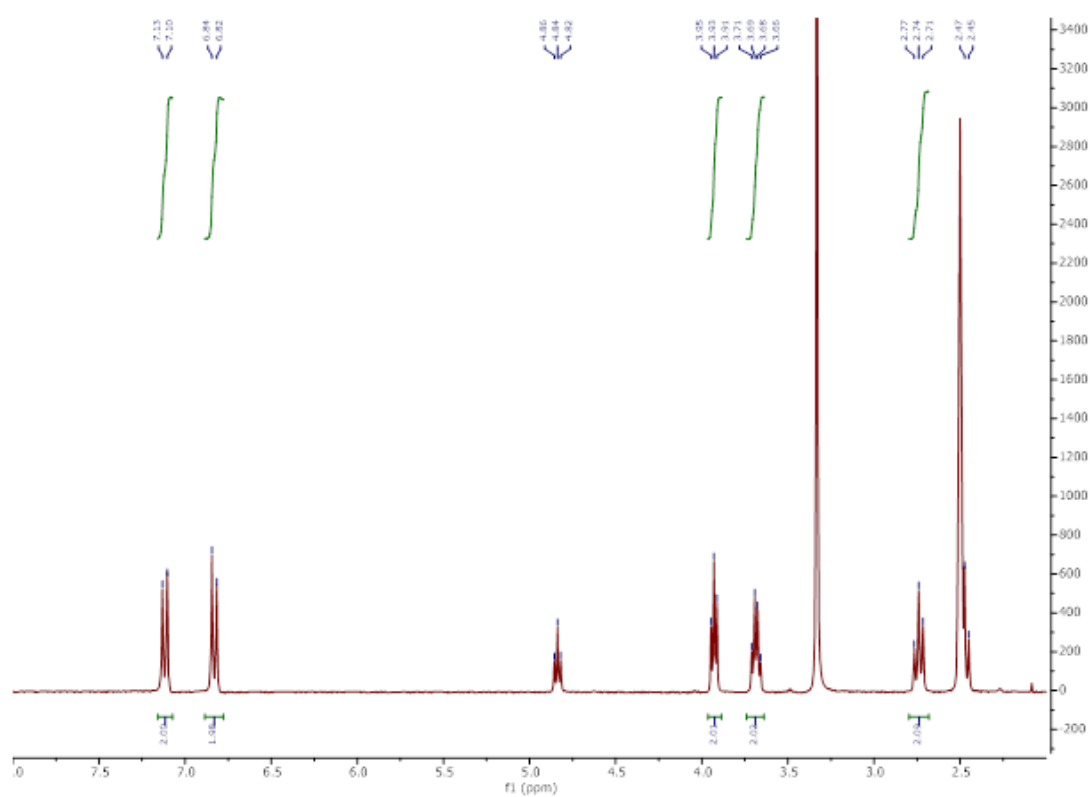


**Figure A.2**  $^1\text{H}$  NMR spectrum of 3-(4-(2-hydroxyethoxy)-3-methoxyphenyl)propanoic acid

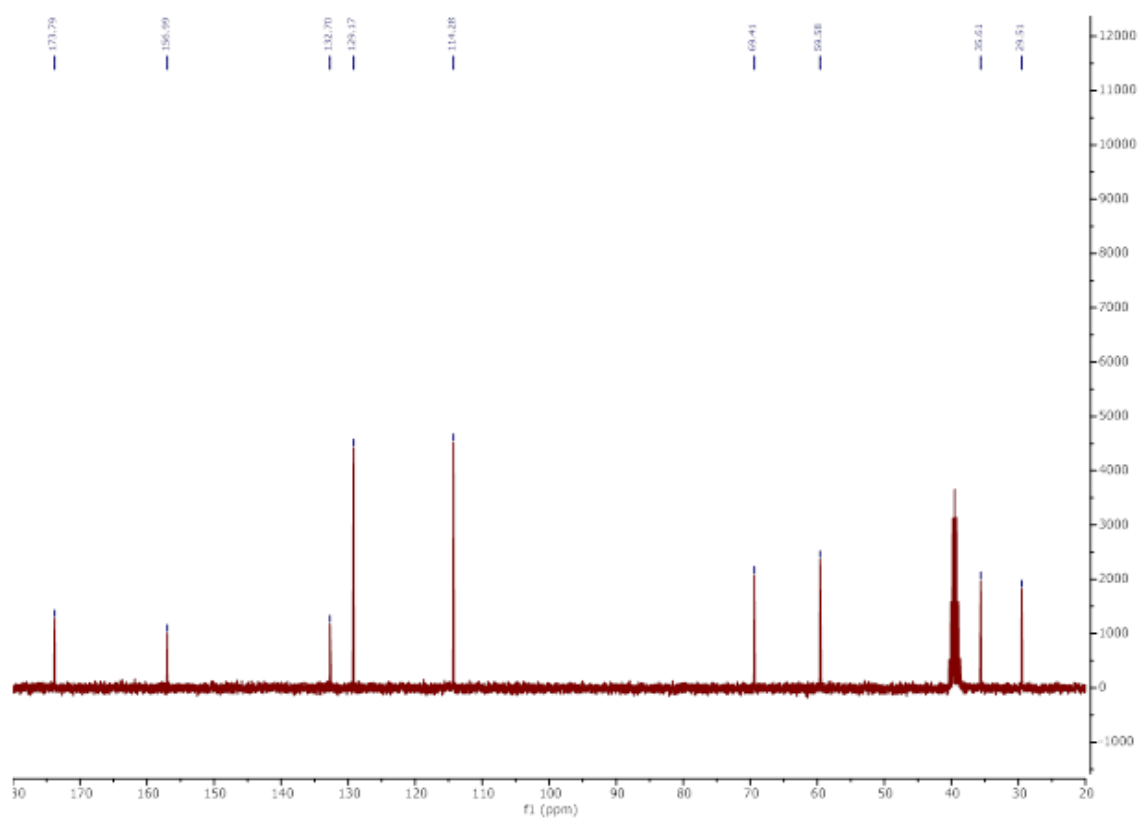


**Figure A.15**  $^{13}\text{C}$  NMR spectrum of 4-(2-hydroxyethoxy)phenylpropanoic acid



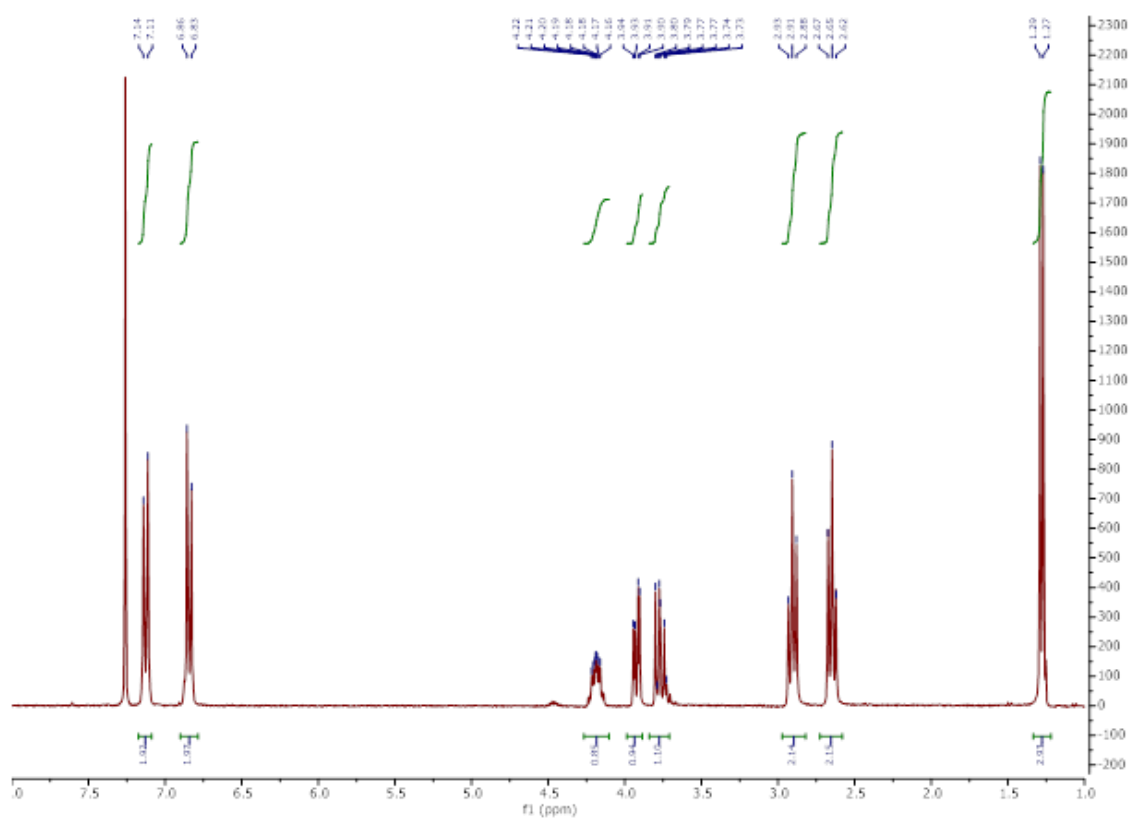


**Figure A.16**  $^1\text{H}$  NMR spectrum of 3-(4-(2-hydroxypropoxy)phenyl)propanoic acid

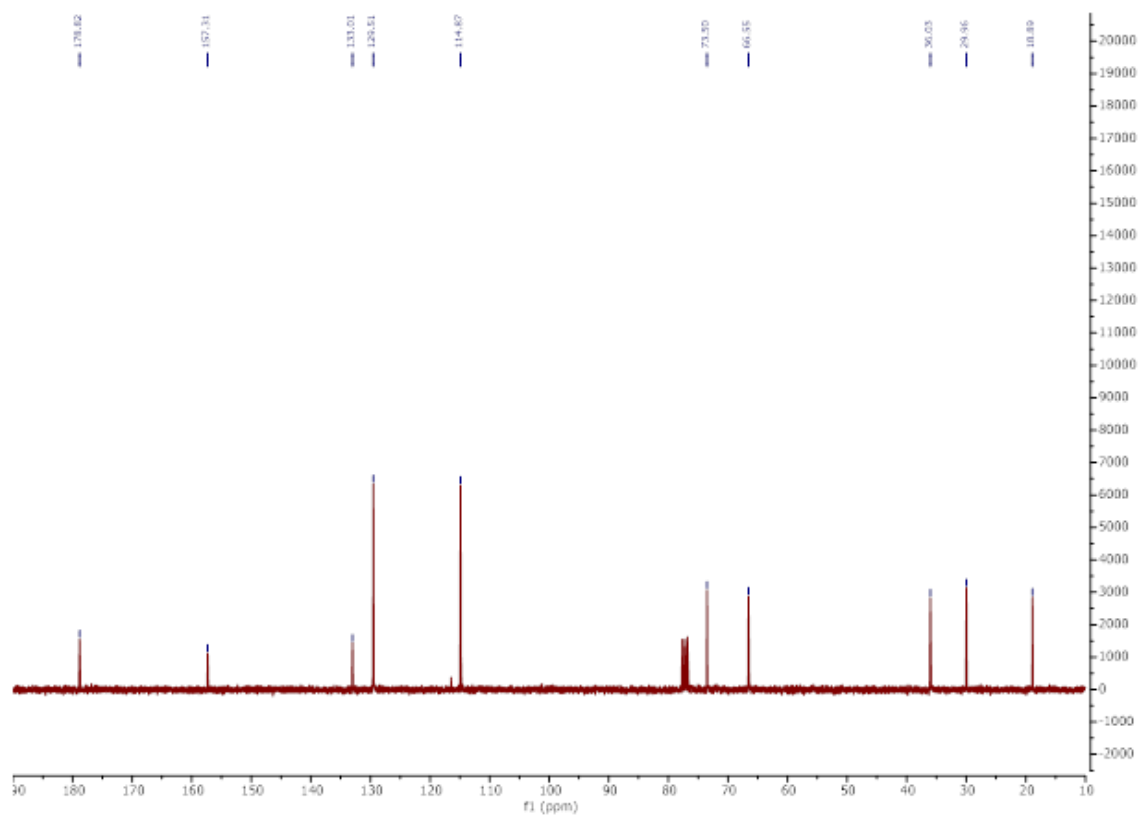


**Figure A.17**  $^{13}\text{C}$  NMR spectrum of 3-(4-(2-hydroxypropoxy)phenyl)propanoic acid

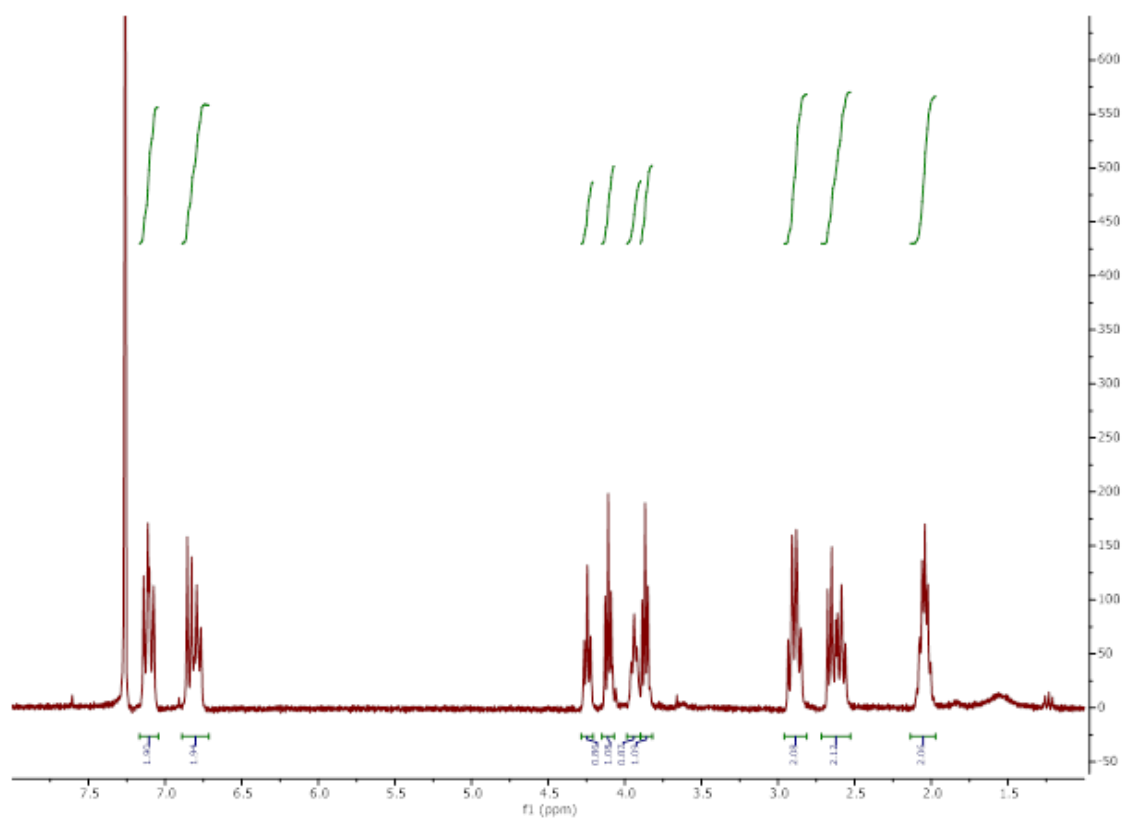


**Figure A.18**  $^1\text{H}$  NMR spectrum of 4-(3-hydroxypropoxy)phenylpropanoic acid

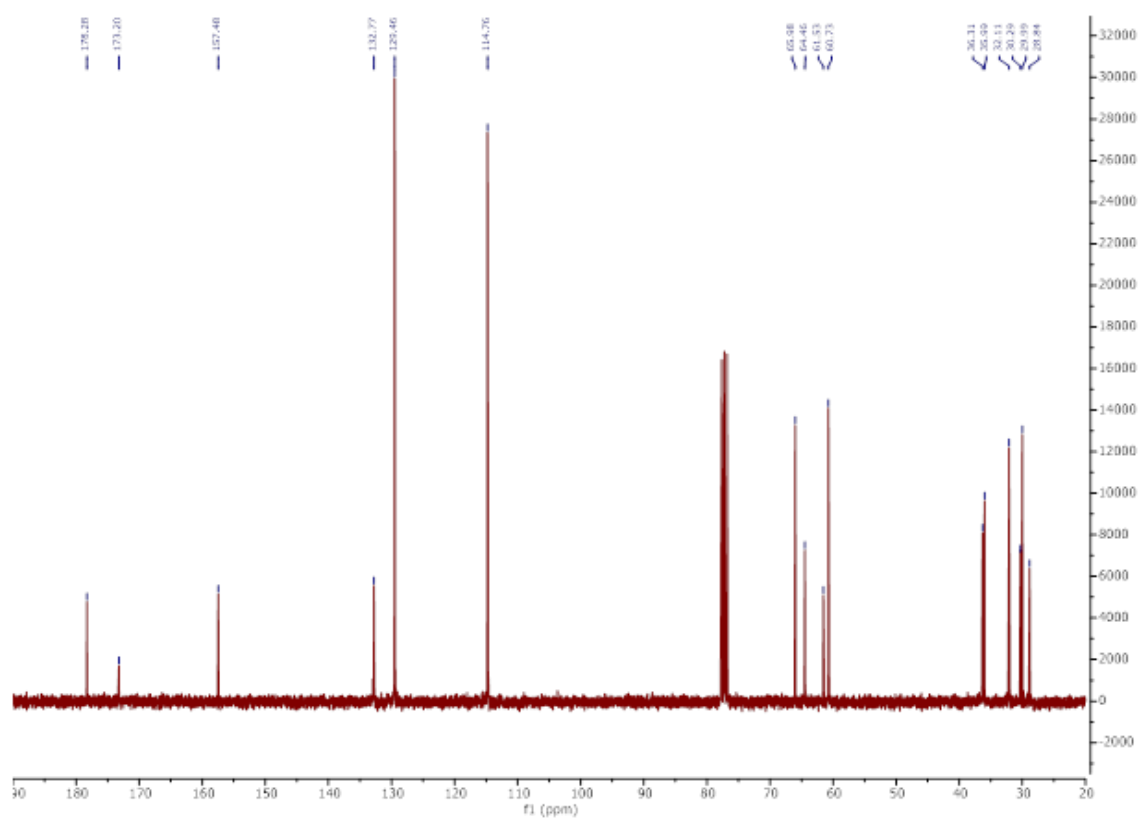


**Figure A.19** <sup>13</sup>C NMR spectrum of 4-(3-hydroxypropoxy)phenylpropanoic acid

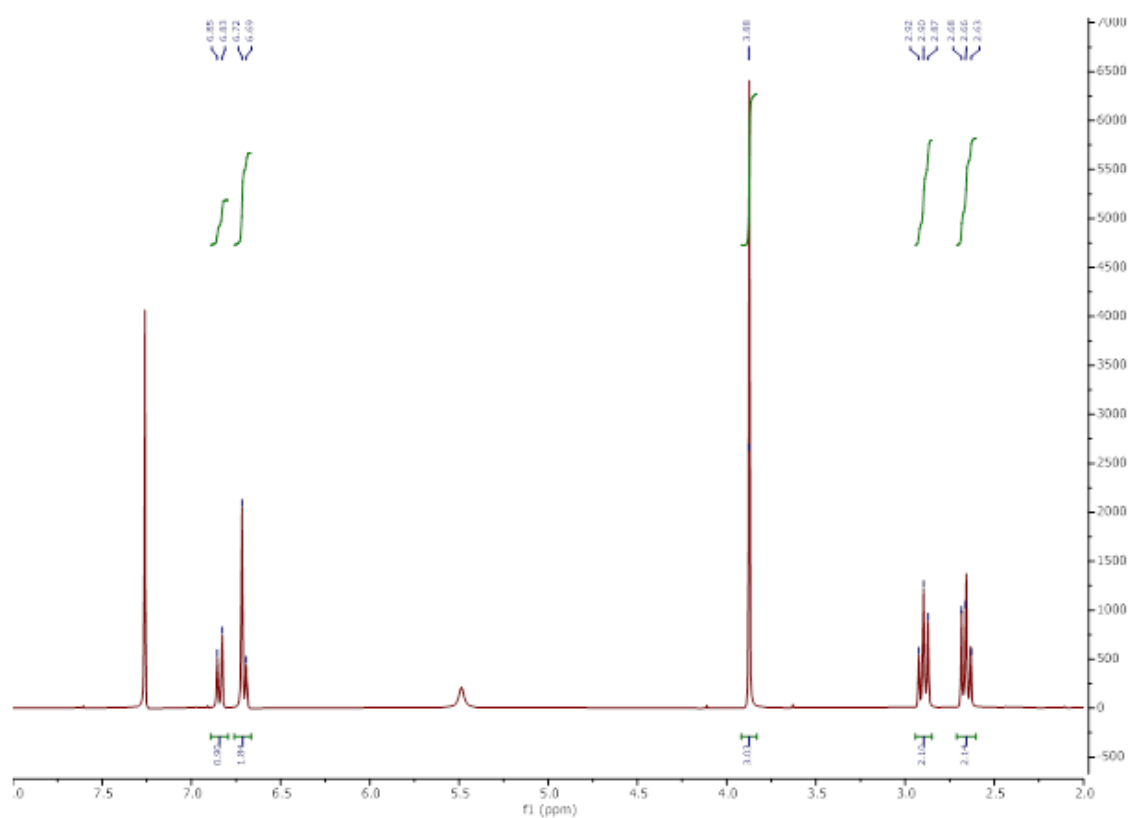


**Figure A.20**  $^1\text{H}$  NMR spectrum of 3-(4-hydroxy-3-methoxyphenyl)propionic Acid

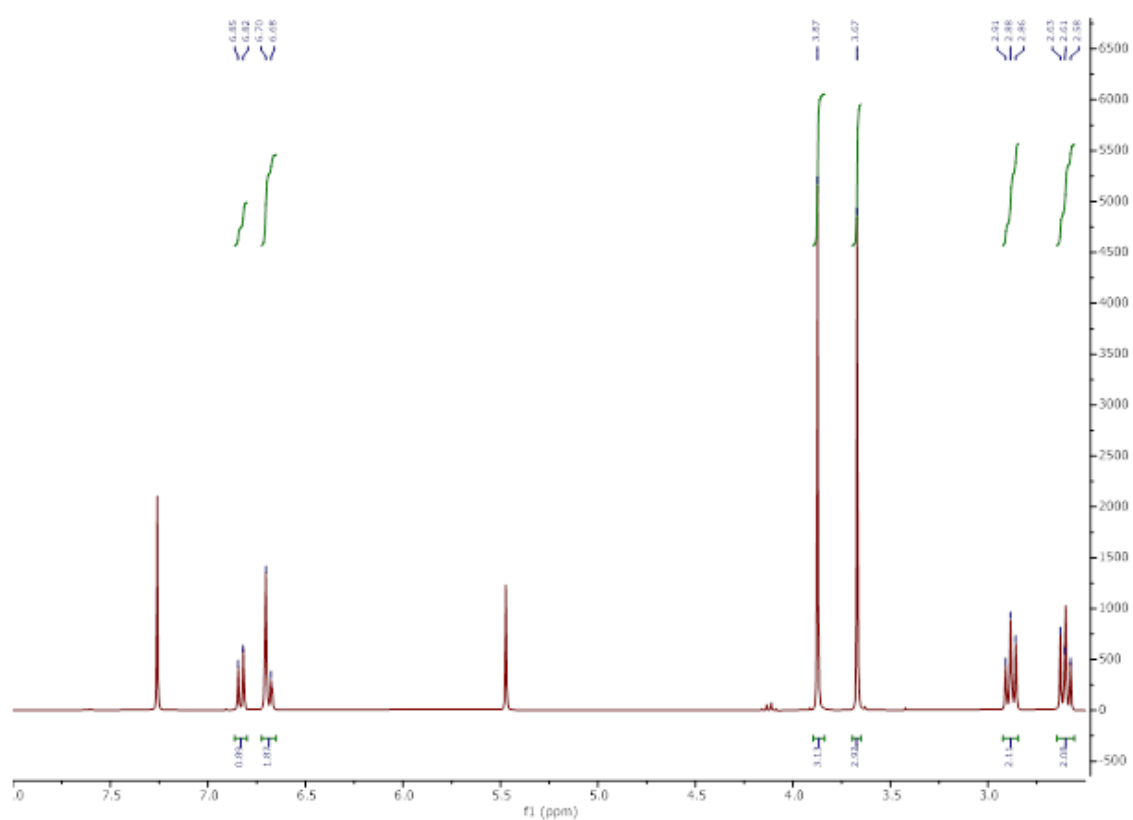


**Figure A.21**  $^1\text{H}$  NMR spectrum of methyl 3-(4-hydroxy-3-methoxyphenyl)propanoate

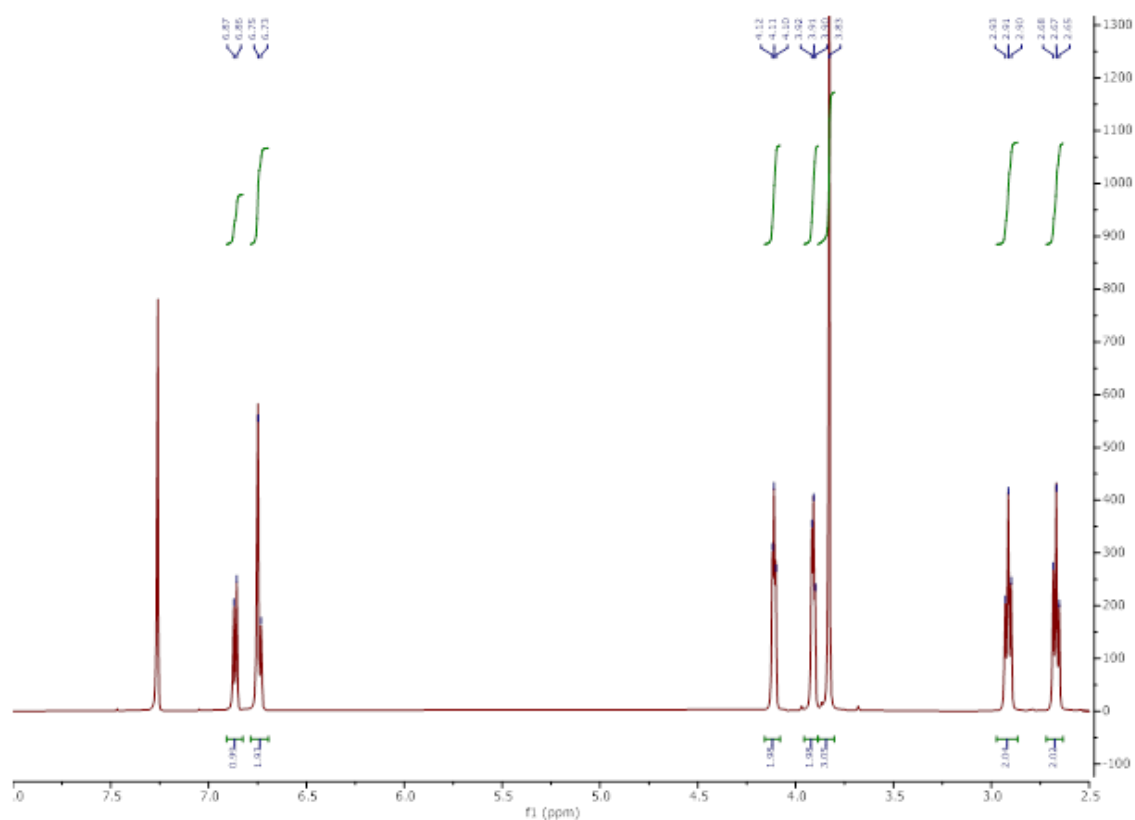


**Figure A.22**  $^1\text{H}$  NMR spectrum of 3-(4-(2-hydroxyethoxy)-3-methoxyphenyl)propanoic acid

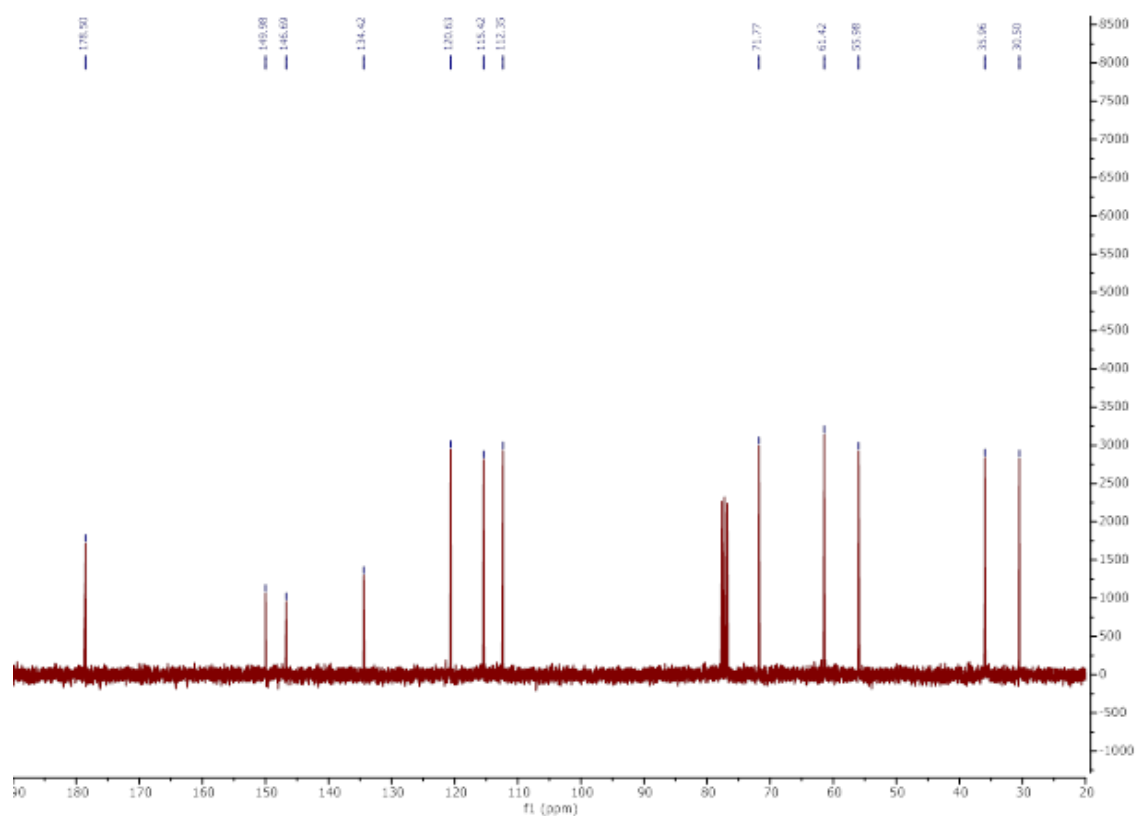


**Figure A.23**  $^{13}\text{C}$  NMR spectrum of 3-(4-(2-hydroxyethoxy)-3-methoxyphenyl)propanoic acid



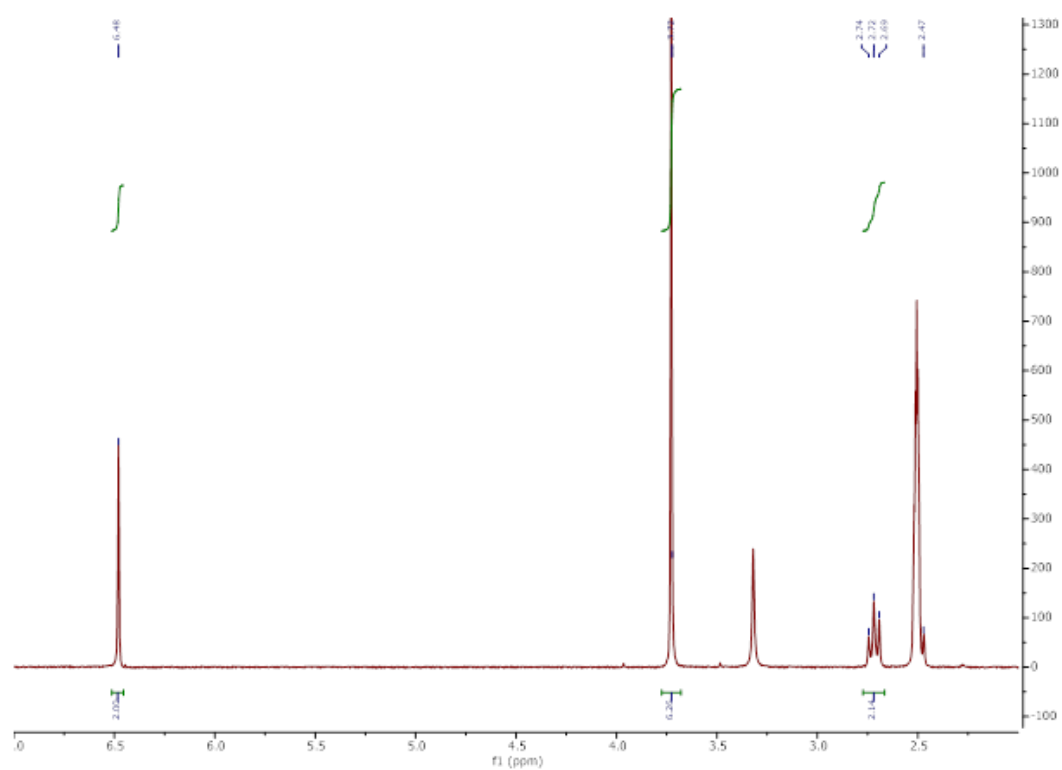


**Figure A.24**  $^1\text{H}$  NMR spectrum of 3-(4-hydroxy-3,5-dimethoxyphenyl)propanoic acid

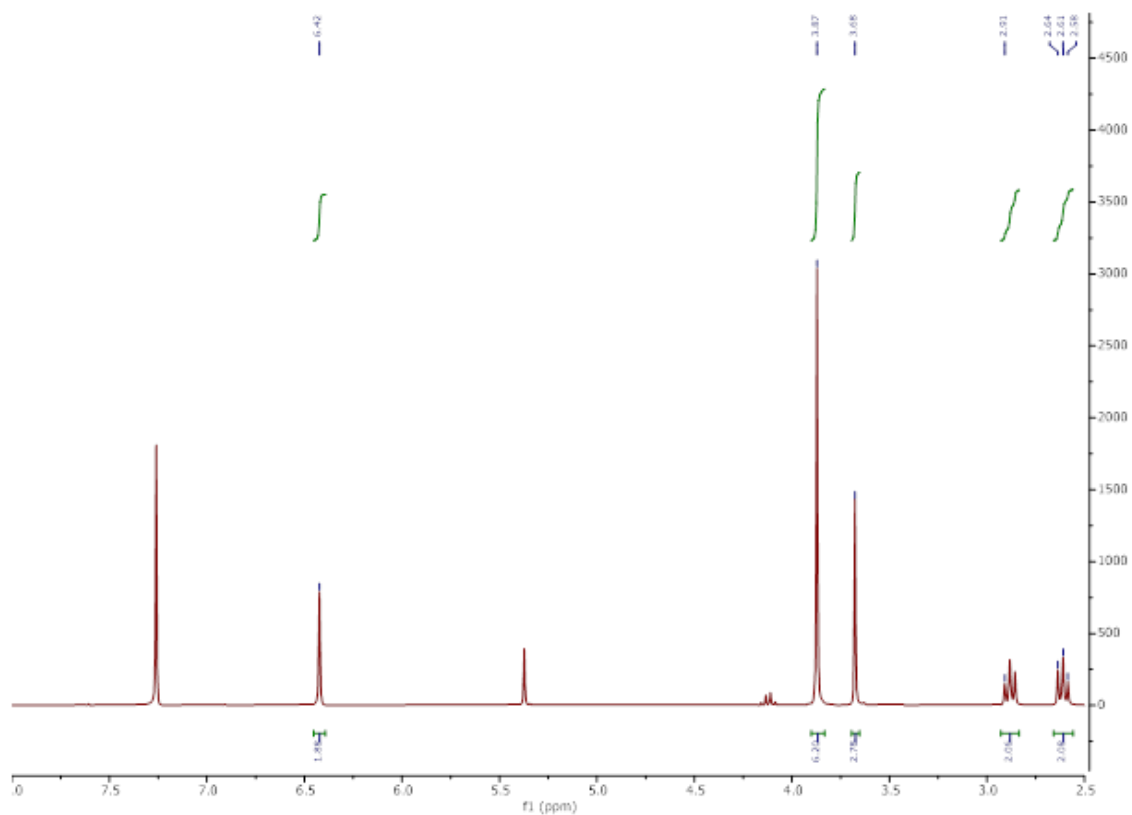


**Figure A.25**  $^1\text{H}$  NMR spectrum of methyl 3-(4-hydroxy-3,5-dimethoxyphenyl)propanoate

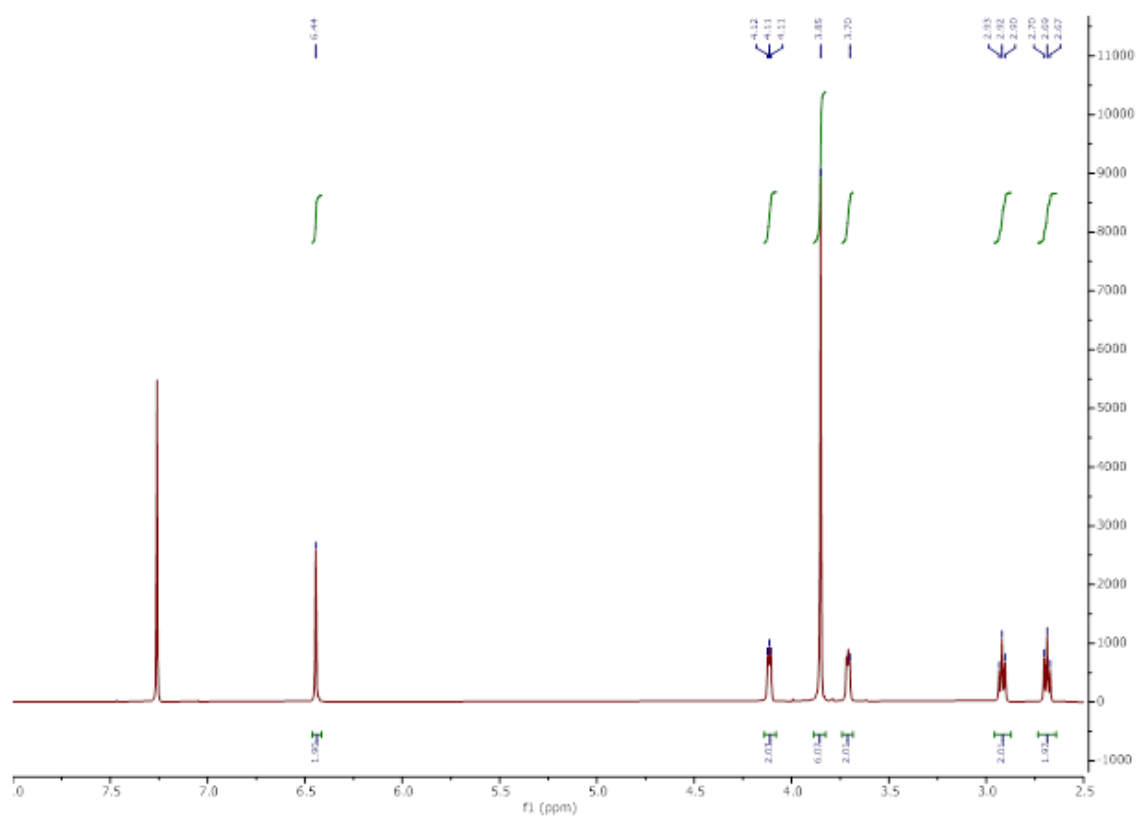


**Figure A.26**  $^1\text{H}$  NMR spectrum of 3-(4-(2-hydroxyethoxy)-3,5-dimethoxyphenyl)propanoic acid

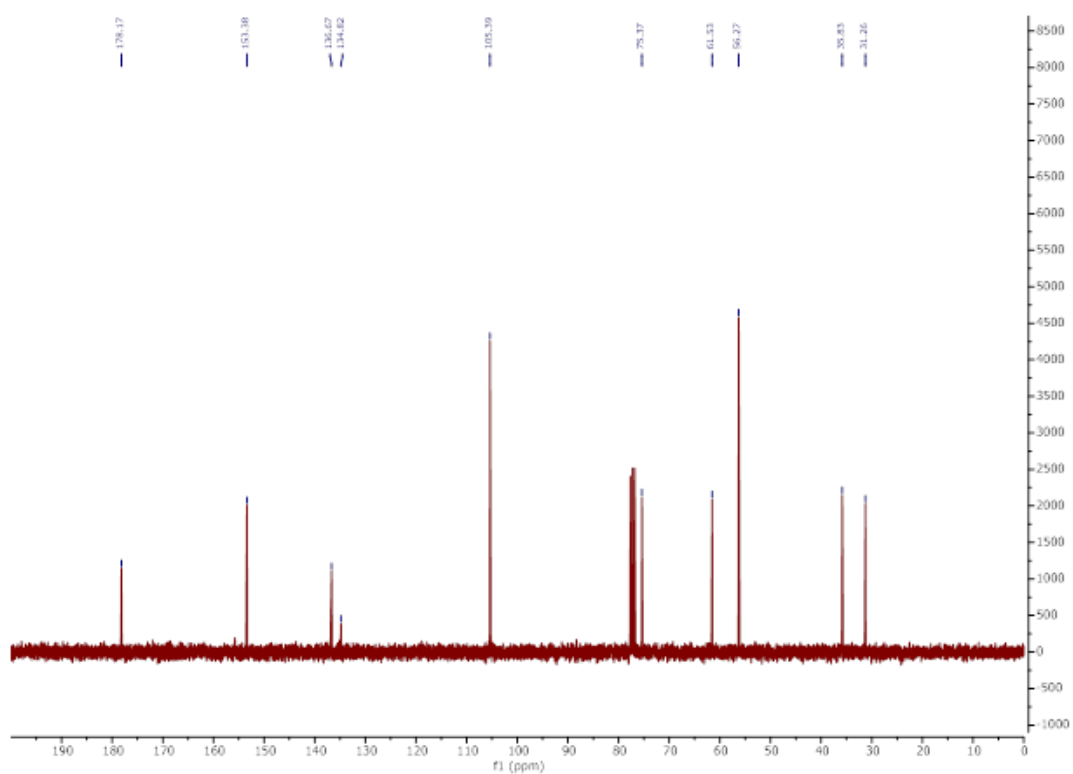


**Figure A.27**  $^{13}\text{C}$  NMR spectrum of 3-(4-(2-hydroxyethoxy)-3,5-dimethoxyphenyl)propanoic acid

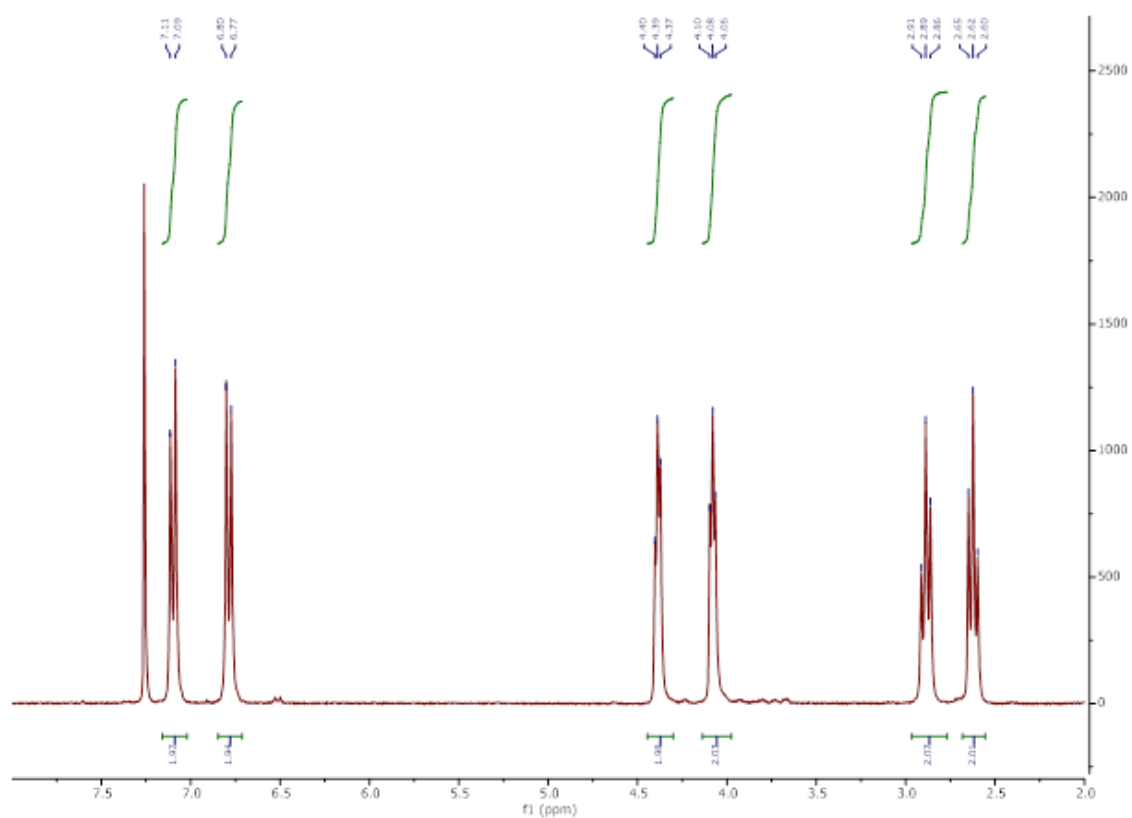


**Figure A.28**  $^1\text{H}$  NMR spectrum of polyethylene phloretate

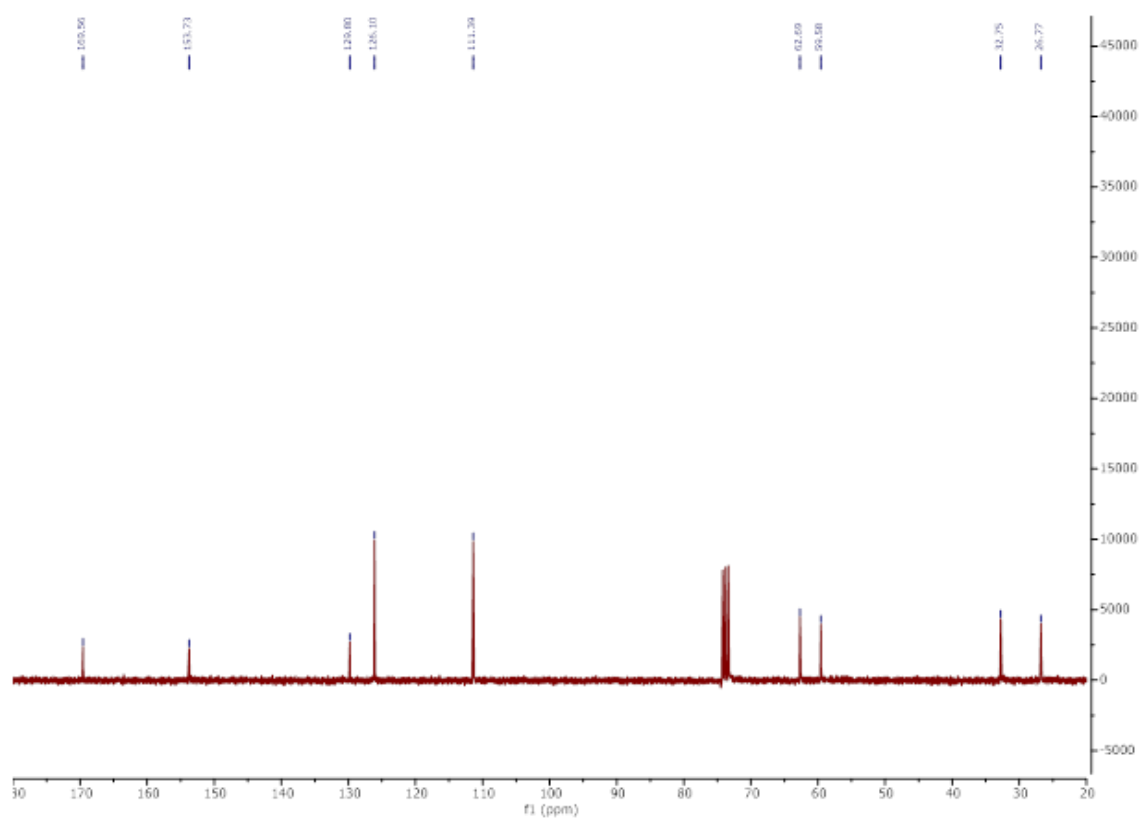


**Figure A.29**  $^{13}\text{C}$  NMR spectrum of polyethylene phloretate

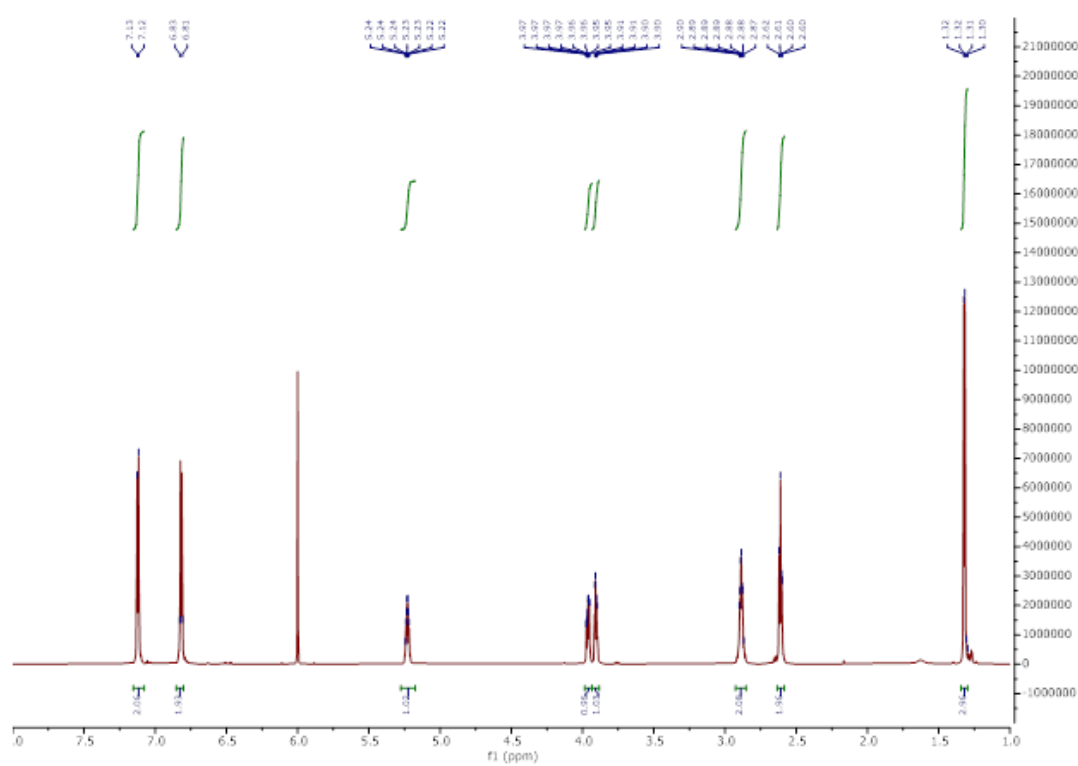


**Figure A.30**  $^1\text{H}$  NMR spectrum of polyisopropyl phloretate (PiPP)

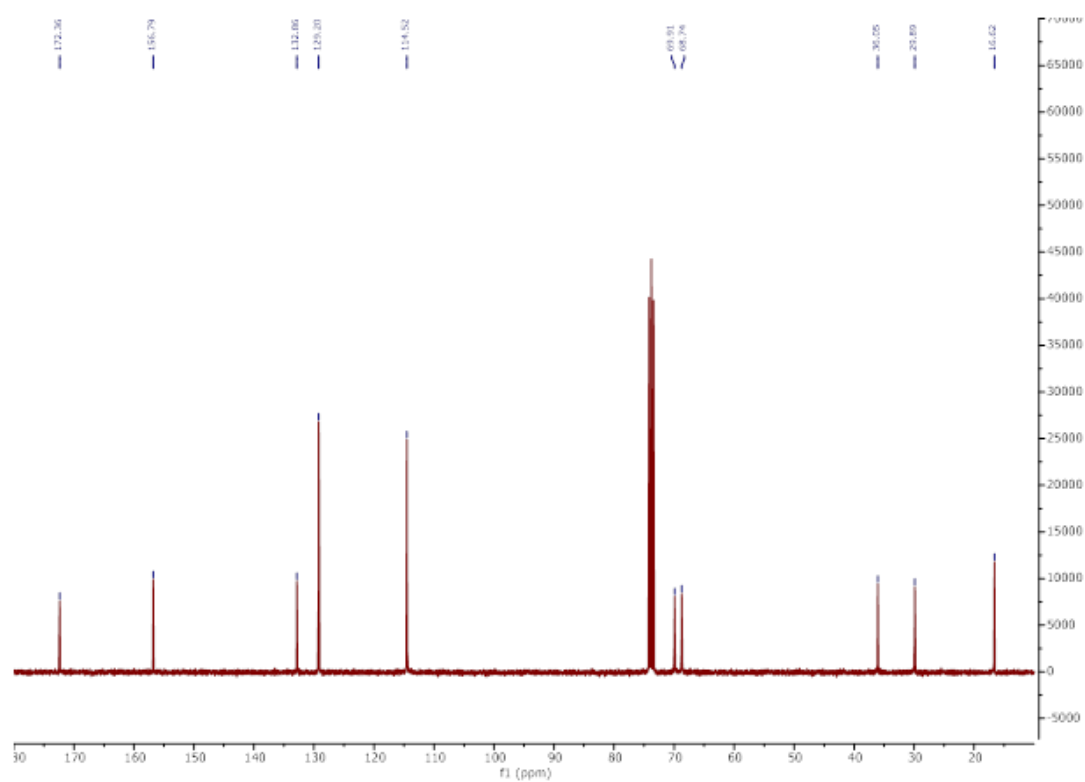


**Figure A.31**  $^{13}\text{C}$  NMR spectrum of polyisopropyl phloretate (PiPP)



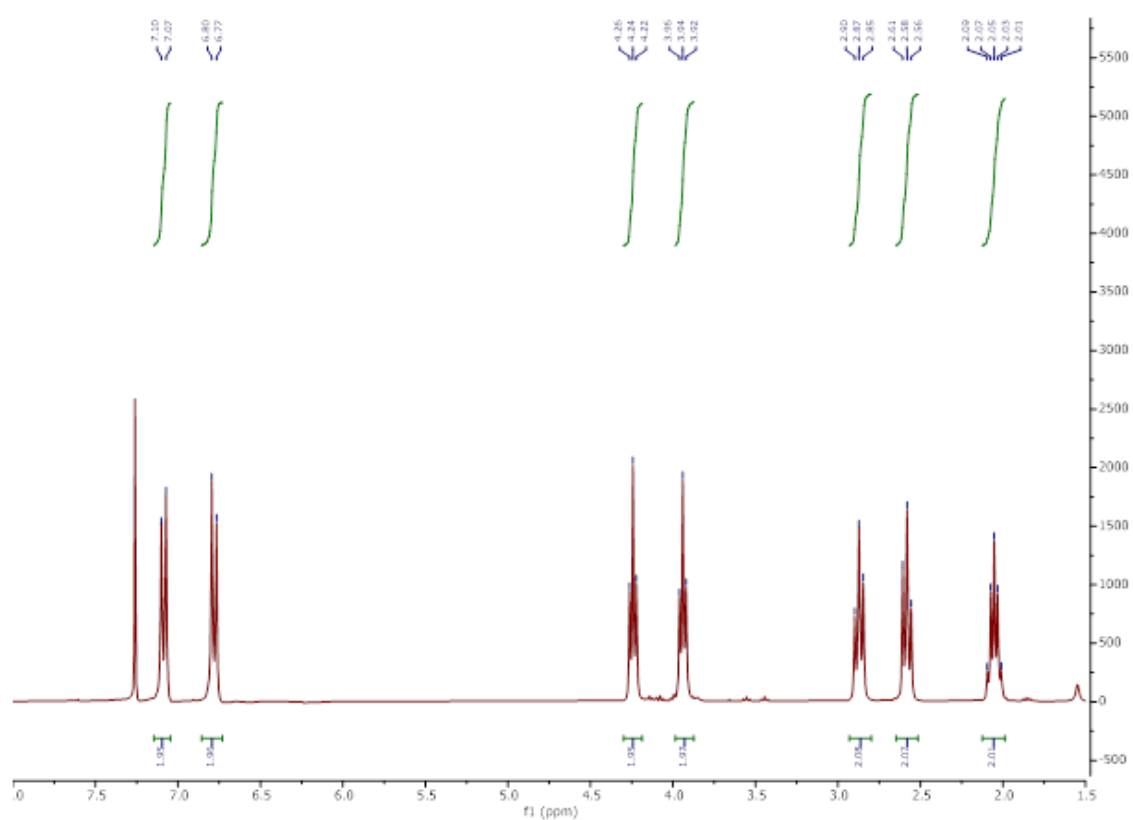


**Figure A.32**  $^1\text{H}$  NMR spectrum of polypropylene phloretate (PPP)

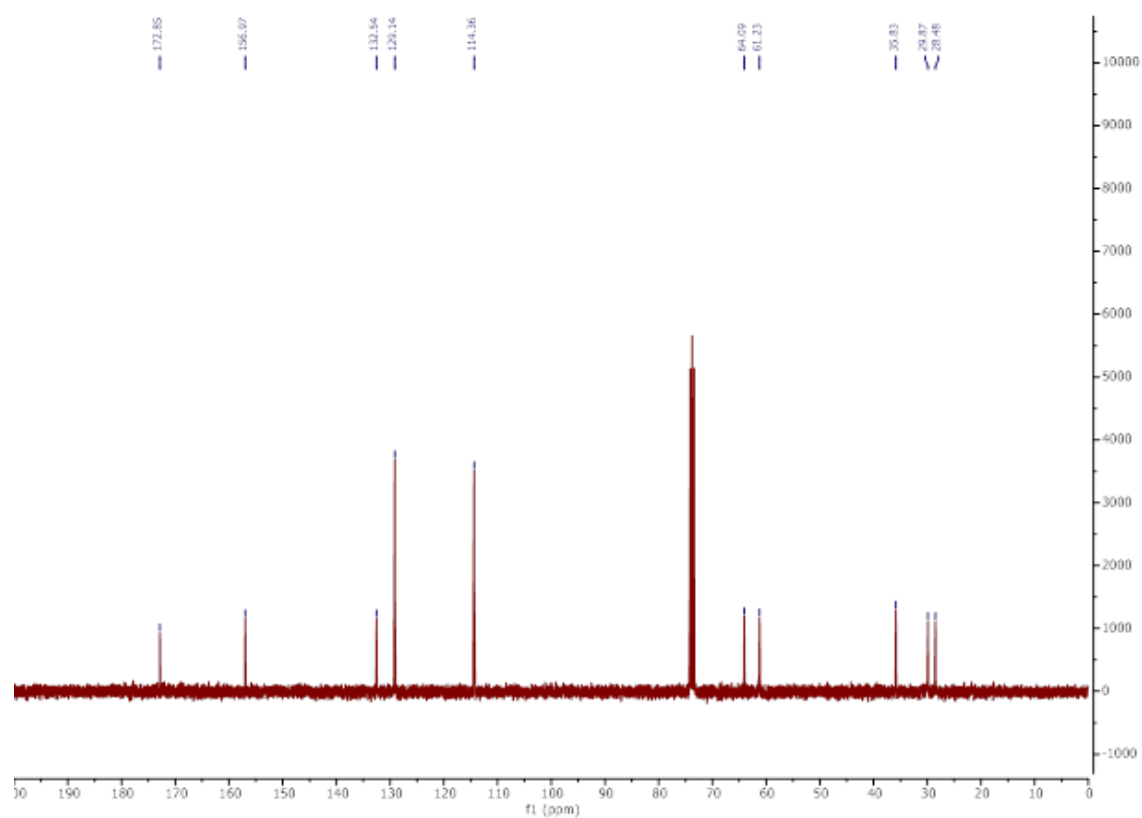


**Figure A.33**  $^{13}\text{C}$  NMR spectrum of polypropylene phloretate (PPP)

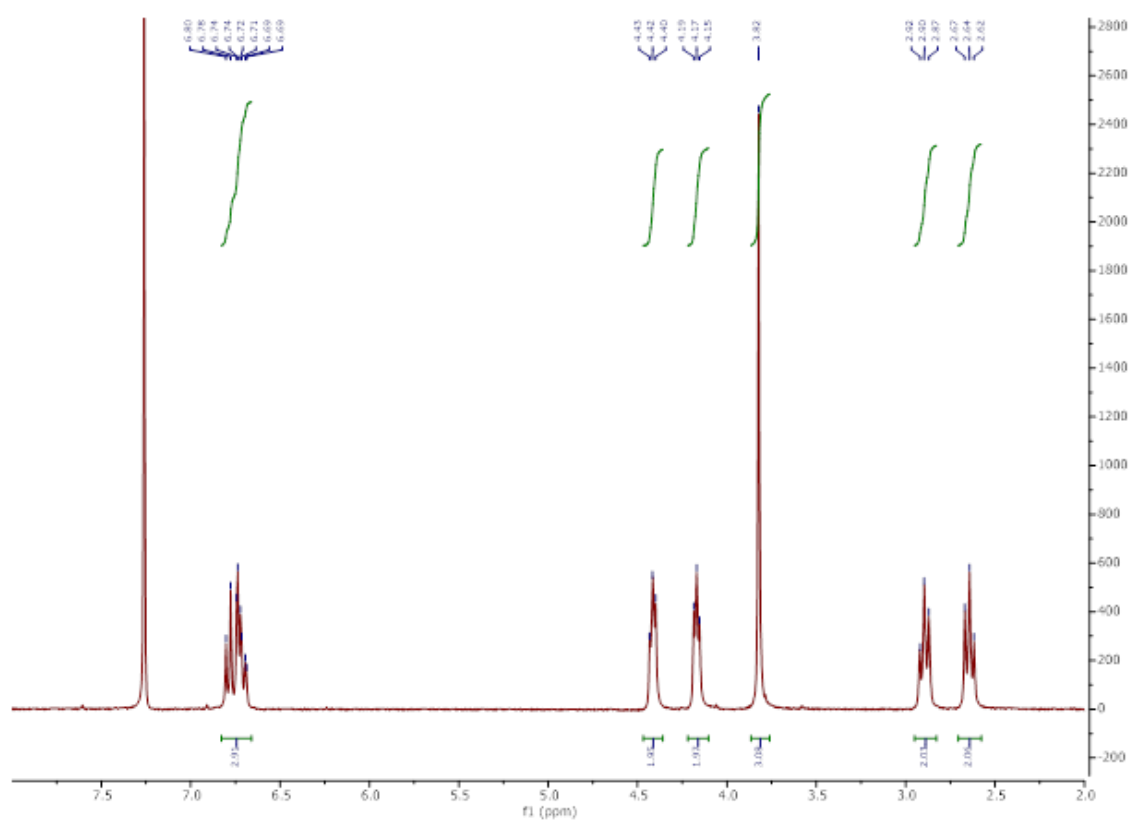


**Figure A.34**  $^1\text{H}$  NMR spectrum of polyethylene dihydroferulate

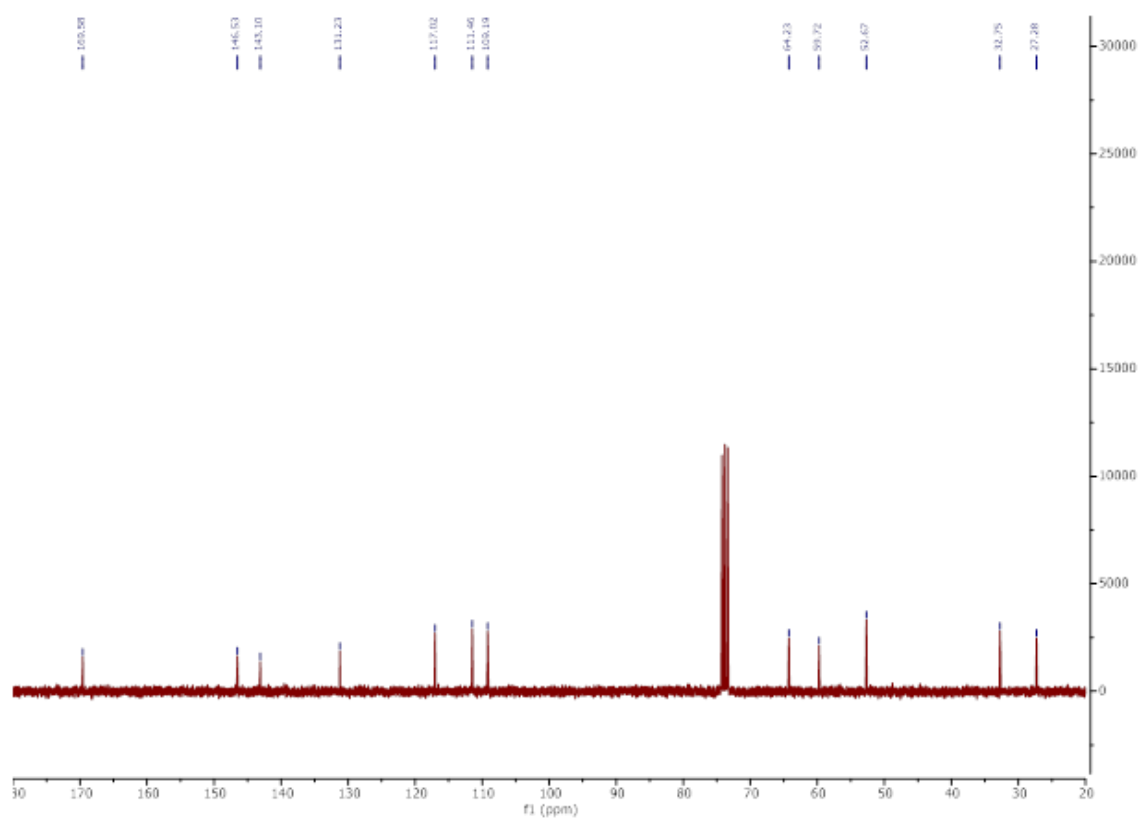


**Figure A.35** <sup>13</sup>C NMR spectrum of polyethylene dihydroferulate

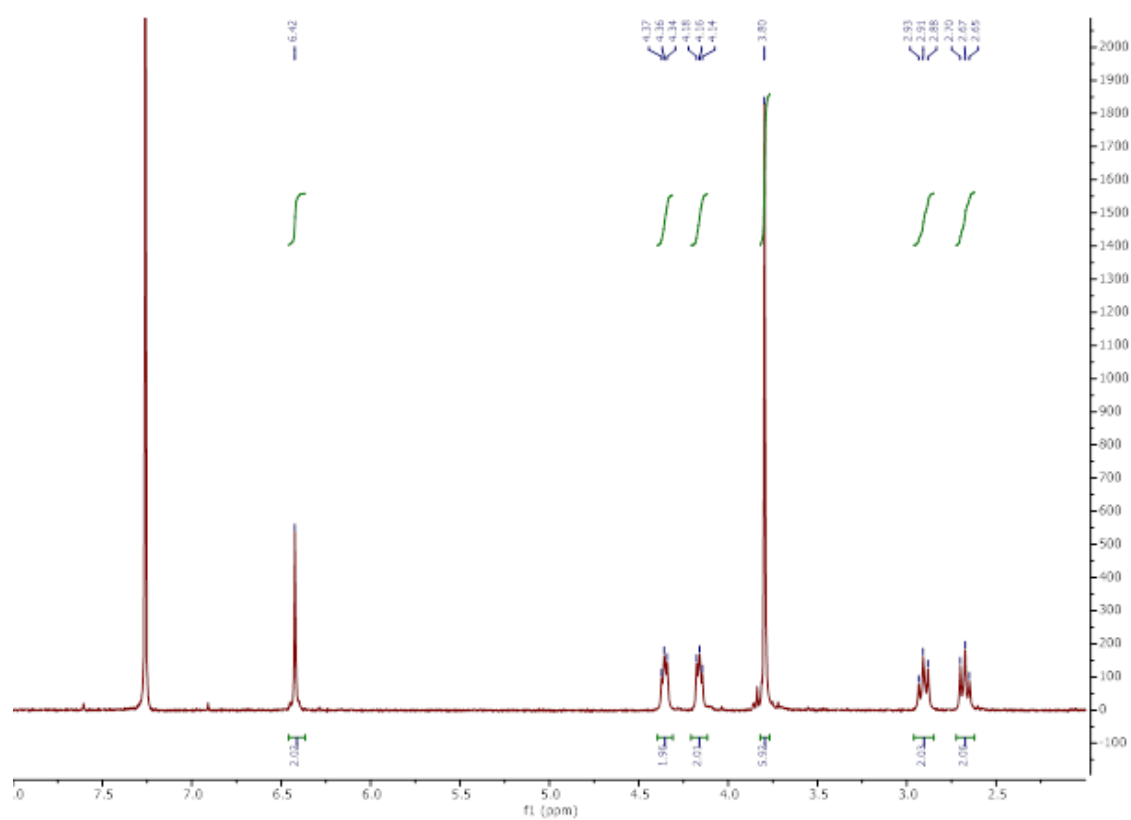


**Figure A.36**  $^1\text{H}$  NMR spectrum for polyethylene dihydrosinapate

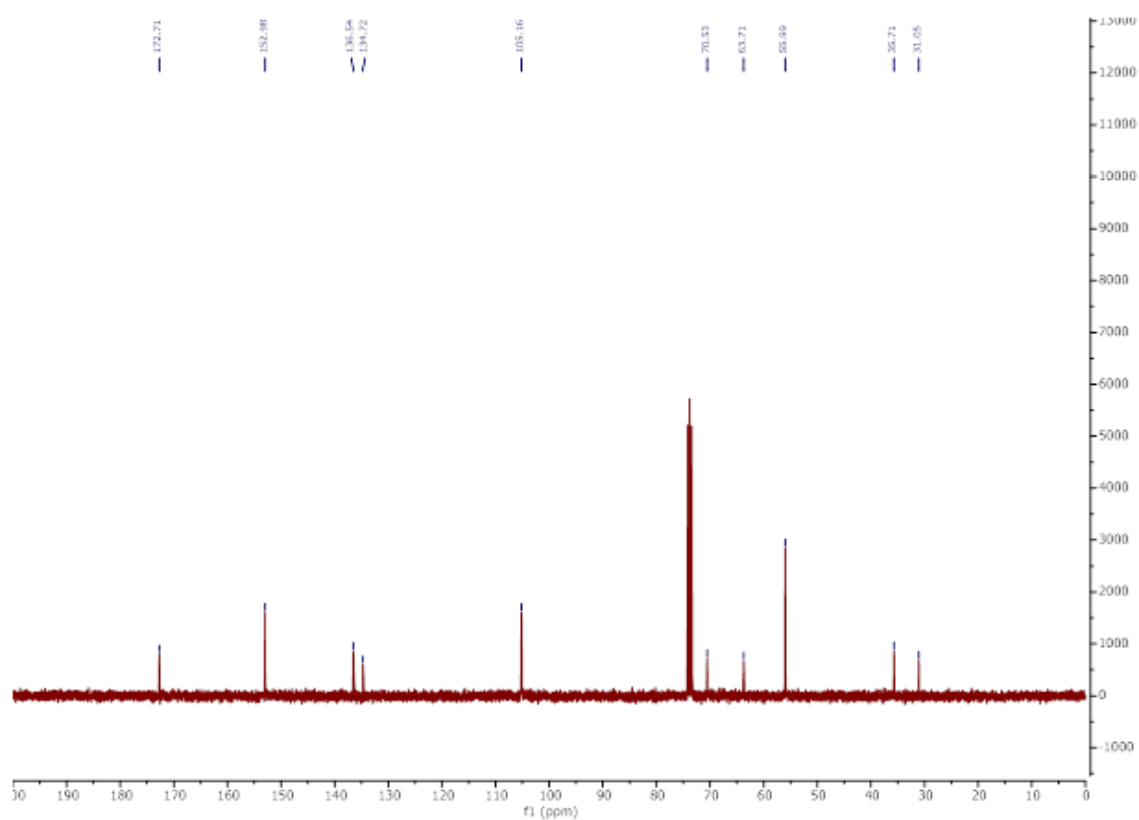


**Figure A.37**  $^{13}\text{C}$  NMR spectrum of polyethylene dihydrosinapate

## Green Metrics

The E-Factor for the synthesis of 4-(2-hydroxyethoxy)phenylpropanoic acid by ethylene carbonate and 1-chloroethanol is present below.

$$E - Factor = \frac{Mass\ of\ Inputs - Mass\ of\ Products\ (g)}{Mass\ of\ Products\ (g)} \quad (\text{Equation A1})$$

**Table A.1** E-Factor evaluation of alkylation via cyclic carbonate over two steps. Sulfuric acid assumed to be negligible

Product	Input Material	Input Weight (g)	Product Weight (g)	E Factor	Process E Factor
PA Methyl Ester	Phloretic acid	50.00	53.61	0	0.97
	MeOH	118.80			
	Sulfuric Acid				
EP monomer	PA Methyl Ester	53.61	50.25	0.97	
	Ethylene carbonate	22.10			
	Potassium Carbonate	1.65			
	NaOH	21.60			
	H <sub>2</sub> O	270.00			

**Table A.2** E-Factor evaluation of alkylation via halo alcohol.

Halo alcohol route	Phloretic acid	166.00	132.45	2.26
EP Monomer	NaOH	100.00		
	NaI	45.00		
	2-chloro ethanol	120.77		
	H <sub>2</sub> O	1000.00		

The general rubric for EcoScale for both routes is shown below.

$$\text{EcoScale} = 100 - \text{Penalty Points} \text{ (Equation A2)}$$

Excellent: 75-100

Acceptable: 50-74

Inadequate: 0-49

**Table A.3** EcoScale Rubric

<b>1. Yield</b>	<b>Penalty Points</b>
(100-%yield)/2	.5-50
<b>2. Price (for 10 mmol product)</b>	
<\$10	0
\$10-\$50	3
>\$50	5
<b>3. Safety (sum all that apply)</b>	
N- dangerous for environment	5
T- toxic	5
F- flammable	5
E- explosive	10
F+ extremely flammable	10
T+ extremely toxic	10
<b>4. Set up (sum all that apply)</b>	
common	0
Controlled addition	1
Unconventional activation	2
Pressure equipment >1atm	3
additional special glassware	1
inert atmosphere	1
glove box	3
<b>5. Temp/Time (sum all that apply)</b>	
rt<1hr	0
rt<24hr	1
heat <1hr	2
heat>1hr	3
cool to 0C	4



Cool < 0C	5
<b>6. Workup/purification (sum all that apply)</b>	
none	0
Cool to rt	0
Adding solvent	0
simple filtration	0
removal of solvent bp <150C	0
Crystallization/filtration	1
removal of solvent bp>150C	2
solid phase extraction	2
distillation	3
sublimation	3
liquid-liquid extraction	3
Chromatography	10

**Table A.4** EcoScale evaluation of alkylation with ethylene carbonate

Parameter	Assessment	Penalty Points
1. Yield	(100-96)/2	2
2. Price PMeEster Ethylene Carbonate K <sub>2</sub> CO <sub>3</sub>	\$ 1.80/10 mmol \$ 0.97/10 mmol \$ 0.69/10 mmol	0
3. Safety	Toxic (ethylene carbonate)	5
4. Set up	Additional special glassware Inert atmosphere	2
5. Temp/Time	heat>1hr	3
6. Workup	Crystallization/Filtration	1
Total Penalty Points		13
Eco-Scale	100-13	<b>87</b>

**Table A.5** EcoScale Evaluation of alkylation with 2-chloroethanol

Parameter	Assessment	Penalty Points
1. Yield	(100-63)/2	18.5
2. Price Phloretic Acid NaOH NaI 2-chloro ethanol	\$ 1.66/10 mmol \$ 1.00/10 mmol \$ 0.45/10 mmol \$ 1.21/10mmol	0
3. Safety	Dangerous for the environment, flammable, extremely toxic (2-chloroethanol)	20
4. Set up	Controlled addition	1
5. Temp/Time	heat>1hr	3
6. Workup	Crystallization/Filtration Liquid-liquid extraction	4
Total Penalty Points		46.5
Eco-Scale	100-46.5	<b>53.5</b>

## DSC Thermograms

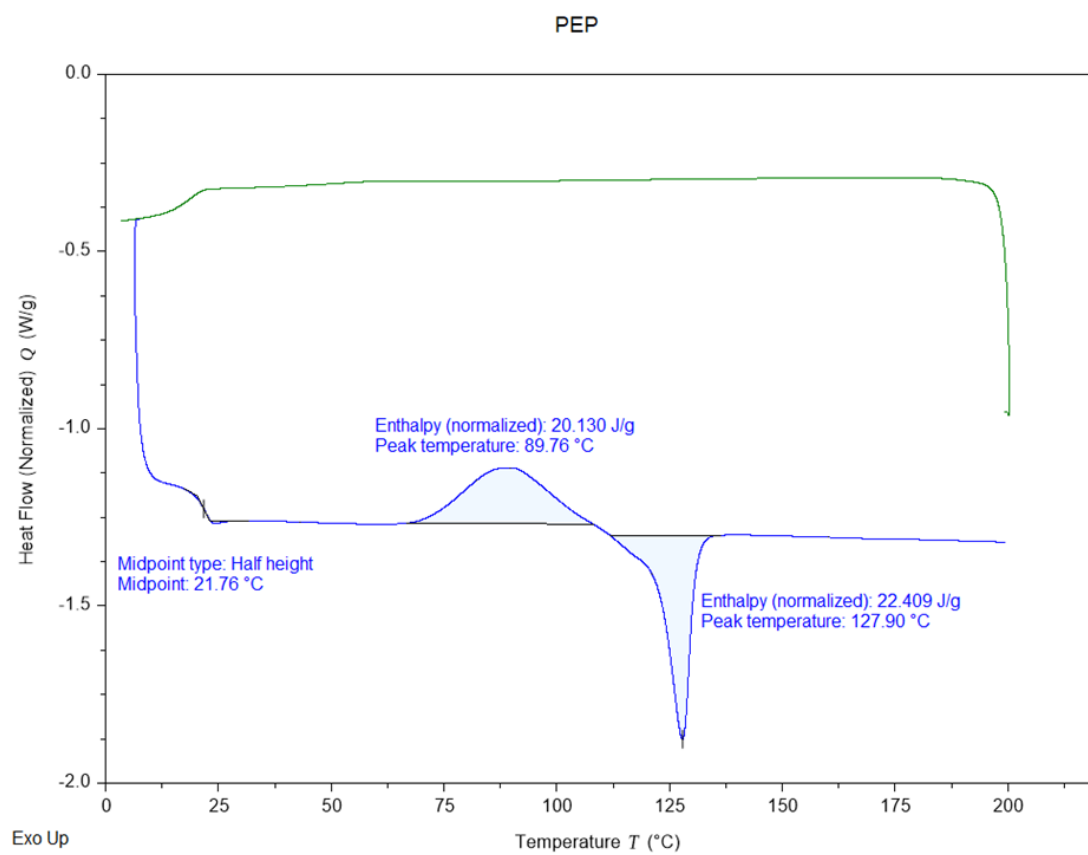


**Figure A.38** Second heating and cooling cycle of PEP

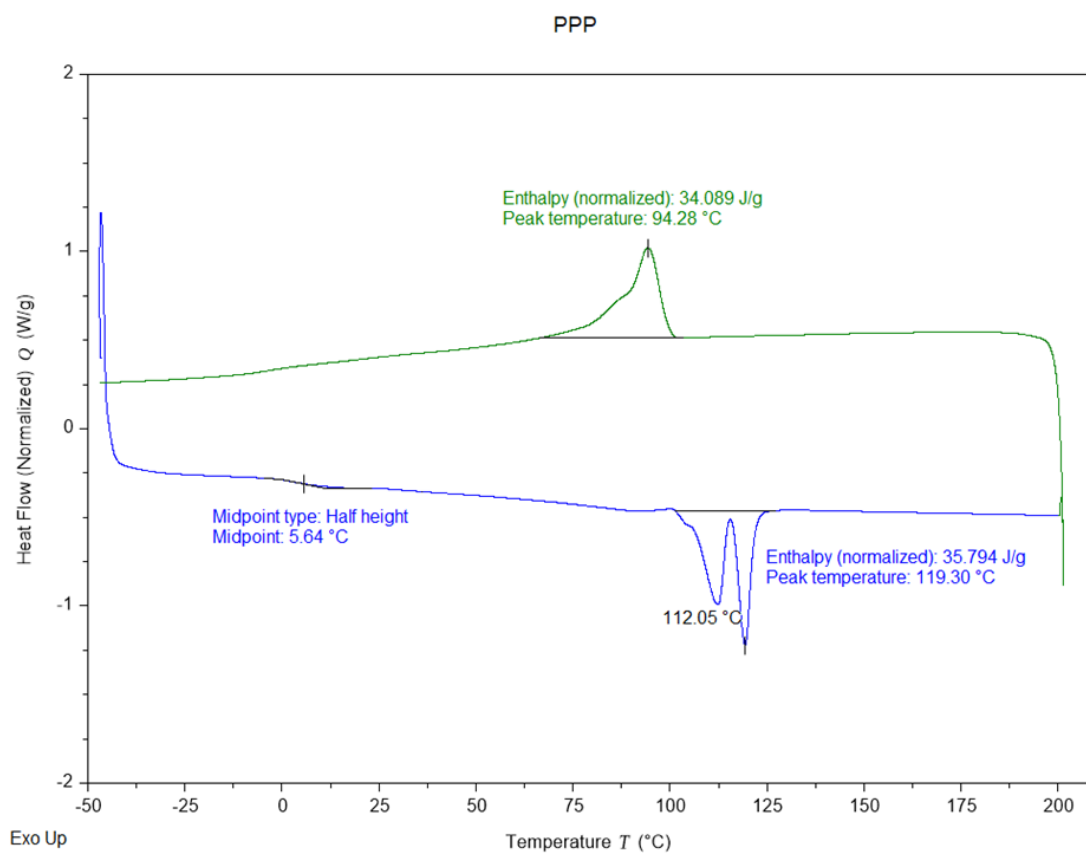


**Figure A.39** Second heating and cooling cycle of PPP

## Tensile Testing

**Table A.6** Tensile properties of PiPP tested at different rates

Rate (mm/min)	Elastic Modulus (MPa)	Tensile Strength (MPa)	Ultimate Elongation (%)
20	3.77	5.40	428.95
50	2.39	2.93	249.80
80	4.76	4.25	273.57

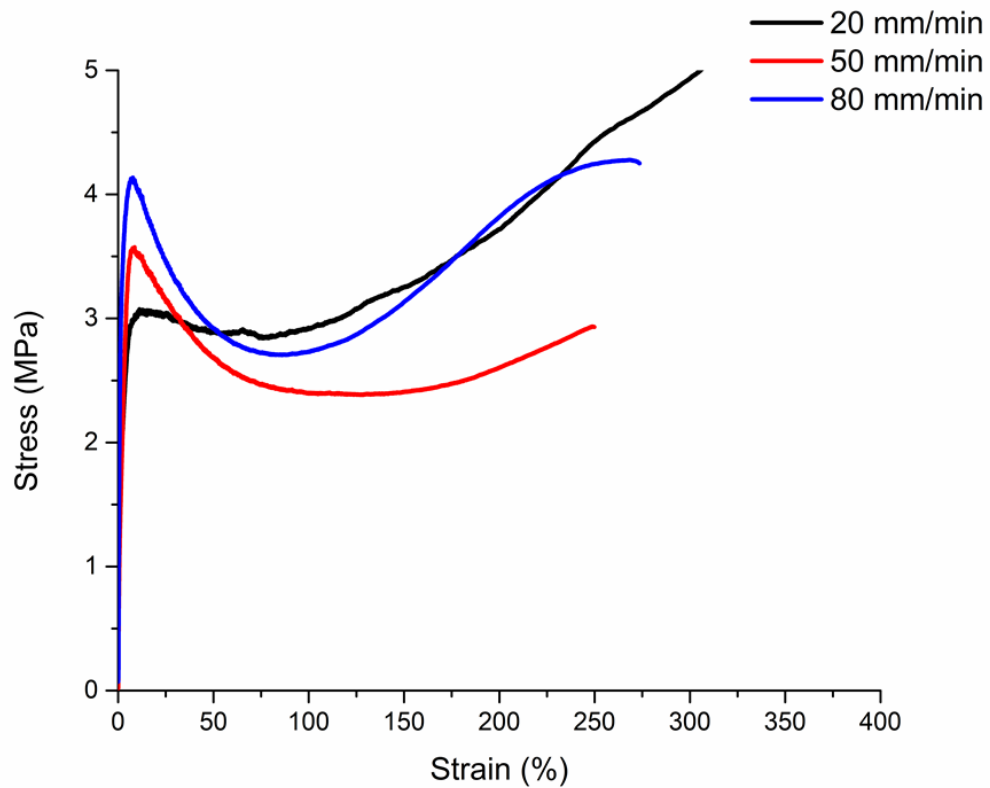


**Figure A.40** Stress strain curve of PiPP tested at different rates

## Composting

The evolved biogas of each sample was calculated daily by the difference of each sample to the average CO<sub>2</sub> contribution from the blank and negative controls as described by **Equation A3**.

$$Sample_{CO_2} = R_{CO_2} - B_{CO_2} \quad (\text{Equation A3})$$

Where  $Sample_{CO_2}$  is the cumulative CO<sub>2</sub> production (mg) from the sample specimen on the  $n^{th}$  day of operation determined from each replicate reactor CO<sub>2</sub> evolution,  $R_{CO_2}$  (mg). No negative control was used in respirometry experiments. Each replicate  $Sample_{CO_2}$  is calculated from the average of the CO<sub>2</sub> evolved from the triplicate control blanks,  $B_{CO_2}$  (mg). The calculated evolved CO<sub>2</sub> for each sample was then used to calculate the daily absolute biodegradation (%), according to **Equation A4**.

$$Absolute\ Biodegradation\ (\%) = \frac{Sample_{CO_2}}{m \times c \times 44.01/12.01} \quad (\text{Equation A4})$$

Where the sample mass,  $m$  (mg) and the percent organic carbon of the sample,  $c$  (%), was used to determine the carbon contributions to CO<sub>2</sub> for each sample. The dimensionless value of 44.01/12.01 is used to account for the carbon mass in CO<sub>2</sub> generated from each reactor. Methane concentrations were monitored to ensure aerobic conditions were maintained throughout the experiment.

These datasets were normalized according to the standard normalization **Equation A5**.

$$y = a + \frac{(y-A)(b-a)}{(B-A)} \quad (\text{Equation A5})$$

Where  $a$  is the minimum value 0,  $b$  is the maximum value of 1,  $A$  is the dataset minimum value, 0, and  $B$  is the dataset maximum value for the absolute biodegradation calculations.

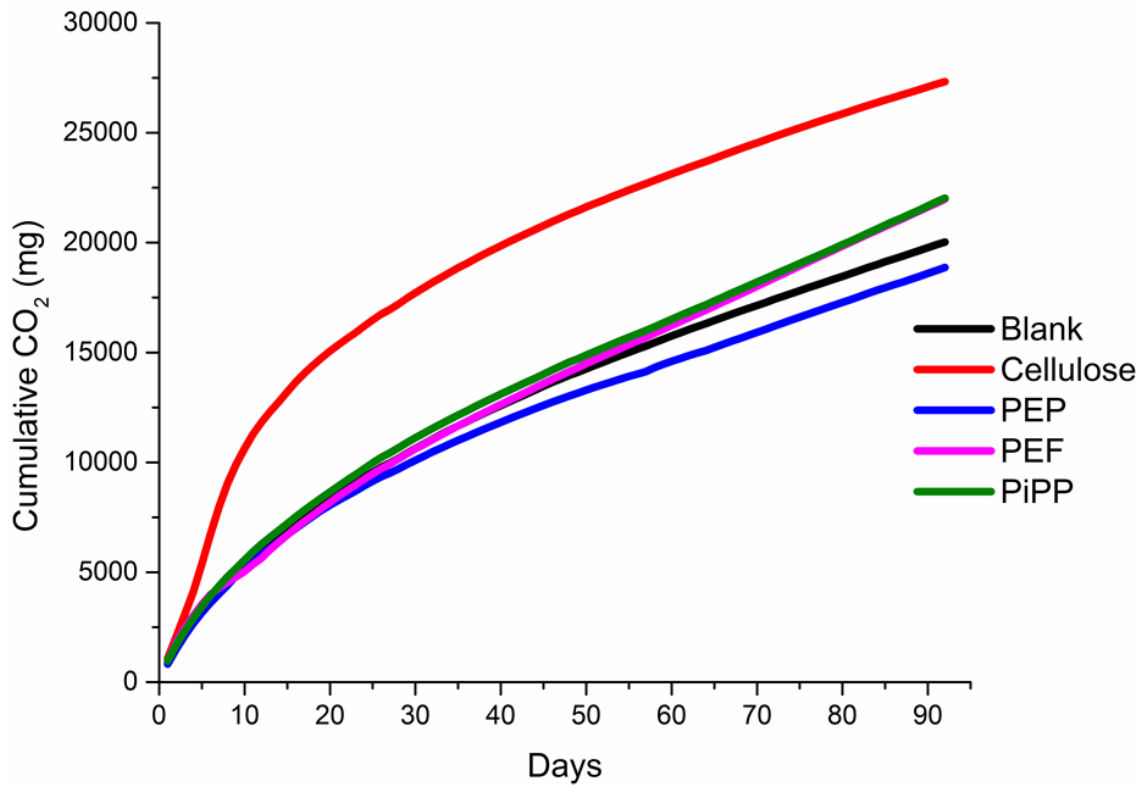


**Figure A.41** Cumulative CO<sub>2</sub> production of compost without sample (blank), cellulose positive control, and tested samples

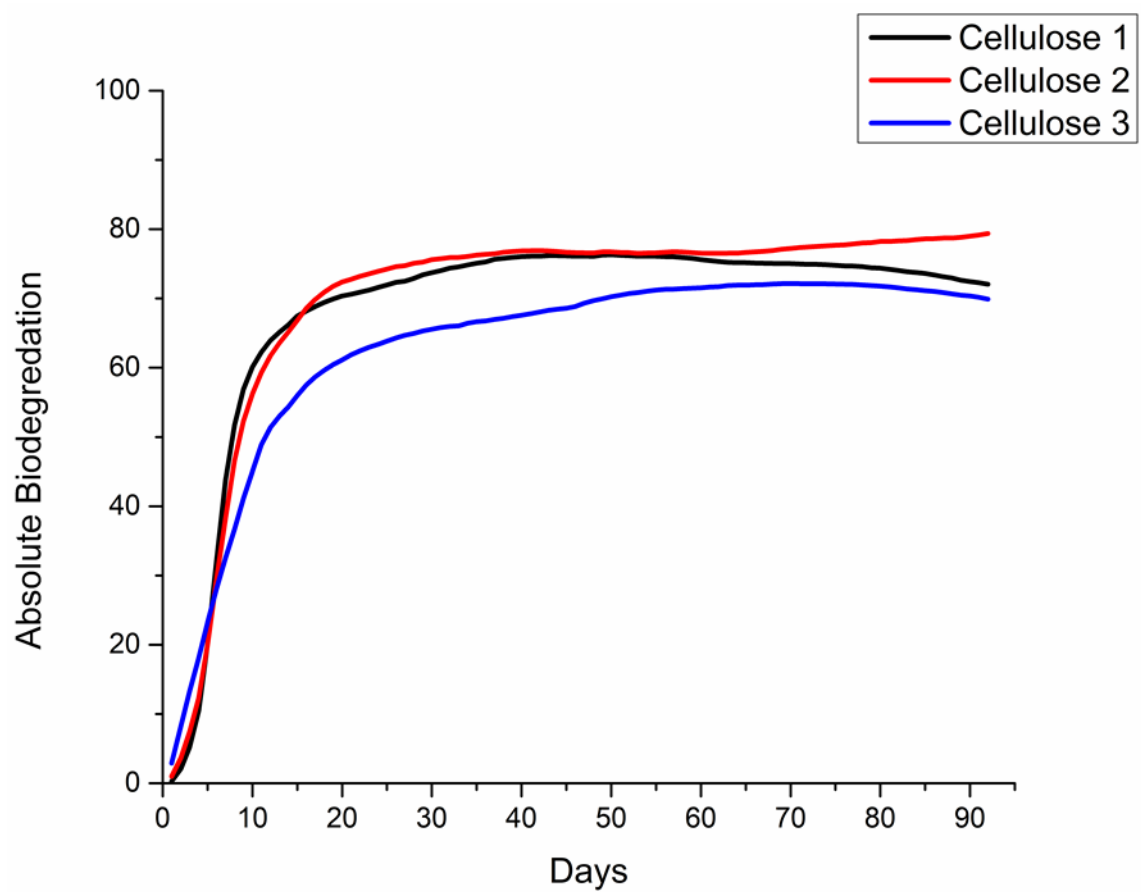


**Figure A.42** Absolute biodegradation of cellulose triplicates



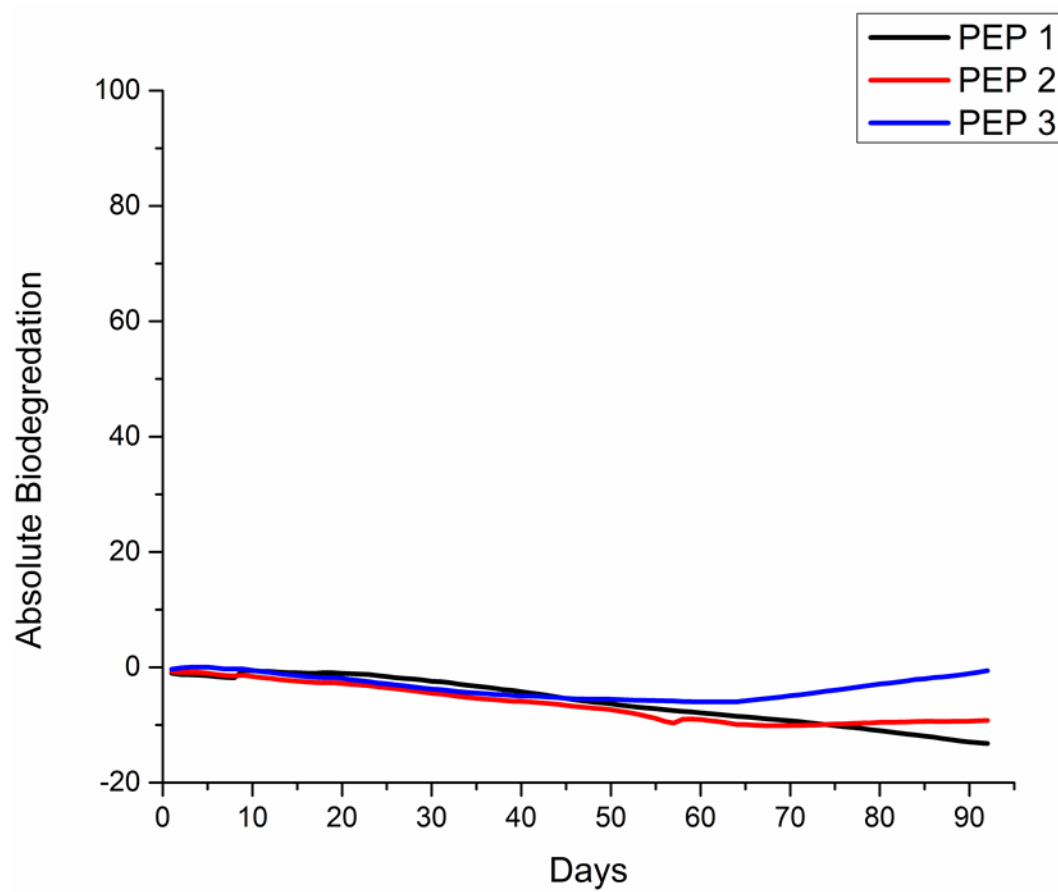


**Figure A.43** Absolute biodegradation of PEP triplicates

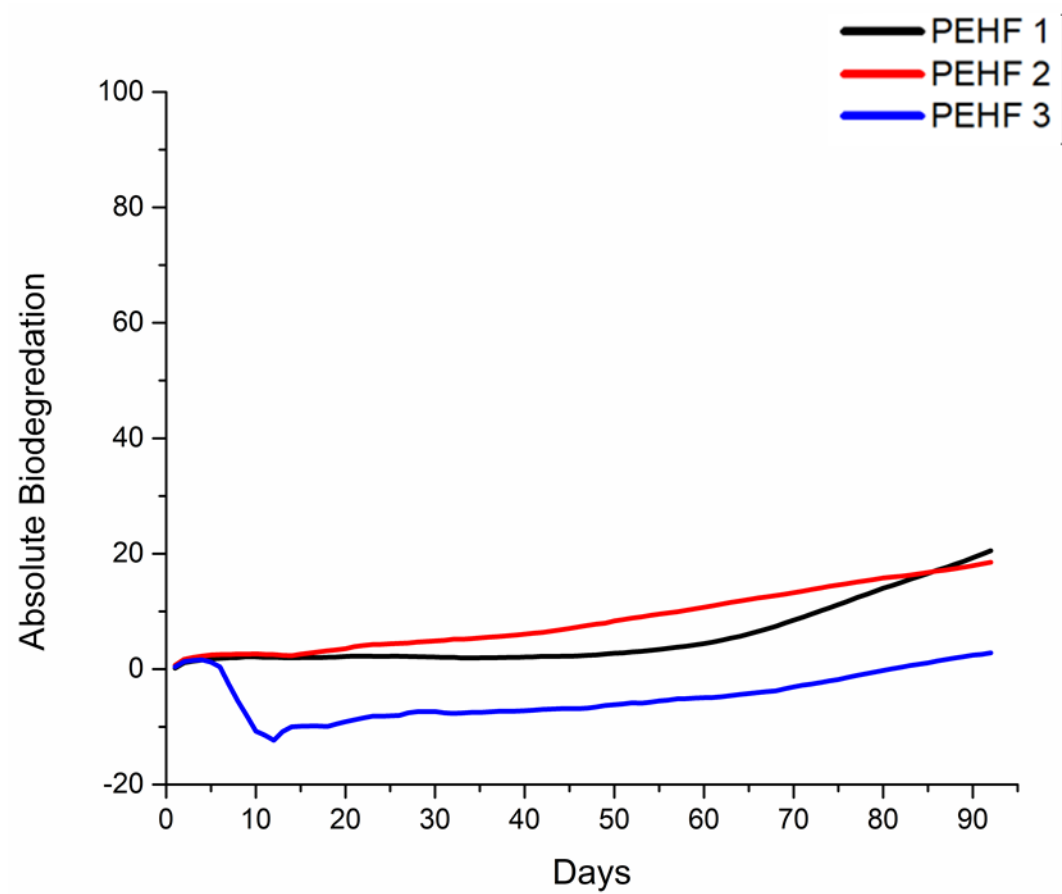


**Figure A.44** Absolute biodegradation of PEHF

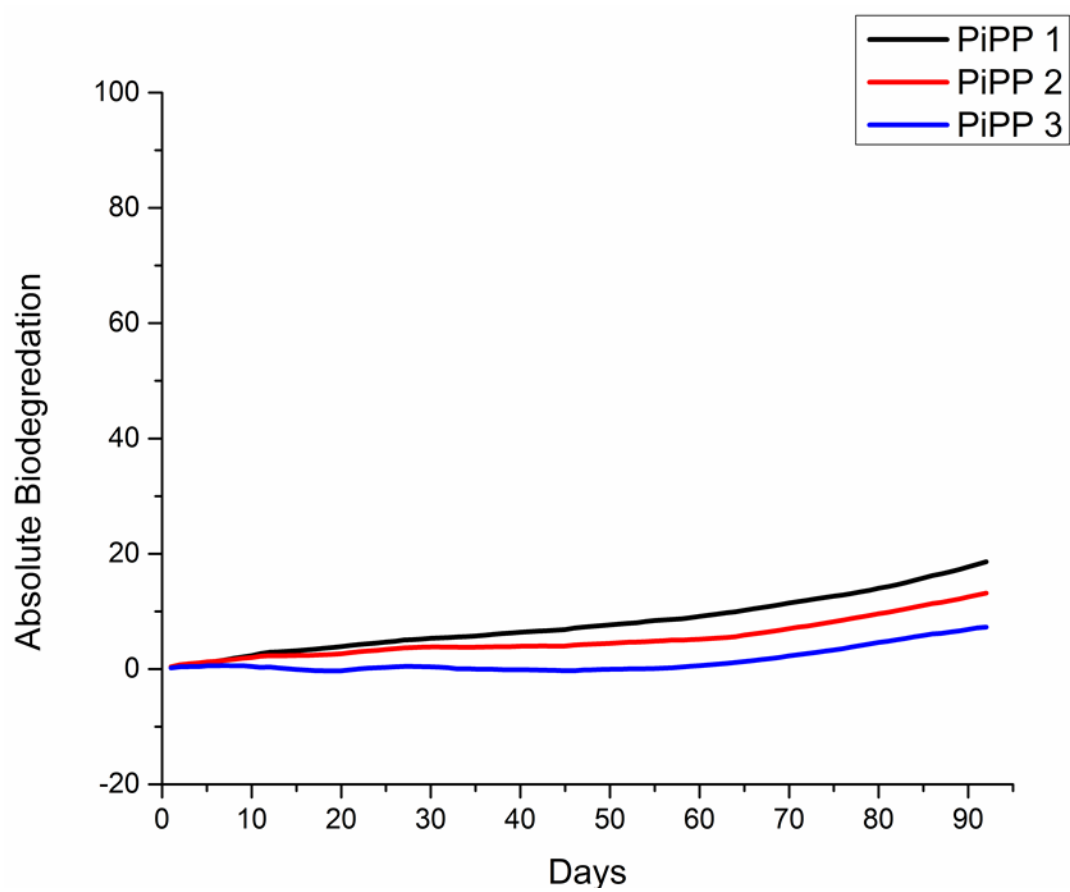


**Figure A.45** Absolute biodegradation of PiPP